İSTANBUL TECHNICAL UNIVERSITY ★ INSTITUTE OF SCIENCE AND TECHNOLOGY

CAVITATION EFFECTS ON STABILITY, ECONOMIC LIFE AND PERFORMANCE OF HYDRAULIC STRUCTURES

M.Sc. Thesis by
Mehdi JAHANI

Department : Civil Engineering

Program : Hydraulic and Water Resources Engineering

SEPTEMBER 2011

İSTANBUL TECHNICAL UNIVERSITY ★ INSTITUTE OF SCIENCE AND TECHNOLOGY

CAVITATION EFFECTS ON STABILITY, ECONOMIC LIFE AND PERFORMANCE OF HYDRAULIC STRUCTURES

M.Sc. Thesis by
Mehdi JAHANI
501091517

Date of submission : 09 September 2011
Date of defence examination : 27 September 2011

Supervisor (Chairman) : Prof. Dr. Ilhan AVCI
Members of the Examining Committee : Prof. Dr. Ismail DURANYILDIZ
Prof. Dr. Mete ŞEN

September 2011

İSTANBUL TEKNİK ÜNİVERSİTESİ ★ FEN BİLİMLERİ ENSTİTÜSÜ

SU YAPILARINDAKİ KAVİTASYON OLAYININ YAPI STABİLİTESİ, EKONOMIK ÖMÜR VE İŞLETME VERİMLİLİĞİ ÜZERİNDEKİ ETKİLERİ

YÜKSEK LİSANS TEZİ
Mehdi JAHANI
501091517

Tezin Enstitüye Verildiği Tarih : 09 Eylul 2011
Tezin Savunulduğu Tarih : 27 Eylul 2011

Tez Danışmanı : Prof. Dr. Ilhan AVCI
Diğer Jüri Üyeleri : Prof. Dr. Ismail DURANYILDIZ
Prof. Dr. Mete ŞEN

EYLUL 2011

FOREWORD

Cavitation is a most unpleasant hydrodynamic phenomenon, whose harmful effects is both widespread and obvious and seriously handicap many phases of science and engineering. Conversely, its basic nature has long been veiled in mystery and only recently is it beginning to be understood.

The generation of cavitation can cause severe damage in hydraulic structures and machinery Therefore, the prevention of cavitation is an important concern for designers of hydraulic structures.

This study is mainly concerned about the characteristics of cavitation and its prevention ways, and it can be very instructive for advanced students, scientists and engineers, who want to understand the true nature of cavitation.

I would like to express my deep appreciation and thanks to my advisor Mr. Prof. Dr. Ilhan AVCI and my grateful thanks to my family members for their support, and my special thanks to my roommate and best friend Mr. Mani BAGHAEI FARD for his patience and tolerance to me, also, my high regards to my friends Burcu ODABAŞI and Volkan ÖGÜT for their helps in writing this thesis.

September 2011

Mehdi JAHANI

Civil Engineer

TABLE OF CONTENTS

Page

ABBREVIATIONS

ASTME	**:** American Society of Tool and Manufacturing Engineers
USSR	**:** Union of Soviet Socialist Republics
RMS	**:** Root Mean Square
LAPC	**:** Low Ambient Pressure Chamber
HFWS	**:** Hartree-Fock-Wigner-Seitz

LIST OF TABLES

Page

LIST OF FIGURES

Page

CAVITATION EFFECTS ON STABILITY, ECONOMIC LIFE AND PERFORMANCE OF HYDRAULIC STRUCTURES

SUMMARY

Cavitation is the formation of bubbles or cavities in a liquid, initiated by surface irregularities and roughnesses that are subjected to high-velocity water flow. The bubble cavities are filled with water vapor and air, and form where the local pressure drops to a value that will cause the water to vaporize at the prevailing water temperature. Cavitation bubbles will grow and travel with the flowing water to an area where the pressure field will cause collapse. When a bubble collapses or implodes close to or against a solid surface, an extremely high pressure is generated, which acts on an infinitesimal area of the surface for a very short time and damages the substrate materials. When cavitation bubbles implode on a metal surface, pressures of up to 1300 kg/cm^{2}are produced, and the velocity of impact of the fluid on the surface may reach 85 m/s.

Cavitation damage in hydraulic structures is a function of the cavitation potential, the duration of the operation, the boundary roughness and alignment, and the strength of the materials from which the boundary is constructed, a method of locating sites of cavitation damage in spillways is presented. Curves delineating damage as a function of the cavitation potential and the duration of operation are given. The formulas allow a determination of areas in which attention to surface tolerances can protect the boundary. These damages are affecting performance and economic life of hydraulic structures and machinery.

In addition, for protecting structures there are some ways that can be used to define when and where aeration grooves must be used. Some methods of preventing cavitation damage, other than aeration grooves, are discussed. The flow conditions that dictate the various cavitation presentation methods are delineated.

Noise and vibration occur in many applications, ranging from all forms of turbo machinery to large valves in industrial plants and spillways. Associated with the deleterious effects of performance breakdown, noise, and vibration, there is the possibility of erosion.

SU YAPILARINDAKİ KAVİTASYON OLAYININ YAPI STABİLİTESİ, EKONOMIK ÖMÜR VE İŞLETME VERİMLİLİĞİ ÜZERİNDEKİ ETKİLERİ

ÖZET

Kavitasyon ; kabarcıkların veya boşlukların bir sıvı içinde, yüksek hızlı su akışına maruz kalan , yüzey düzensizlikleri ve pürüzlülük sebebiyle başlatılan oluşumdur. Kabarcık boşlukları su buharı ve hava ile doludur ve yerel basınç mevcut su sıcaklığında buharlaşma degerinin altina düştüğü anda olusacaktir.

Kavitasyon kabarcıkları büyüyecek ve ta ki bir yerdeki basınç baloncukların patlamasına neden oluncaya kadar akışkanla birlikte hareket edecektir. Ne zamanki bir baloncuk yüzeye yakın bir yerde patlarsa,çok büyük basınçlar oluşur ve cok küçük bir alanda cok kısa zamanda buyuk hasarlar oluşacaktır. Eger baloncuklar metal yüzey yakınlarında patlarsa; yerel hız 85 m/s' e yükselerek 1300 kg/cm^{2}basınç oluşacaktır.

Su yapılarındakı kavitasyon hasarı, işletme zamanına, sınır tabakasındaki pürüzlülüğe ,sınırdaki çıkıntılara ve malzeme kuvvetine bağlıdır. Kavitasyon yerini bulmak için bu çalışmada bir yöntem gösterilmiştir. Bir kaç çizelgede kavitasyon hasarını ve kavitasyon potansiyelini, kavitasyon zamanın etkilerini ve bunlarin bağlantılarını göstermekteyiz. Formüller hangi alanların pürüzlülüklerinin kavitasyon için tehlikeli olabileceklerini tahminine izin verirler.Söz konusu olan hasarlar yapı üzerinde işletme verimliliğini ve ekonomik ömrünü etkilemektedir.

Kavitasyondan korunmak için bir kaç yol vardır. Bunlardan biri de vantuz kullanmaktır.Vantuzdan başka yolları da bahsetmiş bulunmaktayız. Kavitasyona etkili olan akım koşulları da çok önemlidir. Gürültü ve titreşim de kavitasyonun yan etkileridir ki bunları genellikle makinelerde, sanayi valflerinde ve dolu savaklarda görmekteyiz. Bahsedilen işletme verimliliği düşüşü, gürültü ve titreşim bir yerde oluşan erozyonun işaretidir.

1. INTRODUCTION

Cavitation had been postulated theoretically by Reynolds long before it was first observed in the trials of the destroyer HMS Daring in 1893. The speeds reached by HMS Daring were well below those expected and the trouble was traced to poor propeller performance due to formation of vapor bubbles on the blades. A few years later the first turbine ship, the Turbinia, met similar difficulties. She was fitted with seven different propellers in turn but none enabled her to reach anything like the predicted speed. Eventually, it was found necessary to replace the single shaft by triple shafts with three propellers on each; thus equipped, the Turbinia, attained a speed of 32 knots.

Cavitation is caused by the boiling of a liquid at normal temperatures and low pressure. It is accentuated by the presence of dissolved air which is released when pressures are reduced. It is the combination of air release and vaporization caused by low pressures induced in a fluid that we call cavitation.

Since the time of the Daring and the Turbinia investigations, the chemical, physical and engineering aspects of cavitation have been the subject of intensive research. Investigations have been made of the process of bubble formation and collapse, the role of gases dissolved in the liquid, the effect of bubble formation and collapse on pumps, turbines, propellers, dams and similar structures. It has been found for instance that the formation of bubbles upsets the flow of fluid through a machine, causing loss of pressure, efficiency and thrust. Also the collapse of the bubbles causes shock waves which erode the metal of the turbine impeller or propeller.

Its effect on hydrofoils is to cause loss of lift, and a similar effect is caused on the performance of machines, pumps, turbines and propellers. Each type of machine is examined in turn and the cavitation performance characteristic investigated, together with the design recommendation and optimization. Cavitation erosion causes trouble in many machines and static devices.

In the past decade high dams have been constructed and the flow rates discharged over the spillways have been very large. In many projects, the heights of dams are in excess of 200m and the velocities on the concrete chutes of spillway can be of the order of 50m/s. As the velocity on the spillway increases, the threat of damage to the structure by cavitation erosion also increases. Once damage is initiated on the concrete surface, catastrophic damage is accelerated by the combined action of cavitation and impingement attack. An extreme example is shown in Figure 1, which illustrates the damage sustained in the spillway tunnel of the Yellowtail Dam in South Central Montana.

Figure 1.1: Cavitation damage in the spillway tunnel of the Yellowtail Dam (Arndt, 2009).

The following Chapters are mainly subjected to find out more information on the phenomena and ways to predict, prevention of cavitation in large hydraulic structures and Fluid machinery.

2. FUNDAMENTALS OF CAVITATION

2.1. Hydraulic Structures, Hydraulic Structures Stability, Economic Life, and Management Productivity Concepts

A hydraulic structure is a structure submerged or partially submerged in any body of water, which disrupts the natural flow of water. They can be used to divert, disrupt or completely stop the flow. An example of a hydraulic structure would be a dam, which slows the normal flow rate of river in order to power turbines. A hydraulic structure can be built in rivers, a sea, or any body of water where there is a need for a change in the natural flow of water.

One of the main considerations of Dams and turbines design is stability of these structures during their use or economic life.

Since we spend too much money to build such structures and it's important to keep these structures working cause of flood or energy problems, we have to pay attention to stability of these structures.

One of the main problems which endanger the stability and performance of hydraulic structures is Cavitation.

Hydraulic structures are among the most widespread engineering objects with a high economic significance and social and ecological responsibility; Special attention has always been devoted to provision of their reliability and safety.

In Table 2.1 you can see estimated average lives for many thousands of different types of industrial assets. The lives (in years) given for certain elements of hydraulic projects are listed. Such estimates of average lives may be helpful even though they are not necessarily the most appropriate figures to use in any given instance (Mays, 2001).

Table 2.1: Live (in years) for elements of hydraulic projects (Linsley et al, 1992).

Elements	**Years**	**Elements**	**Years**
Barges	12	Pipes, Cast iron 2-4in.	50
Booms, log	15	Pipes, Cast iron 4-6in	65
Canals and ditches	75	Pipes, Cast iron 8-10in	75
Coagulating basins	50	Pipes, Cast iron 12in and over	100
Construction equipment	5	Concrete Pipes	20-30
Crib Dams	25	PVC Pipes	40
Earthen, concrete or masonry Dams	150	Steel Pipes Under 4in	30
Loose rock Dams	60	Steel Pipes over 4in	40
Steel Dams	40	Pumps	18-25
Filters	50	Reservoirs	75
Fossil-fuel power plants	28	Standpipes	50
Generators above 3000kva	28	Concrete Tanks	50
Generators 1000-3000kva	25	Steel Tanks	40
Generators 50hp-1000kva	17-25	Wood Tanks	20
Generators Below 50hp	14-17	Tunnels	100
Hydrants	50	Turbines, Hydraulic	35
Marine construction equipment	12	Wells	40-50
Meters, water	30	Penstocks	50
Nuclear power plants	20		

2.2. Basic Definition of Cavitation

Cavitation is a process that usually is associated with damage to a surface or marked by intense noise. Both phenomena may occur during cavitation, but actually cavitation is neither of these. Instead, Cavitation is defined as the formation of a bubble or void within a liquid. An understanding of the cavitation process can be obtained by examining the process of boiling. When water is heated the temperature increases which results in increases in its vapor pressure. When the vapor pressure equals the local pressure, boiling will occur. At the boiling point, water is changed into water vapor. This change first occurs at localized points within the water and it is observed as small bubbles. The temperature at which boiling occurs is a function of pressure. As pressure decreases, boiling will occur at lower and lower temperatures. Since the pressure is a function of elevation, boiling occurs at lower temperatures at higher elevations as noted on Figure 2.l. If it were possible to go to a high enough elevation, boiling would occur at room temperature.

Although cavities are formed in water by boiling and the process occurs when the local pressure equals the water vapor pressure, a technical difference between boiling and cavitation exists. Boiling is the process of passing from the liquid to the vapor state by changing temperature while holding the local pressure constant. Cavitation is the process of passing from the liquid to the vapor state by changing the local pressure while holding the temperature constant (Fig. 2.1). The local pressure reductions associated with cavitation can be caused by turbulence or vortices in flowing water.

An example of bubble formation within a liquid, which occurs by reductions in pressure, can be seen when a bottle containing a carbonated liquid is opened. Upon opening the bottle, bubbles form within the liquid and rise to the surface. While in the capped bottle, the liquid is under enough pressure to keep the carbon dioxide in solution. However, as the bottle is opened, the pressure is reduced and the liquid becomes supersaturated relative to the carbon dioxide. Therefore, the carbon dioxide begins to diffuse out of the liquid (Falvey, 1990).

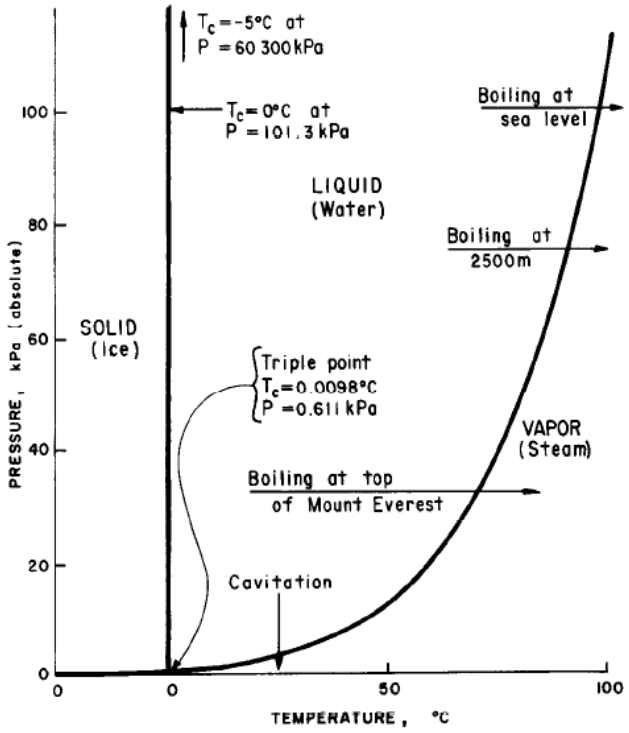

Figure 2.1: Phase diagram for water (Falvey, 1990).

2.3. Mechanism of Happening Cavitation in a Flow

In hydraulic structures, water contains air bubbles and various types of impurities of many different sizes. As will be seen later, microscopic air bubbles or impurities in the water are necessary to initiate cavitation. However, once started, vaporization is the most important factor in the cavitation bubble growth. The presence of air bubbles in the flow also has an effect on damage and noise produced by the cavitation.

Water does not spontaneously change from the liquid to the vapor state as either the temperature is raised or the pressure is decreased. Water which has been distilled and filtered many times can sustain extremely large negative pressures without cavitating. Cavitation and boiling are both observed to begin at the location of impurities in the flow or at minute cracks on a smooth boundary. It is not known if particles of dirt serve as nuclei for the vaporization. However, Katz (1984) observed that the appearance of visible cavitation in flowing water was always preceded by the occurrence of a swarm of microscopic bubbles in a small region of the flow field. The importance of bubbles-as cavitation nuclei-has been known for a long time and

all of the theory, for the formation of cavitation, has been built up around the existence of microscopic bubbles in the flow.

The sizes of these nuclei need to be in the range 0.1 to 10μm, and two theories have been proposed to explain their existence and persistence. The first is that the nuclei are stabilized within the interstices of microscopic dust particles; the second is that an organic film forms around a nucleus and thereby maintains the internal pressure and prevents diffusion of air.

When the ambient pressure in the liquid falls close to the vapor pressure, the nuclei grow rapidly and become visible as a cloud of tiny cavitation bubbles. The inception pressure which triggers this growth is usually slightly lower that the vapor pressure, but depends upon the initial size of the nuclei and upon the ratio of air pressure to vapor pressure within them. The ultimate size of the cavities is determined by the time that they are subject to pressures lower than the inception pressure.

In addition to describing cavitation it can be described by its occurrence. For instance, if the pressure of flowing water is decreased through increases in the flow velocity, a critical condition is reached when cavitation will just begin. This critical condition is called incipient cavitation. Similarly, if cavitation exists and the flow velocity is decreased or the pressure is increased, a critical condition is reached when the cavitation will disappear. This condition is called desinent cavitation. Incipient cavitation and desinent cavitation often do not occur at the same flow conditions. The distinction is especially important in laboratory investigations, but can usually be ignored for all practical purposes in hydraulic structures.

Finally, a set of critical flow conditions exists for which the individual cavitation bubbles suddenly transition into one large void. A condition under which the large void occurs is called variously as cavity flow, developed cavitation, or supercavitation (May, 1987).

2.4. Parameters of Cavitation and Cavitation`s Structure

The preceding section alluded to the existence of a critical combination of the flow velocity, flow pressure, and vapor pressure of the water at which cavitation will appear, disappear, or spontaneously transition into supercavitation. A parameter exists which can be used to define these various occurrences of cavitation. The parameter is known as the cavitation index and is derived below (Falvey, 1990).

The equation for steady flow between two points in a flow stream is known as the Bernoulli equation. It can be written:

$$\frac{\rho V_0^2}{2} + P_0 + Z_0\rho g = \frac{\rho V^2}{2} + P + Z\rho g \qquad \textbf{(2.1)}$$

Where:

P = pressure intensity

P_0 = reference pressure

V = flow velocity

V_0 = reference velocity

Z = elevation

Z_0 = reference elevation

g = gravitational constant (acceleration)

ρ = density of water

(The subscript o refers to upstream flow location as noted on Fig 2.2)

In dimensionless terms, the comparable equation results in a pressure coefficient, $C_{p:}$

$$C_p = \frac{(P+Z\rho g)-(P_0+Z_0\rho g)}{\rho V_0^2/2} = \frac{E_f - E_0}{\rho V_0^2/2} = 1 - (\frac{V}{V_0})^2 \qquad \textbf{(2.2)}$$

Where:

E_f = potential energy of flow (defined by values in parentheses)

E_0 = potential energy at reference point

In many cases, the gravitational terms are small relative to the pressure term or they are about equal; thus, the pressure coefficient can be written:

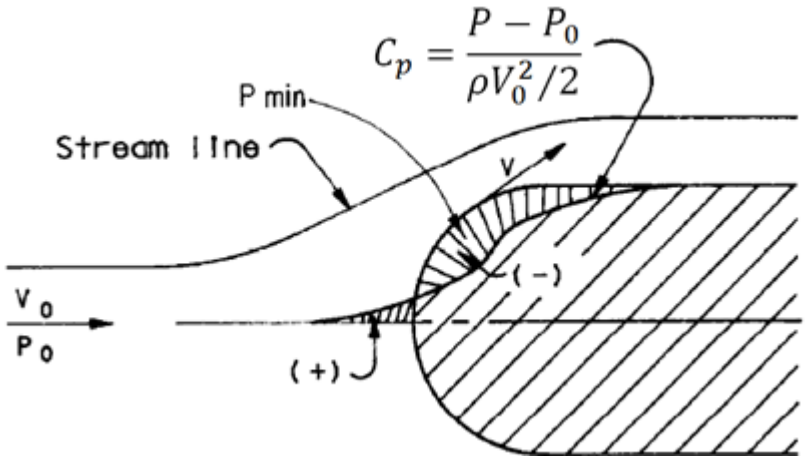

Figure 2.2: Pressure distribution on hemispherical rod (Falvey 1990).

The pressure coefficient is also known as the pressure parameter or Euler number.

The value of the Euler number, at any point on a body, is a constant as long as the minimum pressure on the body is greater than the vapor pressure of water. For example, on Figure 2.2, the pressure at any point on a rod-having a hemispherical end-is predictable in terms of the upstream conditions. However, if the pressure at the location that corresponds to the minimum Euler number drops to vapor pressure, then the pressure at that point will not decrease any further. The upstream conditions that correspond to the onset of cavitation can be calculated by replacing the boundary pressure in Equation 2.2 with vapor pressure and setting the value of the ratio equal to the minimum Euler number. The resulting parameter is known as the cavitation index, σ.

$$\sigma = \frac{E_0 - Z\rho g - P_v}{\rho V_0^2/2} = -(C_p)_{min} \quad \textbf{(2.3)}$$

If elevation Z and Z_0 are equal, the cavitation index is expressed as:

$$\sigma = \frac{P_0 - P_v}{\rho V_0^2/2} = -(C_p)_{min} \quad \textbf{(2.4)}$$

Where P_v is the vapor pressure of water.

For smooth streamlined bodies, the most negative pressure occurs on the boundary. For these cases, the cavitation index can be estimated from pressure measurements made on the surface. However, if the body is not streamlined, the flow will separate from the body and the most negative pressures will occur within the flow. In these cases, the cavitation index will be less than the absolute value of the minimum Euler number on the body.

To avoid ambiguities, both vapor pressure and reference pressure are referenced to absolute zero pressure as shown on Figure 2.3. For example, in absolute units, the reference pressure is given by:

$$P_0 = P_a + P_g \quad \textbf{(2.5)}$$

In the literature, sometimes one notes a reference to a reduced or vacuum pressure. This is done to avoid expressing the gauge pressure as a negative number when the reference pressure is less than the atmospheric pressure. When using values of the vacuum pressure, the appropriate relationship for the reference pressure, P_0 , is given by:

$$P_0 = P_a - P_r \quad \textbf{(2.6)}$$

Where:

P_0 = atmospheric pressure

P_g = gauge pressure

P_r = reduced pressure (vacuum)

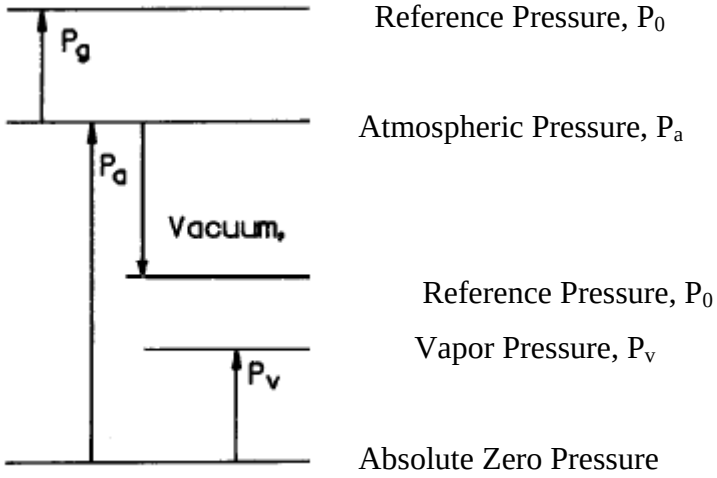

Figure 2.3: Definition of pressure scales.

For example, the cavitation index can be calculated for the following conditions by using Equations 2.4 and 2.5:

$T_c = 10^{\circ}C$ V = 30 m/s

P_v = 1.23 kPa P_g = 9.8 kPa (1.0 m water column)

P_a = 101.0 kPa ρ = 999.7 kg/m^3

$$\sigma = \frac{(101 + 9.8 - 1.23) \times 10^3}{999.7\ [(\frac{30)^2}{2}]} = 0.244$$

Table 2.2 provides values of density, vapor pressure, and viscosity of water as a Function of temperature.

Table 2.2: Properties of pure water (Falvey, 1990)

Temperature℃	Density Kg/m^3	Vapor Pressure KPa	Kinematic viscosity m^2/s×10^4
0	999.868	0.61	1.787
5	999.992	0.87	1.519
10	999.726	1.23	1.307
15	999.125	1.70	1.140
20	998.228	2.33	1.004
25	997.069	3.16	0.893
30	995.671	4.23	0.801
35	994.055	5.62	0.724
40	992.238	7.38	0.658
45	990.233	9.58	0.602
50	988.052	12.3	0.553
60	983.20	19.9	0.475
70	977.77	31.1	0.413
80	971.80	47.3	0.365
90	965.31	70.1	0.326
100	958.36	101.3	0.294

In practical situations, flow conditions are not as ideal as those shown on Figure 2.2. For instance, for a bluff body within a boundary layer, the definition of the cavitation index depends upon the reference location as shown on Figure 2.4. In this case, three different reference locations are noted; the three locations and corresponding cavitation indexes are:

1. Far upstream and outside of the effects of the boundary layer;

$$\sigma_u = \frac{P_u - P_v}{\rho V_u^2/2} \qquad \textbf{(2.7)}$$

2. Immediately upstream of an offset and at the maximum height of the offset;

$$\sigma_h = \frac{P_h - P_v}{\rho V_h^2/2} \quad \textbf{(2.8)}$$

3. Outside of the boundary layer and in the plane of the offset;

$$\sigma_b = \frac{P_h - P_v}{\rho V_b^2/2} \quad \textbf{(2.9)}$$

Where:

P_h = Pressure in free stream in plane of offset

P_u = pressure in free stream upstream of beginning of boundary layer

P_v = vapor pressure of water

V_b = free stream velocity in plane of offset

V_h = velocity at height of offset

V_u = free stream velocity upstream of beginning of boundary layer

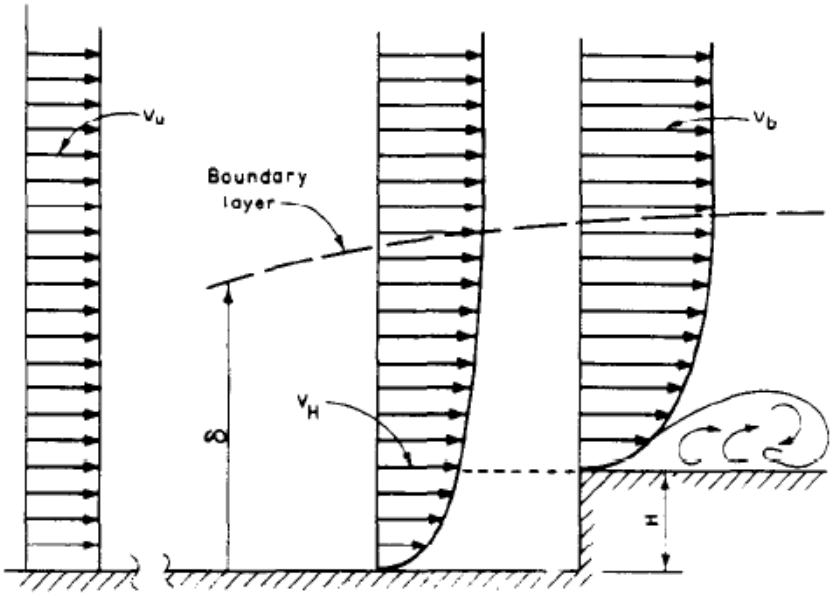

Figure 2.4: Reference Velocity definitions (Falvey, 1990).

For shear flows, several forms of the cavitation parameter have been proposed. Each is based upon easily measurable reference conditions. For example, the cavitation index for a submerged jet, σ_j, is given by:

$$\sigma_j = \frac{P_e - P_v}{\rho V_e^2/2} \quad \textbf{(2.10)}$$

Where:

P_e = Pressure in core of jet

V_e = Velocity in core of jet

Although one parameter such as the cavitation index-in whatever form it is expressed-cannot describe many of the complexities of cavitation, it is an extremely useful parameter to indicate the state of cavitation in a hydraulic structure. For example, for flow past a sudden into-the-flow offset, cavitation will not occur if the cavitation index (defined by Equation 2.7) is greater than about 1.8 as noted on Figure 2.5. As the cavitation index decreases below 1.8, more and more cavitation bubbles form within the flow. To the naked eye, the cavitation appears to be a fuzzy white cloud. However, a flash photograph reveals that the cloud consists of individual bubbles. For even lower values of the cavitation index, the cloud suddenly forms one long supercavitating pocket (Falvey, 1990).

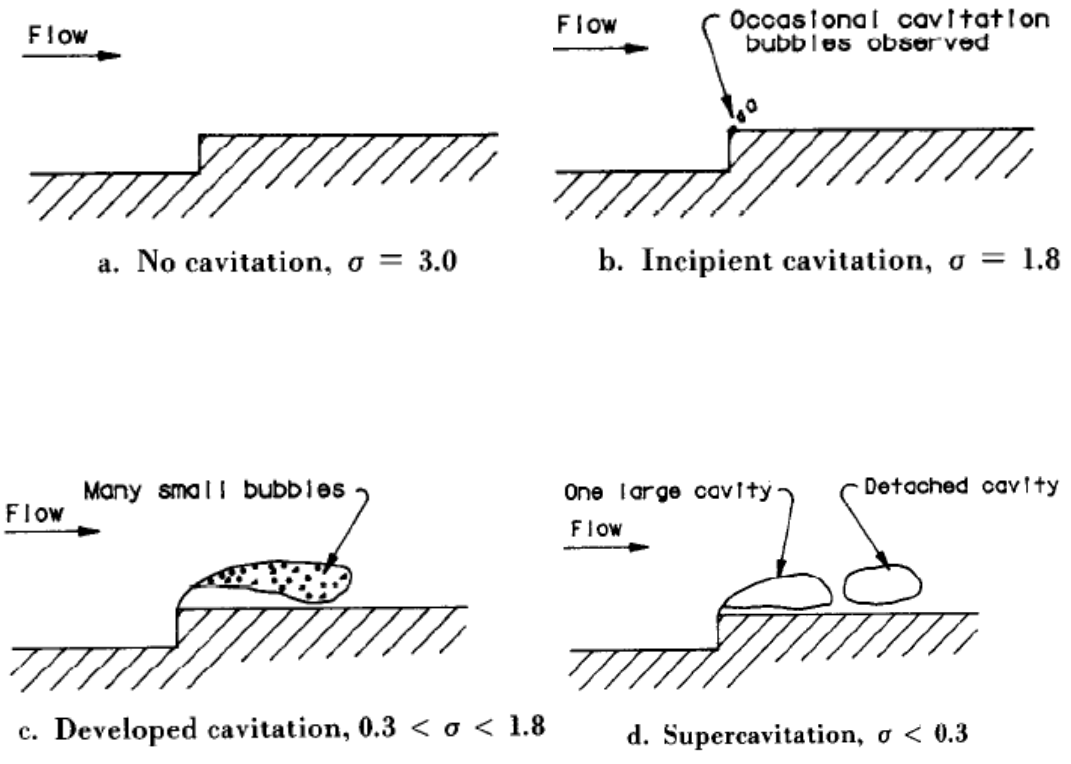

a. No cavitation, $\sigma = 3.0$

b. Incipient cavitation, $\sigma = 1.8$

c. Developed cavitation, $0.3 < \sigma < 1.8$

d. Supercavitation, $\sigma < 0.3$

Figure 2.5: Cavitation development (Falvey, 1990).

3.CAVITATION IN HYDRAULIC STRUCTURES

3.1.Occurrence of Cavitation Phenomena in Hydraulic Structures

In most hydraulic structures the ambient pressure is close to atmospheric, so cavitation is normally associated with flows of high velocity. Cavitation problems can arise when the velocity reaches about 15m/s, and above 25m/s serious damage can be expected if adequate precautions are not taken.

If a flow remains attached to a bounding surface, cavitation-producing pressures are normally the result of turbulent velocity fluctuations in the boundary layer and/or of flow curvature. The point of minimum pressure on a surface can be measured or can sometimes be calculated theoretically from potential theory, with if necessary a suitable allowance for displacement thickness of the boundary layer.

However, turbulent fluctuations may cause cavitation to occur sooner than predicted, while the position at which it starts may be downstream of the point of minimum pressure (due for example to the formation of a laminar separation bubble). If a pressure transducer, mounted at a suitable point on the boundary, indicates transient values close to vapor pressure, the cavitation is likely to occur. Damage will normally take place to the spot at which the cavities are generated.

If a flow separates from a surface, cavities will form first in the fast-rotating eddies that are shed downstream. The pressure in the eddies will be lower than at the point of separation, so surface –mounted transducers will not provide a good indication of the likelihood of cavitation. The cavities will be swept downstream and will collapse when they enter a region of high pressure (May, 1987).

3.1.1. Typical situations favorable to cavitation

- Wall geometry may give rise to sharp local velocity increases and resulting pressure drops within a globally steady flow. This happens in the case of a restriction in the cross-sectional area of liquid ducts (Venturi nozzles), or due

to curvature imposed on flow streamlines by the local geometry (bends in pipe flow, upper sides of blades in propellers and pumps).

- Cavitation can also occur in shear flows due to large turbulent pressure fluctuations Damage caused by shear flows can therefore occur a considerable distance downstream of the point of separation. This type of cavitation can be produced by local irregularities in the boundary (e.g. sharp steps at joints) or by the overall geometry of the structure. Examples of the latter include horizontal shear flows generated by high-velocity submerged jets, or vertical shear flows created by a sudden increase in channel width (e.g. two or more control gates discharging to a single tunnel).
- The basic unsteady nature of some flows (e.g. water hammer in hydraulic control circuits or ducts of hydraulic power plants, or in the fuel feed lines of Diesel engines) can result in strong fluid acceleration and consequently in the instantaneous production of low pressures at some points in the flow leading to cavitation.
- The local roughness of the walls (e.g. the concrete walls of dam spillways) produces local wakes in which small attached cavities may develop.
- As a consequence of the vibratory motion of the walls (e.g. liquid cooling of Diesel engines, standard A.S.T.M.E. erosion device) oscillating pressure fields are created and superimposed on an otherwise uniform pressure field. If the oscillation amplitude is large enough, cavitation can appear when the negative oscillation occurs.
- Finally, attention has to be drawn to the case of solid bodies that are suddenly accelerated by a shock in a quiescent liquid, particularly if they have sharp edges. The liquid acceleration needed to get round these edges produces low pressures even if the velocities are relatively small immediately after the shock (Pierre Franc and Marine Michel, 2004).

Structures where damage has been reported include:

1. Open-Channel spillways
2. Bottom outlets in dams
3. High-Head gates and gate slots
4. Energy dissipaters including hydraulic-jump stilling basin.

In next parts we will mention cavitation in Tunnels and Energy dissipaters.

3.2. The Main Effects of Cavitation in Hydraulic Structures

If a hydraulic system is designed to operate with a homogeneous liquid, additional vapor structures due to cavitation can be interpreted, by analogy with the case of mechanical systems, as mechanical clearances. The vapor structures are often unstable, and when they reach a region of increased pressure, they often violently collapse since the internal pressure hardly varies and remains close to the vapor pressure. The collapse can be considered analogous to shocks in mechanical systems by which clearances between neighboring pieces disappear. Following this, a number of consequences can be expected:

— Alteration of the performance of the system (reduction in lift and increase in drag of a foil, fall in turbo machinery efficiency, reduced capacity to evacuate water in spillways, energy dissipation, etc.);

— The appearance of additional forces on the solid structures;

— Production of noise and vibrations;

— wall erosion, in the case of developed cavitation if the velocity difference between the liquid and the solid wall is high enough.

Thus, at first glance, cavitation appears as a harmful phenomenon that must be avoided. In many cases, the free cavitation condition is the most severe condition with which the designer is faced. To avoid the excessive financial charges that would be associated with this, a certain degree of cavitation development may be allowed. Of course, this can be done only if the effects of developed cavitation are controlled. The negative effects of cavitation are often stressed (Pierre Franc and Marine Michel, 2004).

3.3. Significant Causes of Flow and Structure Profile Parameters on Happening a Cavitation

Categories of Surface Roughness

Upon examining the flow surface of a hydraulic structure, the flow surface irregularities & or the surface roughness can be characterized usually as belonging to one of two main categories (1) singular (isolated) roughnesses or (2) uniformly distributed roughnesses. Singular roughnesses are irregularities in a surface that are

large relative to the surface irregularities from where they protrude. A uniformly distributed roughness is a surface texture that does not contain singular roughnesses.

Sometimes, singular roughnesses are referred to as local asperities. Typical examples of these in hydraulic structures include:

1. offset into-the flow, Fig 3.la;
2. offset away-from the flow, Fig 3.lb, c, d;
3. Voids or grooves, Fig 3.le; and
4. Protruding joints Fig 3.lg.

In all these cases, cavitation is formed by turbulence in the shear zone; the action is produced by the sudden change in flow direction at the irregularity. The location of the shear zone can be predicted from the shape of the roughness.

Depending upon the shape of the roughness, cavitation bubbles will collapse either within the flow or near the flow boundary.

Figure 3.lf depicts cavitation above a distributed roughness. Cavitation occurs within the flow because of turbulence generated by the roughness of the boundary. The cavitation location is not predictable; however, cavitation always occurs within the body of the flow for distributed roughnesses (Falvey, 1990).

The principal method of predicting whether a surface irregularity will cause cavitation in a prototype structure is to calculate the cavitation number σ of the flow from Equation (2.4), and compare it with previously determined values of the incipient cavitation index σ_i for that type of irregularity; cavitation will occur if $\sigma < \sigma_i$.

Values of σ_i have been obtained for many types of irregularity, some of which are shown above. The methods of determining σ_i include:

1. Theoretical predictions of the minimum pressure on the surface of the irregularity;
2. Laboratory measurements of the minimum pressure on the surface of the irregularity;
3. Laboratory observations of cavity formation using cavitation tunnels (no free surface) or vacuum test rigs (with free surface);

4. Field measurements of surface pressure or cavitation damage at irregularities.

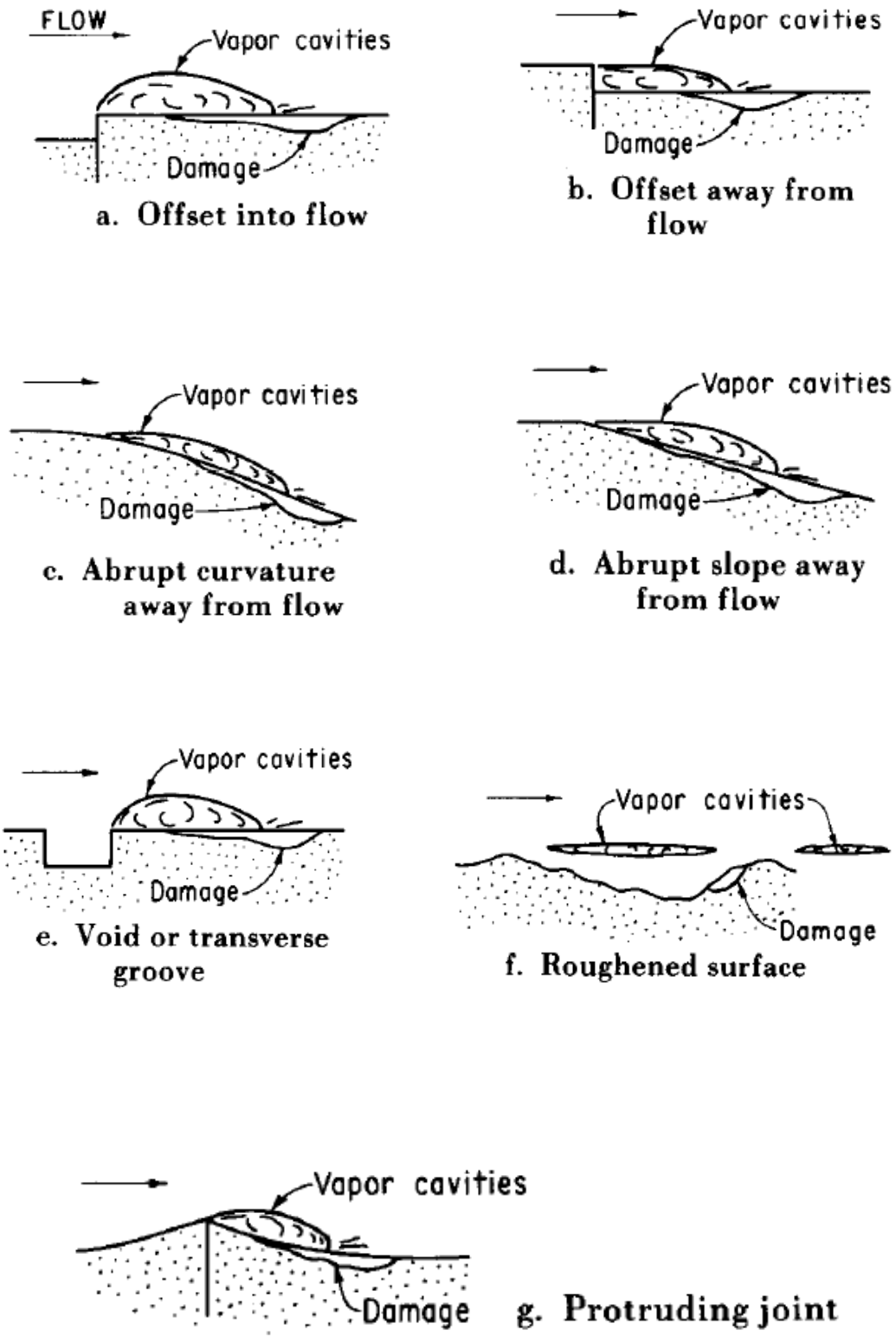

Figure 3.1: Typical isolated roughness elements found in hydraulic structures (Falvey, 1990).

Results based on field studies are the most appropriate, but very few are available because of the difficulties of carrying out controlled tests. If the flow separates at an irregularity, the lowest pressures will occur in eddies within the fluid; values of σ_i determined from measured or predicted surface pressures may thus be under-estimated. Data from cavitation tunnels and vacuum test rigs, backed up by field measurements, should therefore be used where possible.

In general, most of the experimental results for a given type of irregularity are in reasonable agreement. Discrepancies between tests do exist, but they are normally fairly small in comparison with the effects produced by minor changes in shape (e.g. rounded edges instead of sharp edges). Moreover, irregularities due to construction faults in spillways and tunnels have three-dimensional shapes which will seldom match precisely those tested in the laboratory.

Movement of concrete formwork is the most common cause of irregularities, and can give rise to abrupt offsets and chamfers (both into and away from the flow), sudden changes in slope, cusped joints, and undulations (see types a, b, c, d, e, f, g in Figure 3.1). Of these, abrupt offsets into the flow (Type a) have the greatest cavitation potential, and a suitable formula for calculating the σ_i value is that due to (Liu, 1983),

$$\sigma_i = 1.02h^{0.326} \ , \ h \leq 15mm \qquad \textbf{(3.1)}$$

Where h is the height of the step in mm.

If the edge of the offset is rounded to a radius of r=0.5h, the value of σ_i is reduced to 86% of that given by Equation (3.1).

Figure 3.2: Abrupt offsets into the flow

When calculating the cavitation number σ of the flow from equation 2.4, the values of velocity V_0 and absolute static pressure P_0 should be those at the level of the top of the offset; Surface irregularities just downstream of high-head gates are particularly liable to cause cavitation because the boundary layers are very thin, and do not protect the irregularities from the high free-stream velocities.

The cavitation potential of construction faults can be reduced by grinding them to form chamfers (May, 1987).

Data for chamfers angled away from the flow (Type c, d on Fig 3.1) are limited, and may not be comparable because of different definitions of the characteristic velocity (e.g. near the bed, or depth-averaged). Laboratory studies indicate that the values of σ_i tend to be higher than for into-flow chamfers of equal slope.

As the flow velocity is increased, the standards of surface finish required to prevent cavitation eventually become impracticable, particularly in cases where a convex surface reduces the static pressure, or the boundary layers are not fully developed. Some references suggest that use of the parameter σ_i for cavitation inception is not appropriate in design, because damage does not occur until the cavitation index σ of the flow falls below σ_i. Wang & Chou (1979) proposed that the design criterion should be $\sigma \geq 0.8\,\sigma_i$. Field tests at Bratsk Dam (USSR) reported by Galpertin et al (1977) and Oskolkov & Semenkov (1979) provided values of the index σ_i for incipient damage at chamfers angled into and away from the flow.

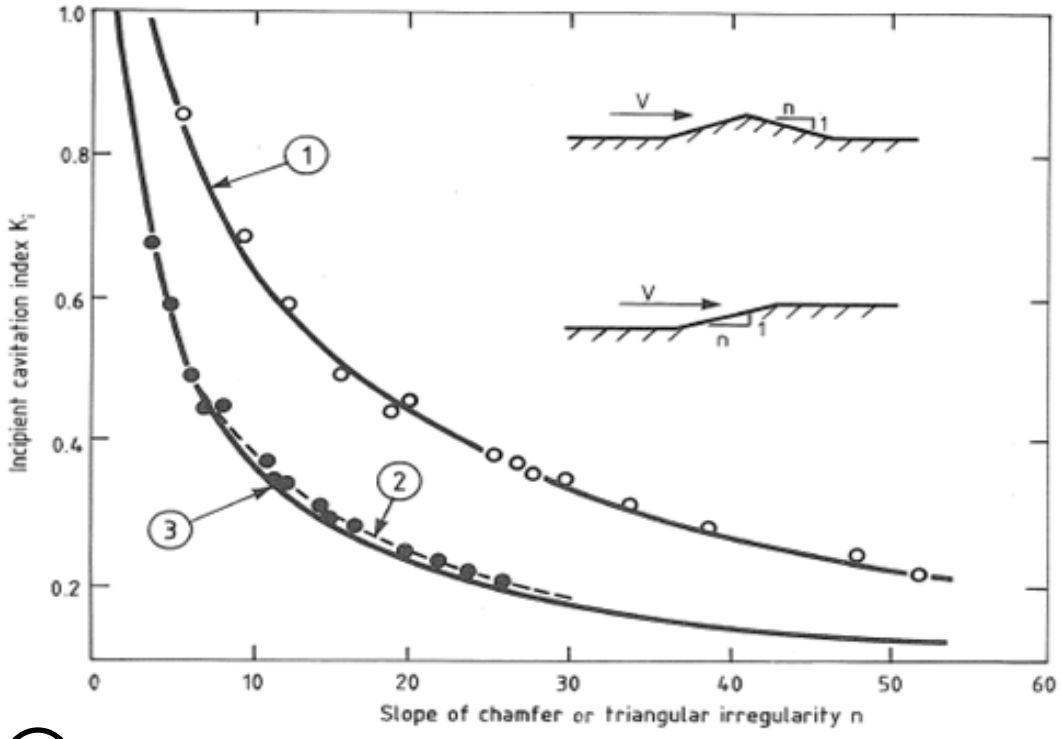

1 Triangular irregularity

2 Into-flow Chamfer

3 Into-flow chamfer (Ball's Data)

Figure 3.3: Values of σ_i for surface irregularities (Wang & Chou, 1979).

The results are presented in Figure 3.4, and indicate that chamfers away from the flow have slightly higher values of σ_i than chamfers projecting into the flow.

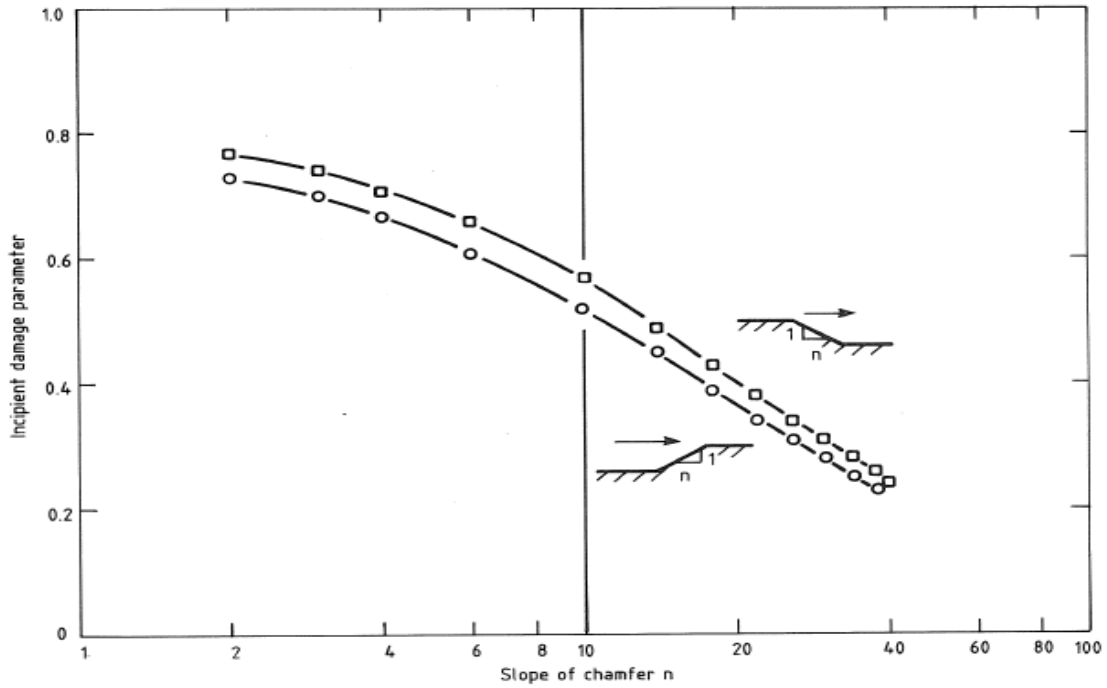

Figure 3.4: Values of σ_i for surface irregularities (Oskolkov & Semenkov, 1979)

Another factor to be considered in design is the likely duration of the cavitation attack; as the cavitation number σ of the flow decreases, the safe operating time is reduced. Falvey (1983) used field data to produce Figure 3.5, which shows a relationship between the value of cavitation parameter, its duration and the amount of cavitation damage.

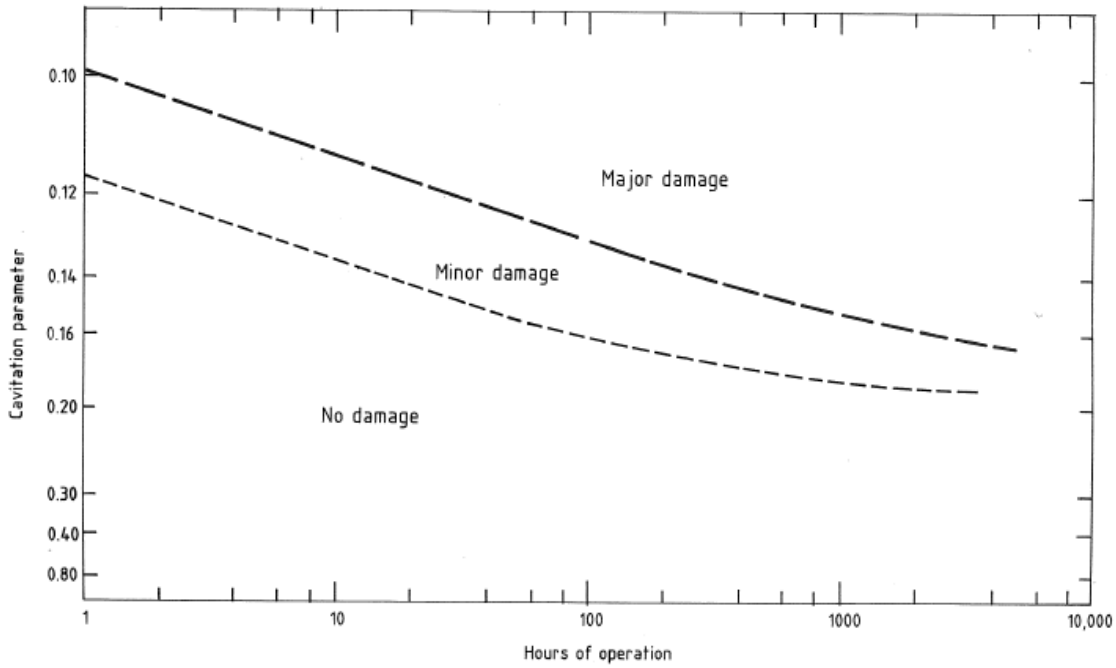

Figure 3.5: Cavitation damage curve (Falvey, 1983)

When the geometry of flow boundaries causes streamlines to curve or converge, the pressure will drop in the direction toward the center of curvature or in the direction along the converging streamlines. For example, Fig. 3.6 shows a tunnel contraction in which a cloud of cavities could start to form at Point c and then collapse at Point d. The velocity near Point c is much higher than the average velocity in the tunnel upstream, and the streamlines near Point c are curved. Thus, for proper values of flow rate and tunnel pressure at 0, the local pressure near Point c will drop to the vapor pressure of water and cavities will occur.

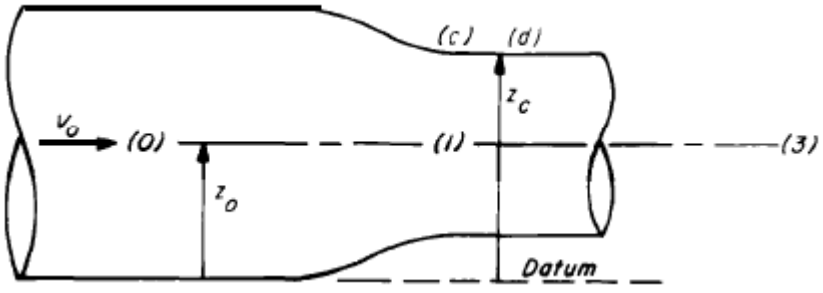

Figure 3.6: Tunnel Contraction

3.4. Happening of Cavitation in Tunnels and Gates

Cavitation can be a potentially serious problem in intermediate and low-level outlets in dams, and may occur at inlets to tunnels, at high-head gates, and in tunnels downstream of gates.

Convergence and curvature of the flow entering a tunnel can produce sub-atmospheric pressures, which together with the effect of turbulent fluctuations may be low enough to cause cavitation. If the flow separates in an inlet, these methods will under-estimate the likelihood of cavitation, because the lowest pressures will not occur at the boundaries but within the fluid. Separation may be caused by a poorly-designed transition, by a notch or slot, or by a secondary flow issuing from a connecting shaft.

The supporters and lifting mechanisms for vertical leaf gates are normally located on the downstream side of the gate, and are accommodated in slots in the side walls so as to protect them from high velocity flow. Such slots have often been a cause of cavitation damage. High velocity flow past a rectangular slot (Figure 3.7) may produce cavitation in three ways:

1. Flow separation at the upstream corner, with cavities being generated in the free shear layer and carried downstream by the flow;
2. Flow separation at the downstream corner, with cavities collapsing where the flow re-attaches to the wall of the tunnel;
3. Vortex formation within the slot, with possible damage to the sides and the gate supports (May, 1987).

The relative importance of these sources various with the aspect ratio of the slot, and may be altered by the use of offsets and transitions.

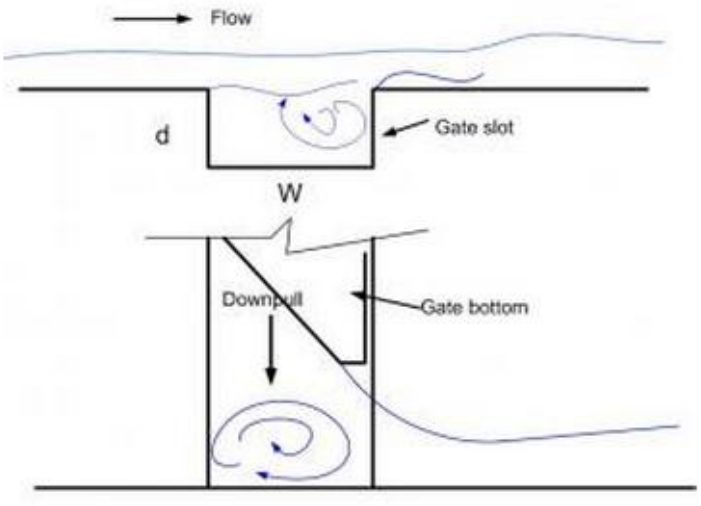

Figure 3.7: Flow around rectangular slot.

Many studies have been made of two-dimensional flow past various shapes of slot, some of which are shown in Figure 3.8. The tests correspond approximately to the conditions which exist when a gate is fully open and the slot is not occupied by the lifting mechanism. Some studies have compared different shapes of slot on the basis of pressure measurements around the boundaries. However, studies carried out in cavitation tunnels are more useful and reliable, because the conditions for cavitation inception can be measured directly.

There is general agreement between studies about which types of gate slot have the lowest cavitation potential. A plan rectangular slot (Type 1A in Figure 3.8) is satisfactory for low heads, but Jin et al (1980) recommend that the length/ depth ratio should be kept in the range $1.4 \leq L/h \leq 2.5$, and if possible between $1.6 \leq L/h \leq 1.8$ for the best performance.

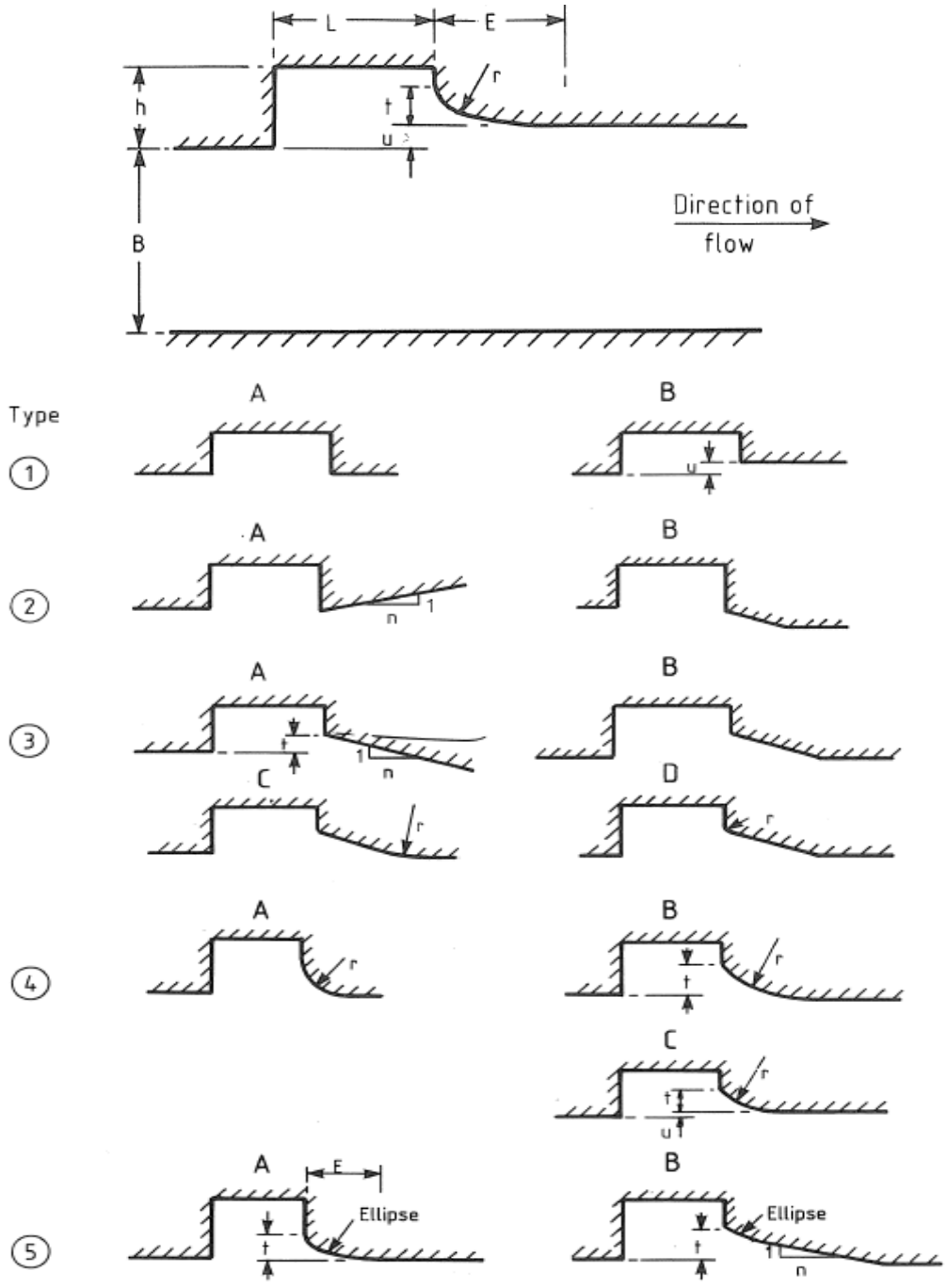

Figure 3.8: Types of Gate Slots

Strong vortex action occurs if L/h < 1.2, and cavitation due to flow separation becomes serious if L /h > 2.5. Offsetting the wall downstream of the slot (as in Type 1B in Fig 3.8) is, by itself, not effective; the offset reduces the risk of cavitation at the downstream corner of the slot, but increases it at the upstream one. The designs which were found to have the lowest cavitation potential were slots with an offset ($t/h \approx 0.2$) and either a radiused transition (Type 4B, $100 < r/t < 250$) or an elliptical transition (Type 5A, E/t =5).

Separate values of σ_i are calculated for the upstream and downstream corners of the slot, and take account of the width of the conduit, the aspect ratio of the slot, the amount of any downstream offset, and the relative thickness of the boundary layer.

In the presence of a gate rail can alter the flow conditions at the downstream corner. If a gate rail projects into the slot, the notch between the edge of the rail and the downstream face of the slot should be faired in order to prevent flow separation.

When a leaf gate is partially open, the flow past the slot becomes three-dimensional, and is influenced by the shape and proximity of the gate. The incipient cavitation number σ_i of a gate is higher if it is submerged on the downstream side than if it discharges freely. Above the level of the gate lip, the lifting mechanism should, if possible, fully occupy the slot. If it does not, downward flow develops in the slot; this increases the value of σ_i, and can result in additional cavitation damage on the wall near the floor of the tunnel.

Gate lips should be designed to produce a clean flow separation without re-attachment. A lip with a smooth upstream profile produces less intense separation under submerged conditions, and reduces the risk of cavities forming in the horizontal shear layer between the high-velocity jet and the water above it. Cavitation in such shear layers can cause serious damage along walls downstream of partially-open gates.

Radial gates with attached seals have the advantage of not requiring slots. Under submerged conditions, cavitation occurs along the bottom edge of the gate, and is particularly intense at the side walls.

Alternatively, radial gates may close against recessed seals mounted in offsets in the walls and floor of the tunnel. The values of σ_i for the offsets are similar to those for the upstream corners of gate slots.

High-velocity flow through small gaps and at gate seals can lead to cavitation damage. Seals should have smooth profiles in order to prevent flow separation. Gaps of more than 2mm can result in serious erosion, and the seals may themselves be damaged by vibrations induced by unstable cavity formation (May, 1987).

3.5. Energy Dissipaters

Most types of energy dissipater produce large amounts of flow turbulence. Cavitation will occur if the velocity fluctuations are large enough to cause the static pressure to fall occasionally to the vapor pressure of the water.

Laboratory and prototype measurements of pressures beneath hydraulic jumps indicate that the maximum root mean-square (rms) values of the fluctuations are typically between 3% and 9% of the velocity head entering the jump. Using a sill to produce a forced jump shortens the distance over which the energy dissipation occurs, and tends, as might be expected, to increase the magnitude of the rms fluctuations on the floor of the basin. Flow separation behind baffle blocks and chute blocks can produce much larger variations in pressure; for example, Lopardo et al (1982) measured rms fluctuations on the rear face of a chute block equal to 27% of the upstream velocity head.

Near the toe of a jump, the positive pressure fluctuations tend to be larger than the negative ones, but further downstream the departures from the mean become more symmetrical and conform approximately to a Gaussian probability distribution. However, in zones of flow separation, the negative fluctuations may become bigger than the positive ones. Thus, for a given rms level of turbulence, cavitation is more likely behind a sill or baffle block than on a level floor.

Lopardo et al (1985) compared model and prototype data, and suggested that cavitation may occur if the pressure falls to vapor pressure for more than 0.1% of the time. This limit can be used to obtain a very approximate guide as to when cavitation might be expected to develop on the floor of a stilling basin. Assuming an rms pressure fluctuation of 9% of the upstream velocity head, a Gaussian distribution, and a mean absolute pressure of 13m head of water, leads to a limiting velocity of about 30m/s. For stills and baffle blocks, a higher turbulence level of 27% would indicate that cavitation might occur at velocities above about 17m/s. As explained above, all these assumptions are affected by changes in the flow conditions and the configuration of the basin, so each case needs to be assessed individually.

Chute blocks and baffle blocks are the features most vulnerable to cavitation damage in hydraulic jump basins, because they are subject to the highest velocities and produce the largest pressure fluctuations. Thus, although they allow the use of

shorter basins, they are often omitted in high-head installations. To be effective, blocks need to have high drag coefficients (C_d), but this also results in high values of the cavitation inception parameter $K_{i;}$ rounding the corners reduces K_i but also C_d. Shapes of baffle blocks investigated by Oskolkov & Semenkov (1979) and by Rozanova & Ariel (1983) are shown in Figure 3.9. Cavitation damage can be reduced or avoided by using a super-cavitating design which causes the flow to separate at the upstream face and form a large fixed cavity that encloses the block; damage is avoided by removing the solid surfaces from the region in which the individual cavity bubbles collapse. This can be achieved by sloping the sides of the block away from the flow in the downstream direction and by introducing a step in the floor (see, for example, Type 1 in Figure 3.9).

Prototype study:

The Bureau of Reclamation and the US Army Corps of Engineers have joined together to build a new Auxiliary Spillway on Folsom Dam to comply with dam safety requirements and reduce the flood risk in Sacramento. Folsom Dam is located on the American River approximately 32 km (20 miles) northeast of Sacramento California. The Auxiliary Spillway consists of six submerged tainter gates, each 7 m (23 ft) wide by 10 m (33 ft) high, with a maximum discharge greater than 8,495m^3/s.

Baffle blocks designed for a unique stilling basin have been tested in Reclamation's Low Ambient Pressure Chamber (LAPC) to evaluate their cavitation potential and to compare modified block designs for possible prototype use. Standard block designs have long been known to be susceptible to cavitation damage and are not recommended for designs where the baffle blocks are exposed to velocities of 15m/s (50 ft/s) and above without realization that cavitation and resulting damage will occur.

A sectional model was constructed in Reclamation's LAPC to evaluate the cavitation potential of several different baffle block configurations. A closed conduit section included a full block with two half-blocks. The water tunnel could be exposed to a reduced ambient pressure by applying up to 74 kPa (10.7 lb/in^2) vacuum. Velocities up to 6 m/s (19.7 ft/s) were possible. Instrumentation allowed for relative comparisons of forces on the center baffle block, detection of cavitation inception, and some evidence of the type of cavitation present.

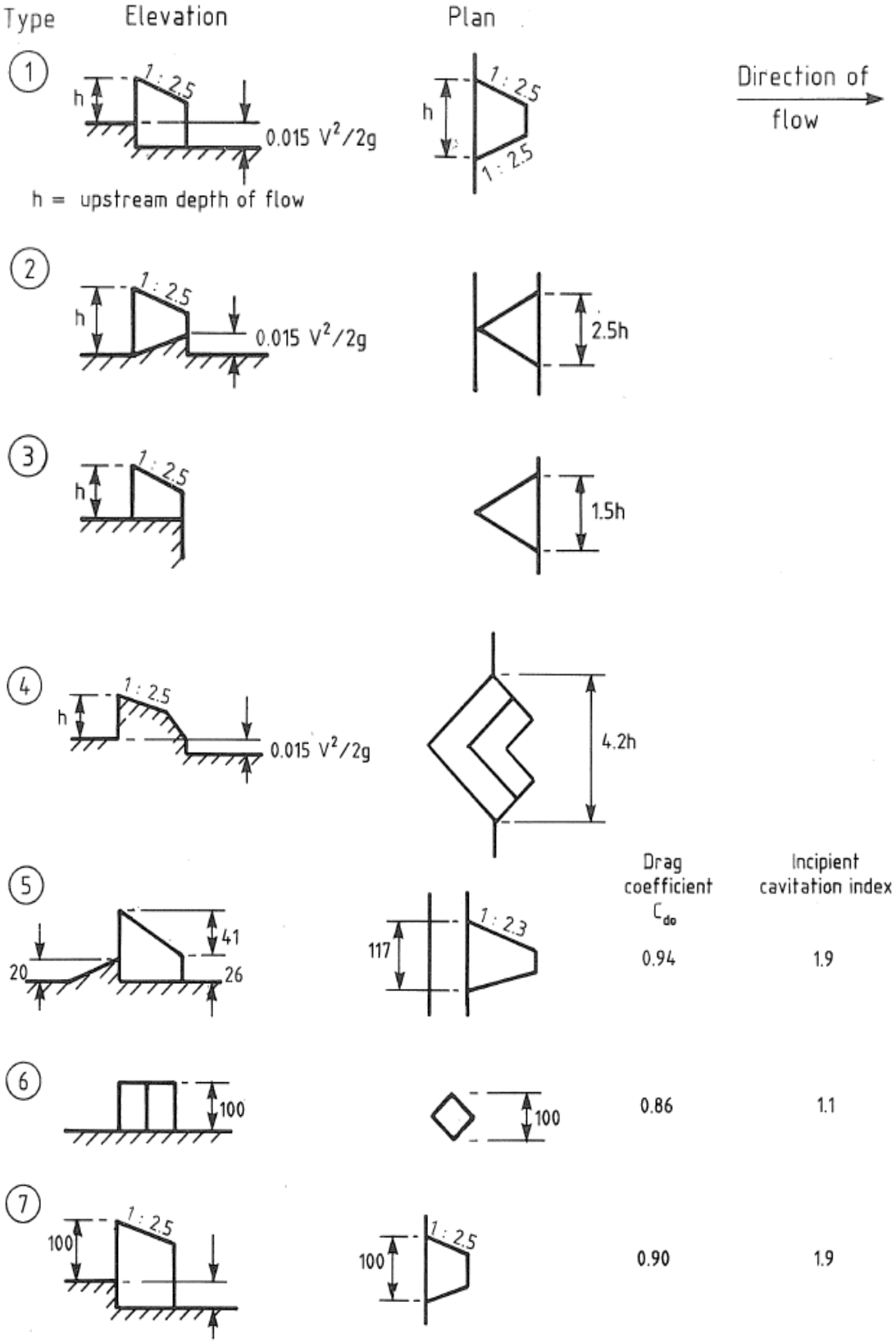

Figure 3.9: Types of baffle block

Visual observations of cavitation were performed with the aid of a high-speed video camera. Three configurations were tested, the standard "original" baffle block design, the original block with a 1V: 3H ramp upstream from the blocks, and a modified block shape with various ramp combinations. Elimination of cavitation is not possible under the flow conditions that are present, so creating supercavitation or the formation of a large vapor cavity that envelope the entire baffle block is desired in order to prevent typical damage that would occur with the standard block shape. Baffle blocks with the addition of the upstream ramp were able to achieve supercaviting conditions at much lower velocities and this condition was much more stable than the blocks without ramps.

Schematic views of the block and ramp configurations tested appear in Figure 3.10.a to 3.10.e.

These views show the central full block with a half-width block on either side.

The original block design did show substantial cavitation potential. As with all the blocks, the first sign of cavitation takes the form of a horseshoe vortex out in front of the blocks, near the floor, Figure 3.11. This vortex is formed by the interaction of the streamlines due to the stagnation at the block face and the floor intersection.

This vortex occurred for all block/ramp combinations that were tested. The ramp location preceding the block caused the horseshoe vortex to be slightly closer to the ramp surface due to the change in pressure gradient over the flat floor approach.

High-speed video allowed the observation of attached vortices at the downstream corners of the blocks, Figure 3.12. These vortices were formed in the shear layer of the block but attached to the floor and remained attached until dissipation or implosion. This location is typical of where damage at previous locations with similar designs has occurred. These vortices intensified in strength with lowering of the cavitation parameter. In addition, this shape would not pass into a supercavitating regime within the operating range of the facility. Addition of the ramp to the original block reduced the intensity and consistency of the floor attached vortices, however it transferred the attachment point up onto the down sloping edge of the block itself, still creating the potential to severely damage the baffle blocks during operation. On a positive note, the ramp prompted supercavition at the design condition (Frizell and Cox, 2009).

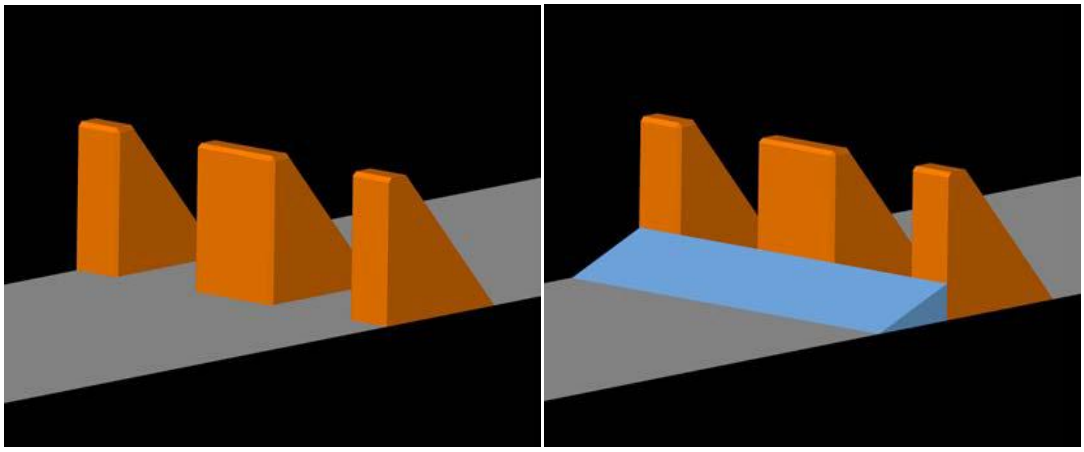

a.) Original block design. b.) 1V:3H ramp (1.22-m-high (4-ft-high))

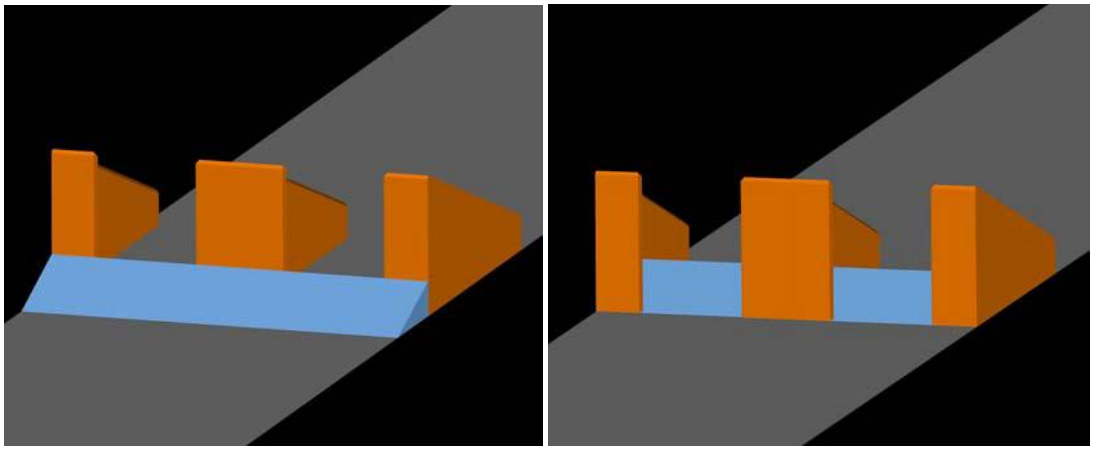

c.) tapered block with ramp preceding d.) Tapered block with 1V:3H ramp inside

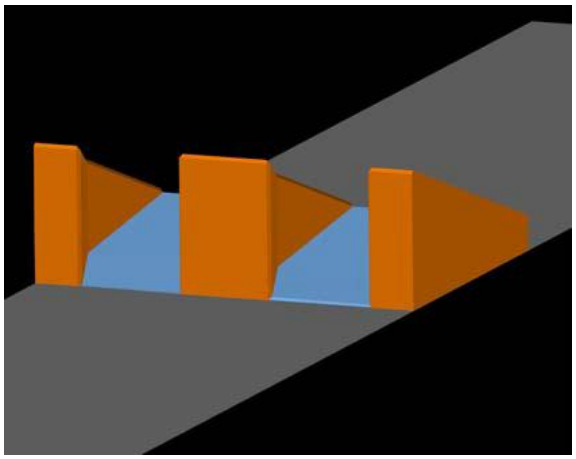

e.) tapered block with 1V:9H ramp between

Figure 3.10: Block/ramp combinations testing in the LAPC (Frizell and Cox, 2009).

Figure3.11: Horseshoe vortex upstream from baffle block face (Frizell & Cox, 2009)

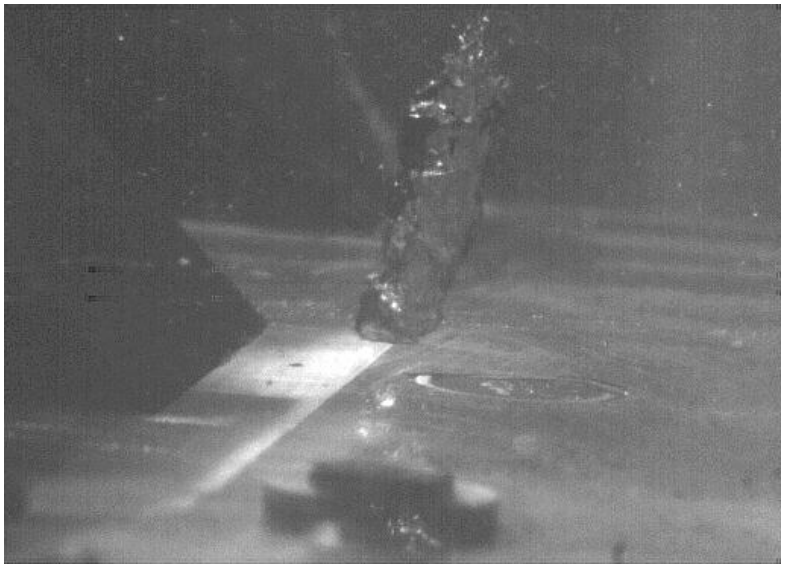

Figure 3.12: Floor attached vortex at downstream corner of baffle blocks (Frizell & Cox, 2009).

Testing of the new tapered block design was accomplished in three steps, each with a different ramp configuration. The first configuration was with a 1V:3H ramp preceding the block. All ramps had a maximum height of 1.22 m (4 ft). The general flow conditions featured many vertically oriented free stream vortices that traveled downstream from the front edge of the block, Figure 3.13. The floor attached vortices observed with the original design were not present. There was still indication

of vortices that contacted the floor between the blocks even during ventilated supercavitation. Top and side views of this block/ramp combination in a supercavitating condition are shown on Figure 3.14.

Two ramp configurations were tested, the same 1V:3H ramp as previously tested placed between the blocks starting at the front edge, and a 1V:9H ramp that began at the front edge and ended at the rear edge of the blocks. The first ramp showed general improvement but there was still visual evidence of possible vortex collapse on the floor between the blocks. The extension of the ramp to the end of the blocks lessened the occurrence of collapse or possible implosions on the blocks and floor ramp. For the design condition, any chance of damage with this final configuration will be relegated to downstream from the blocks on the floor of the basin.

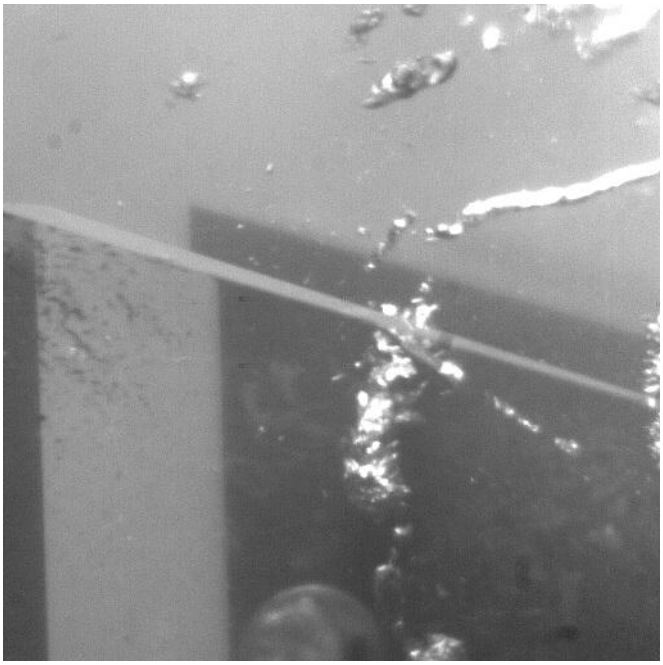

Figure 3.13: Near vertically oriented vortices in the shear layer between blocks (Frizell and Cox, 2009).

Half block against wall in clear acrylic to facilitate viewing between the blocks.

The original goal was to produce a baffle block that would not have cavitation damage during basin operation. The velocities entering the basin for almost all flow conditions are well above any recommended values so to accomplish this; the block must operate within a supercavitating regime with the cavity enveloping the entire block. This was accomplished with the new tapered block design that was tested. Possible collapse of shear layer vortices on the floor between the blocks was

addressed by moving the ramp such that it fills the entire area between the blocks, resembling an “oversized” dentated end-sill. Supercavitation resulted in a very stable condition and should be present at the design condition for the basin. Smaller flows leading up to the transition to supercavitation could possibly result in some minor damage to the floor downstream from the baffle blocks if operated for a long durations (Frizell and Cox, 2009).

a.) Side View

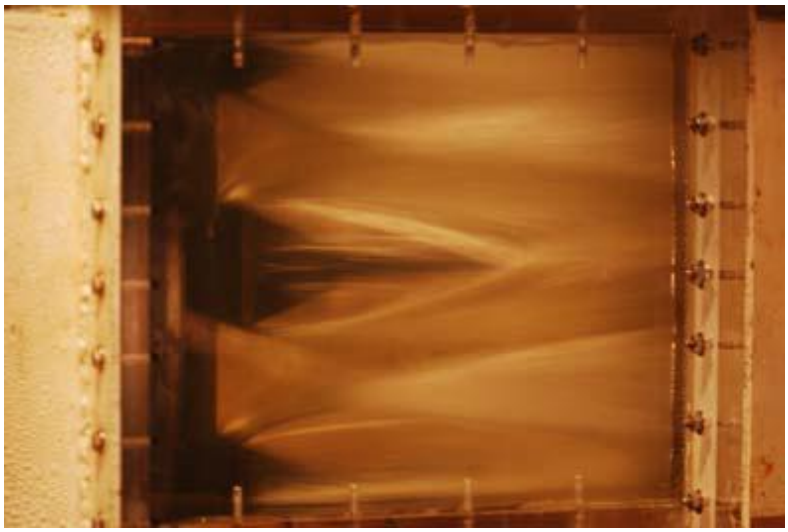

b.) Top View

Figure 3.14: New block with preceding ramp in a supercavitating – ventilated cavity condition (Frizell and Cox, 2009).

Sudden expansions in high-head tunnels can be used to convert kinetic energy to turbulence. Cavities are liable to be formed around the perimeter of the high velocity jet, and can damage the walls of the chamber if they are too close. The performance

of the expansion chamber can be affected by small changes in configuration, and model tests are normally necessary (Frizell and Cox, 2009).

3.6. Cavitation in Siphon Spillways

The discharge over an overflow spillway is a function of the head measured over its crest. Enclosing the crest and making the resulting conduit flow full can substantially increase this effective head. The head on the spillway (as shown in Figure 3.15) is then the difference in elevation between the reservoir surface and the spillway outlet. However, the flow near the crest of the spillway would then be under a negative pressure. In other words, the conduit becomes a siphon. All necessary precautions must be taken to ensure that the vacuum is maintained and that it does not become so excessive as to cause cavitation. The maximum negative pressure at the spillway crest is theoretically 10 m of water at sea level. Allowing for the vapor pressure of water, loss due to turbulence, etc., the maximum net effective head is rarely more than about 7.5 m. This corresponds to a velocity of $\sqrt{2 \times 9.81 \times 7.5} \approx 12$ m/s. This means that the initial velocity in any siphon cannot exceed about 12 m/s at the inlet. The essence of the hydraulic design of siphon spillways, therefore, lies in ensuring maximum discharge capacity without harmful negative pressures.

To have that velocity, we have to restrict the income discharge and for that reason we can change the outlet section, or changing the operating head (Khatsuria, 2005).

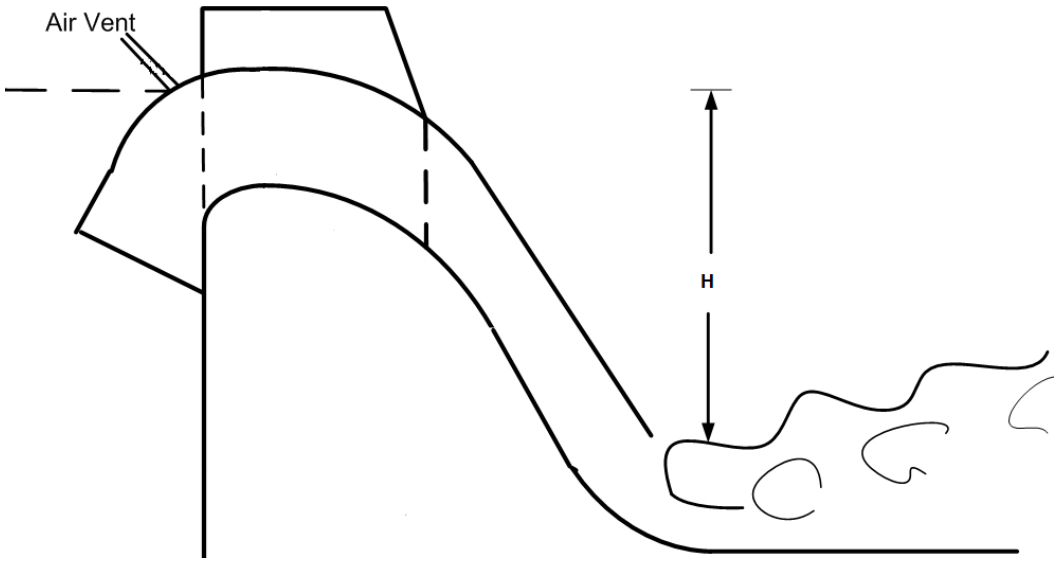

Figure 3.15: Siphon spillway

4. CAVITATION DAMAGES ON HYDRAULIC STRUCTURES

4.1. Definition of Cavitation Damage

Collapse Dynamics:

As we know, growth and decay of bubbles was considered using a theory that assumed water to be incompressible. In addition, the vapor pressure, surface tension, and temperature were all considered to be constant. In reality, as a bubble collapses these assumptions are not valid. To simulate the collapse dynamics it is necessary to consider the compressibility of water, the compressibility of the gas in the bubble, and the enthalpy changes. These considerations result in six differential equations and four algebraic equations that must be solved simultaneously (Knapp et al, 1970).

Numerical solution of the equations reveals that bubble collapse consists of phases in which the bubble diameter decreases, reaches a minimum value, and then grows or rebounds as shown on Figure 4.1. The process is repeated for several cycles with the bubble diameter decreasing during each cycle until it finally becomes microscopic.

During the reversal or rebound phase, a shock wave forms. The shock wave velocity-as it radiates outward from the center of collapse-is equal to the speed of sound in water. Assuming that water is incompressible, Hickling and Plesset (1964) found that the shock wave intensity varies inversely with the distance from the collapse center. At a distance of two times the initial bubble radius from the collapse center, the pressure intensity is about 200 times the ambient pressure at the collapse site. The following example illustrates a method of estimating the collapse pressure.

Assume a bubble diameter of 0.1 millimeter and a flow depth of 2.0 meters, then

Water pressure = 2.0 m (999 kg/m^3) 9.8 m/s^2 =19580 Pa

Ambient pressure = water pressure + barometric pressure

= 19.58 kPa + 101.3 kPa = 120.9 kPa

Pressure intensity 0.1mm from collapse center:

200 × 120.9 kPa=24 200 kPa

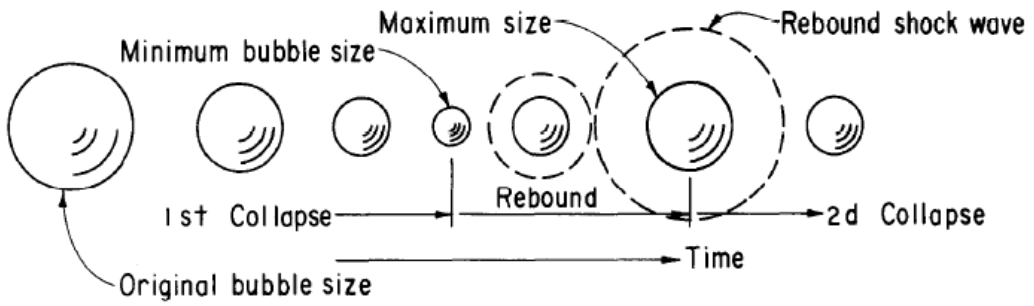

a. Collapse of an individual bubble in a quiscent fluid

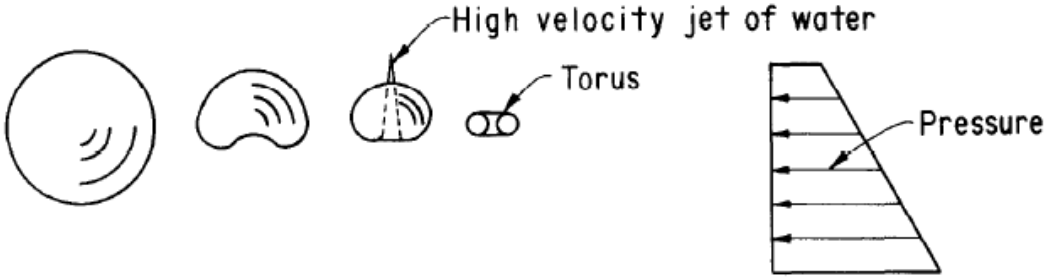

b. Collapse of an individual bubble in a hydraulic gradient

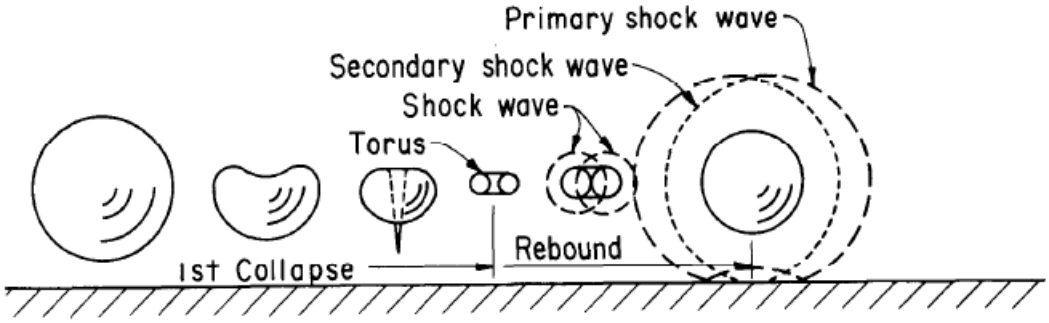

c. Collapse of an individual bubble near a boundary

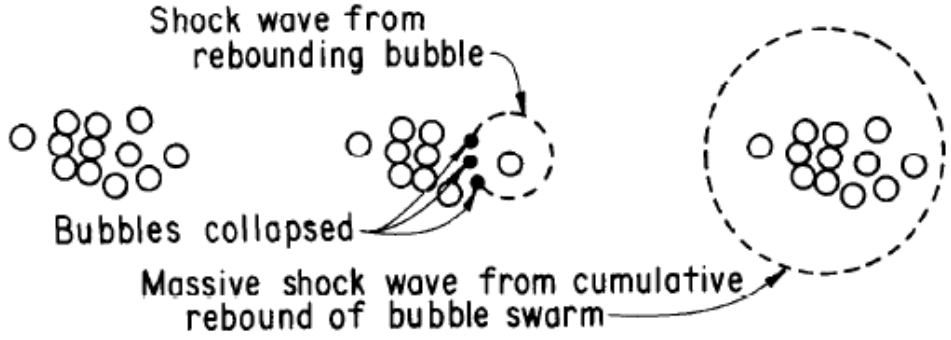

d. Collapse of a swarm of bubbles

Figure 4.1: Collapse mechanisms of bubbles.

These computations ignore the effect of the initial bubble diameter and the water temperature on collapse pressure. Fujikawa and Akamatsu (1980) show that both parameters have a significant influence.

They found that the collapse pressure increased as either the initial bubble diameter or the water temperature decreases.

Theory also allows estimating the time for a bubble to collapse. The collapse time is given approximately by Knapp et al (1970):

$$\tau = R_0(\frac{\rho}{P_0})^{\frac{1}{2}} \quad \textbf{(4.1)}$$

Where:

P_0 = reference pressure (at collapse site)

R_0 = initial radius of bubble

ρ = density of water

For a bubble having an initial diameter of 0.1 millimeter and an ambient pressure corresponding to 2.0 meters of water, the collapse time is:

$$\tau = 0.0001\ (\frac{999}{120900})^{\frac{1}{2}} = 9.1\ microseconds$$

Several factors modify the collapse mechanism of a purely spherical bubble. For instance, if the bubble collapses in the presence of a pressure gradient, the shape of the bubble does not remain symmetrical. Pressure gradients exist in flow around submerged bodies. If the bubble collapses near a boundary, the boundary restricts the flow toward the bubble which also causes an asymmetric collapse.

Both cases cause one side of the bubble to deform into a jet which penetrates the opposite side of the bubble as depicted on Figure 4.1. The jet formed by the unsymmetrical collapse of a single bubble is called a micro jet. The velocities of micro jets are large. Hammitt (1979) concluded that in most cases cavitation damage was due primarily to the liquid micro jet impact on the surface and not to the spherical shock waves which emanate from the rebounding bubble. However, more recent photo elastic studies Fujikawa and Akamatsu (1980) have shown that the shock wave generates much higher pressure impulses than the jet.

If more than one bubble is present, the collapse of the first will produce shock waves that radiate to other bubbles. These shock waves will cause the sudden unsymmetrical collapse of neighboring bubbles. The jet formed by the unsymmetrical collapse of a bubble caused by shock waves is called an ultra-jet. The velocities produced by ultra-jets are on the order of one-half the sonic velocity of the liquid (Tomita and Shima, 1986). Ultra jets generate higher pressure intensities than either spherical shock waves or micro jets.

Unfortunately, theory does not exist to predict the magnitude of the pressures generated by the collapse of a swarm of bubbles. One can hypothesize: if one bubble in a swarm collapses, the shock wave the bubble produced during rebound will cause other bubbles in the vicinity to collapse. The process will continue in the form of a chain reaction until the remainder of the swarm effectively collapses simultaneously. It is logical that the synchronous collapse of a bubble swarm would produce higher pressure intensity than the random collapse of individual bubbles in the swarm.

Another important factor influencing collapse of the cavitation bubble is the presence of vortices within the flow. Shear flows generate vortices that collect bubbles on their axes. Depending upon the proximity of bubbles, they may remain near each other in a swarm or they may coalesce into one filament shaped bubble (Falvey, 1990).

Damage caused by the group of bubbles-trapped on the axis of a vortex- can be many times greater than that caused by the collapse of an individual bubble or even a swarm of bubbles. For example, an individual bubble having a 2.7-millimeter diameter can create a depression in aluminum which is about 0.2 millimeter in diameter (Knapp et al, 1970). However, cavitation occurring in the vortices of the shear layer formed by a partially opened slide gate (operating submerged) has caused depressions up to I6 millimeters long and measured pressure intensities of 1500 megapascals (Lesleighter, 1983).

4.1.1. Mode of damage

Several mechanisms are usually involved in damage of hydraulic structures. For example, when cavitation forms because of a surface irregularity, surface damage will begin at the downstream end of the cloud of collapsing cavitation bubbles. After some time, an elongated hole will form in the concrete surface. As time progresses,

the hole will get larger with high velocity flow impinging on the downstream end of the hole. This flow creates high pressures within the minute cracks around individual pieces of aggregate or within temperature cracks which form during the curing process. Pressure differentials between the impact zone and the surrounding area are created which can cause aggregate or even chunks of concrete, to be broken from the surface and swept away by the flow. This damage process can be accurately regarded as erosion; whereas, the loss of material due to cavitation is not strictly erosion. Here, erosion is defined as an abrasion, dissolution, or transport process. As erosion from high velocity flow continues, reinforcing bars can become exposed. The bars may begin to vibrate which can lead to mechanical damage of the surface.

At the Bureau's Glen Canyon Dam, concrete lumps were found attached to the end of the reinforcing steel. At this stage, high velocity flow acting on the lumps rip reinforcement bars from the concrete even though the steel may be imbedded as deep as 150 millimeters. After the structure's lining has been penetrated, erosion can continue into the underlying foundation material. When damage penetrates the liner, the integrity of the structure is the first concern (Falvey, 1990).

4.2. Parameters Which Affecting Cavitation Damage on Surface

As high velocity flow passes over a surface, a potential exists for the surface to be damaged by cavitation. Various factors that determine whether or not the surface will be damaged include:

- Cause of the cavitation
- Location of the damage
- Intensity of the cavitation
- Magnitude of the flow velocity
- Air content of the water
- Resistance of the surface to damage
- Length of time the surface is exposed

4.2.1. Cavitation and causes of cavitation erosion

It is well-known that cavitation can severely damage solid walls by removing material from the surface. The phenomenon of cavitation erosion is complex since it includes both hydrodynamic and material aspects.

From a hydrodynamic viewpoint, vapor structures are produced in the low pressure regions of a cavitating flow. They are entrained by the flow and may violently collapse when entering regions of pressure recovery, causing the erosion of the solid walls.

Erosion is due to the concentration of mechanical energy on very small areas of the walls exposed to cavitation, following the collapse of vapor structures. This energy concentration results in high stress levels which can exceed the resistance of the material, such as its yield strength, ultimate strength or fatigue limit. The response of the material to such a micro-bombardment by a myriad of collapsing vapor structures from the standpoint of continuum mechanics, solid physics and metallurgy is also a key point in cavitation erosion (Pierre Franc & Marie Michel, 2004).

4.2.2. Location and intensity of damage zone

Observations of damage zones in many types of hydraulic equipment are in agreement with the laboratory experiments in that the zone of maximum damage is located at the downstream end of the mean length of the cavity, but the zone is relatively broad, extending both upstream and downstream from the maximum damage point (Knapp et al, 1970).

Stinehring (1976) showed for a cylinder-with its end facing into the flow-that the damage begins when the length of the cavitation cloud is equal to the diameter of the cylinder. Also, he found that the length of the cavitation cloud, L_k, was given by:

$$\frac{L_k}{H} = 2\left(\frac{\sigma_s}{\sigma}\right)^{2.63} \quad \textbf{(4.2)}$$

Where:

H = characteristic dimension, offset height, radius of cylinder, etc.

L_k = length of cavitation cloud

σ = cavitation index of the flow

σ_s = cavitation index when damage begins, σ_s corresponds to cavitation index when $L_k/H= 1$

Stinehring (1976) also showed that maximum damage occurs near the end of the cavitation cloud. His experiments agree relatively well with observations of cavitation damage in the Glen Canyon Dam tunnel spillways.

After approximately 20 days of operation, at a discharge of about 205m^3/s, damage was observed in the left tunnel spillway downstream of a calcite deposit which formed in a shrinkage crack as shown on figure 4.2a. After 3-day operation, at an average discharge of about 425m^3/s, a second damaged area was observed downstream of the first as shown on Figure 4.2b.

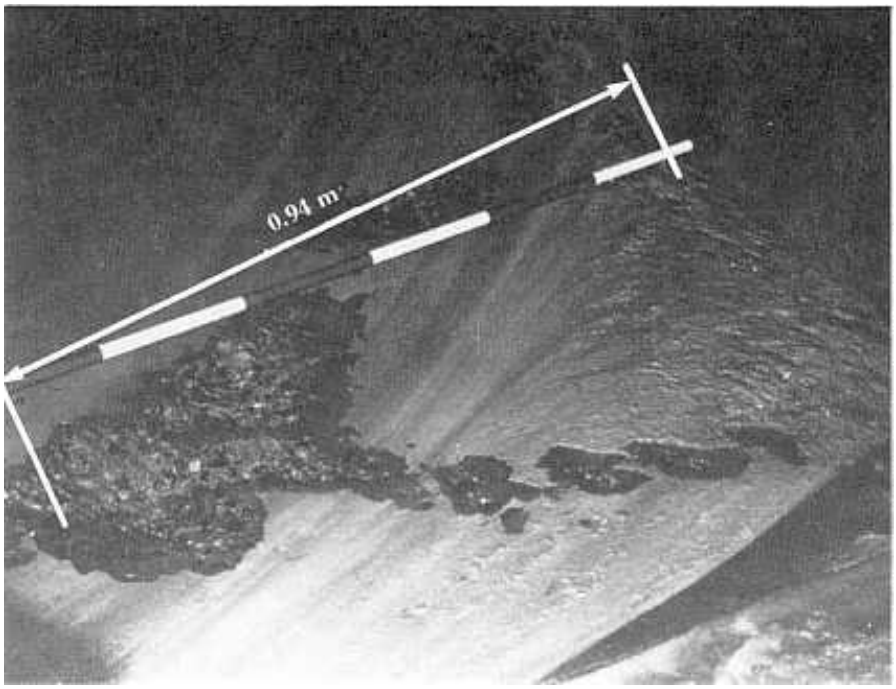

Figure 4.2a: Damage observed during a photographic survey (Fall, 1981)

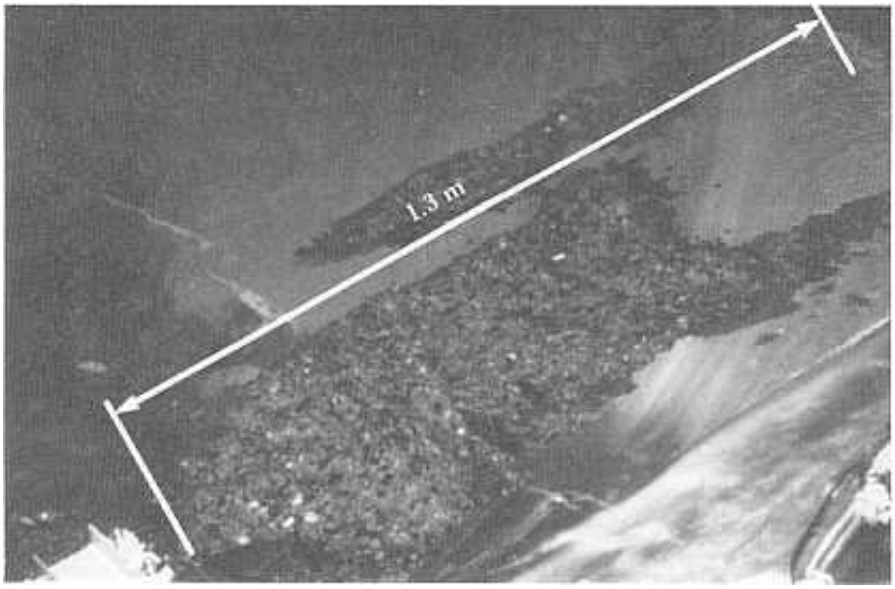

b. Damage observed on June 6, 1983

Figure 4.2: Glen Canyon Dam, left tunnel spillway-station 760.70 (Falvey, 1990)

Equation (4.2) can be used to predict the distance to maximum damaged areas. Appropriate values are given in Table 4.1. Note the locations were estimated relatively well for the approximations that must be made for the estimated height of the calcite deposits and their cavitation characteristics.

This analysis shows that the distance to maximum damage increases as both the discharge and the height of the surface irregularity increase. The photographic survey indicates the extent of damage; that is, the length of the damaged area also increases as the height of the irregularity increases.

Table 4.1: Length of cavitation cavities in Glen Canyon Dam left tunnel spillway-station 760.70 (m) (Falvey, 1990).

Discharge m^3/s	Estimated height of deposit, mm	Cavitation index of deposit	Distance to maximum damage
205	7	0.713	0.99
425	7	0.728	1.22

Farther up-in the spillway-damage was observed, but two distinct areas of damage did not develop as shown on Figures 4.3a and 4.3b. Stinebring's equation predicts a difference between the two damaged areas as shown in Table 4.2. However, the

difference is so small relative to the size of the damaged area that two areas of damage cannot be discerned.

Table 4.2: Length of cavitation cavities in Glen Canyon Dam left tunnel spillway-station 739.38 (m) (Falvey, 1990).

Discharge m^3/s	Estimated height of deposit, mm	Cavitation index of deposit	Distance to maximum damage
205	5	0.635	0.57
425	5	0.652	0.67

These two observations bring into question a widely held assumption about the formation of cavitation damage. This assumption is that cavitation tends to "leapfrog-forming a Christmas-tree shaped damage pattern as shown on Figure 4.4. That is, once cavitation damage has formed, it is assumed that the damaged area becomes a source of cavitation which then creates another damage area downstream.

Because the damaged area is larger than the irregularity which caused it, the process continues to produce larger and larger damage areas.

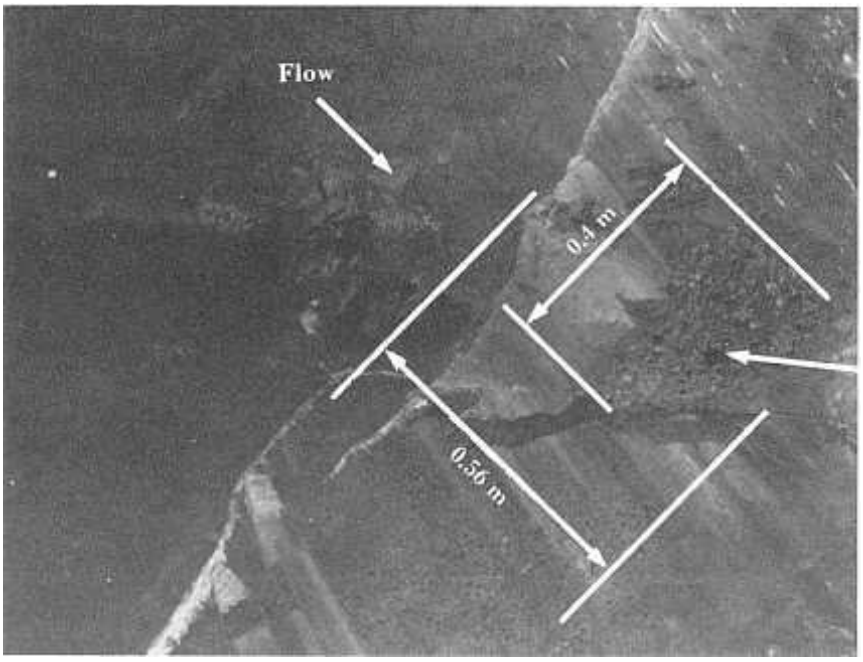

Figure 4.3a: Damage observed during a photographic survey (Fall, 1981)

b. Damage observed on June 6.1983

Figure 4.3: Glen Canyon Dam left tunnel spillway - station 739.38 (m) (Falvey, 1990)

Once cavitation damage has substantially altered the flow regime, other mechanisms then begin to act on the surface. These, fatigue due to vibrations of the mass, include high water velocities striking the irregular surface and mechanical failure due to vibrating reinforcing steel. Significant amounts of material may be removed by these added forces, thereby accelerating failure of the structure (Graham ACI Report, 1998).

The excellent prediction of the observed damage patterns using equation (4.2) shows that only consideration of changes in discharge is sufficient to explain the leapfrog pattern in the damage observed in the Glen Canyon tunnel spillway.

The Christmas-tree pattern of damage develops only after the depth of the cavitation damage becomes large relative to the flow depth. For a large hole, the damage mechanism is undoubtedly more that of erosion-by a high velocity jet on a rough surface-than that of cavitation. The erosion of a surface by a high velocity jet in the absence of cavitation has not been systematically studied (Falvey, 1990).

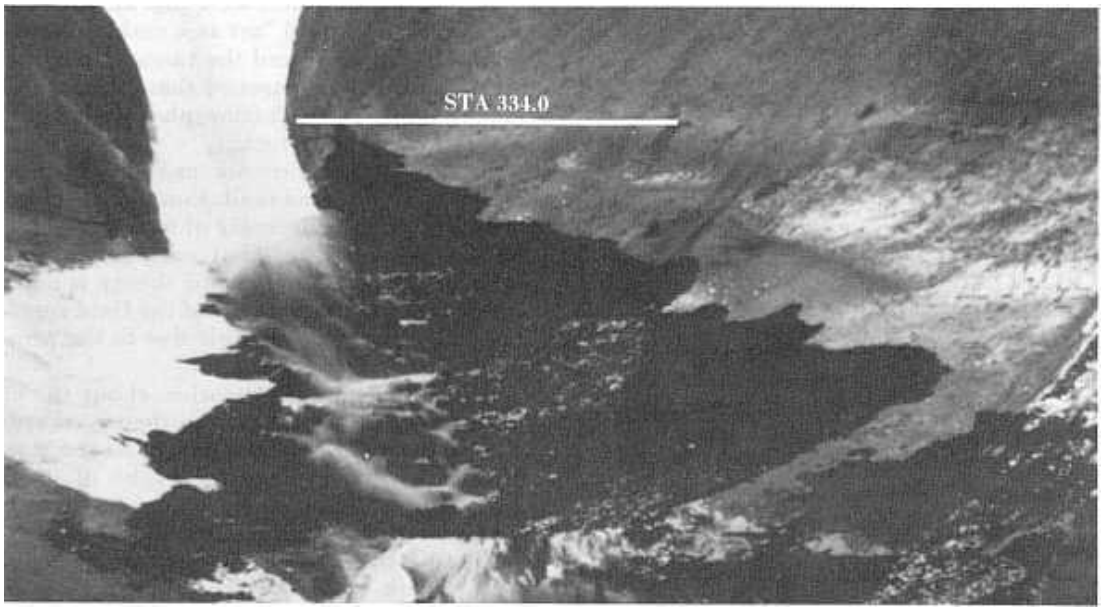

Figure 4.4: Hoover Dam, Nevada tunnel spillway- Christmas tree pattern of damage.

Cavitation Intensity:

Cavitation intensity is an extremely difficult parameter to quantify. Stinebring (1976) observed that as the cavitation index, σ, decreases relative to the incipient index, σ_i, the damage rate increases slowly as noted on Figure 4.5. If the cavitation index is decreased further, a zone is reached where the damage rate (expressed as pits per square centimeter per second) is inversely proportional to the cavitation index. Further decreasing the index will results in a point being reached where the damage rate has a maximum value. As the index is decreased even further, the damage rate decreases. From this, it appears that the cavitation intensity increases and then decreases as the cavitation index are lowered below the value of the incipient cavitation index. The noise spectrum has a similar behavior.

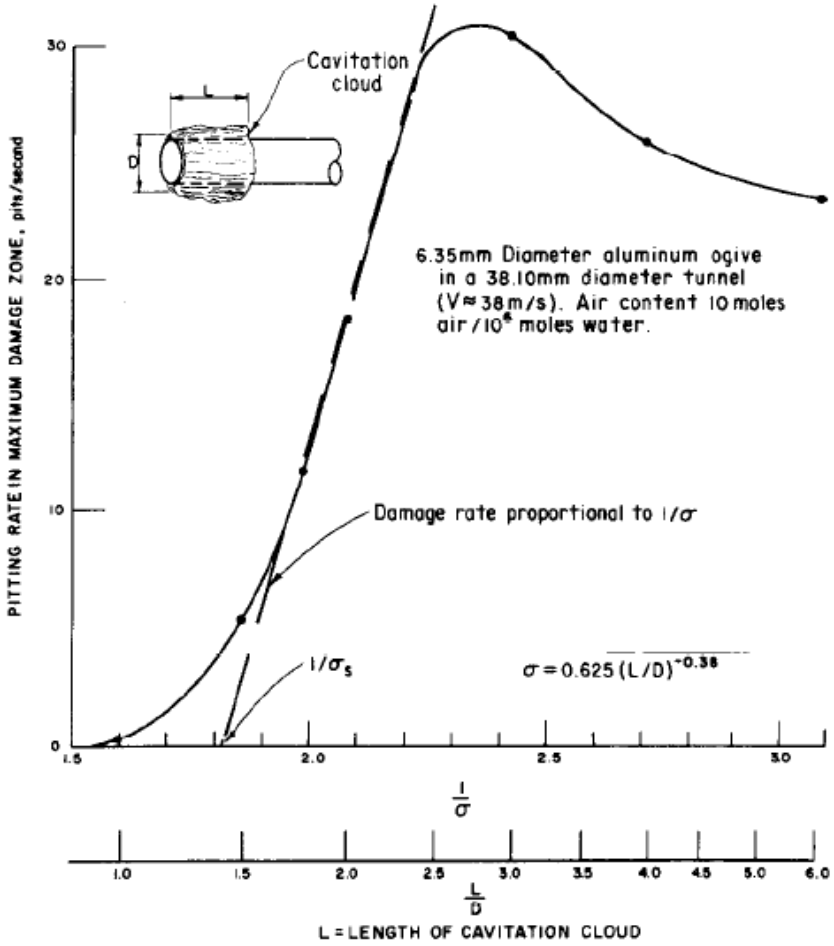

Figure 4.5: Cavitation damage rate (Stinebring, 1976).

Colgate (1977) proposed a similarly shaped curve for the damage intensity as the cavitation index decreases (decreasing ambient pressure). Also, he indicated the maximum of the total damage curve does not coincide with the maximum of the damage intensity curve. In addition, he showed the area of damage continues to grow larger as the cavitation index decreases as shown on Figure 4.6.

Colgate's observations can be explained by the following reasoning. As damage rate increases-for decreasing values of the cavitation index-the length of the cavitation cloud increases. However, length of the cavitation cloud is sensitive to variations in velocity. Therefore, length of the damage area tends to get larger and larger as the difference between the incipient cavitation index and the cavitation index of the flow increases. Thus, the intensity, measured in pits per square centimeter per second, may decrease while the total amount of material removed actually increases.

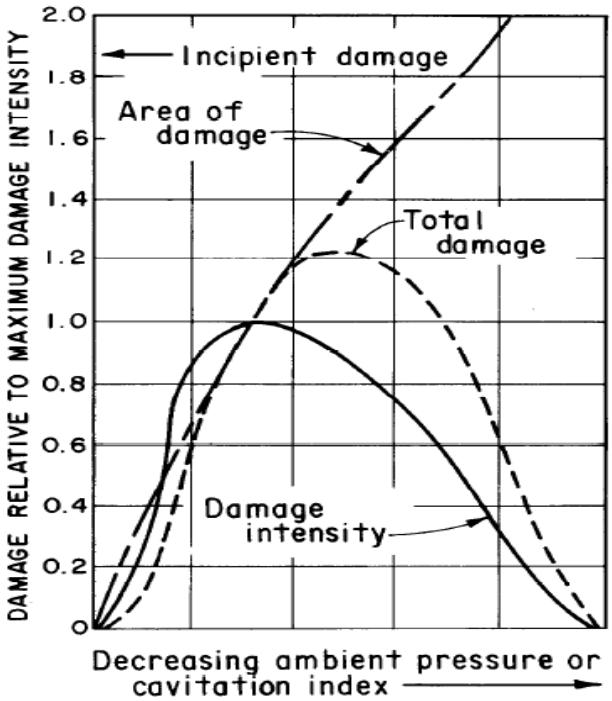

Figure 4.6: Cavitation damage with respect to cavitation index (Colgate, 1977).

Damage observed in hydraulic structures occurs downstream of an irregularity at distances up to 100 times the height of the irregularity. A solution of Equation (4.2), for these distances to height ratios, indicates the cavitation index of the flow must be on the order of one-sixth of the incipient cavitation index. Therefore, based upon Figure 4.5, damage which occurs in hydraulic structures is in the decreasing range of damage rates. Rarely are laboratory experiments made in this range because of the difficulty to create a facility that will produce damage at such low values of the cavitation index. Consequently, the only reliable data must come from field observations. Unfortunately, there is a paucity of good data (Falvey, 1990).

4.2.3. Flow velocity and importance of air amount in the flow

A common assumption is that a potential for damage exists when the flow velocity exceeds some critical value (Figure 4.7). Some justification exists for this assumption. For instance, a typical value of the incipient cavitation index for abrupt changes in geometry is on the order of 2.0. If this value is substituted into equation (2.4), along with the assumption that the reference pressure is equal to the barometric pressure at sea level, the resulting velocity is equal to 10m/s. Therefore, it is prudent to investigate the possibility of cavitation for velocities exceeding 10 m/s.

If a surface is exposed to cavitation, at a constant velocity, for a while material will not be lost from the surface. This period is known as the incubation phase. The surface then enters an accumulation phase wherein the rate of loss increases dramatically with time. This is followed by a steady-state phase and the rate of loss is constant. The steady-state phase may be preceded by an attenuation phase in which the rate of loss decreases (Falvey, 1990).

Tests on aluminum plate show that the surface is being pitted during the incubation phase (Stinebring, 1976). The average energy per pit increases as the 5th power and the number of pits increases as the 6th power of velocity. Therefore, the total energy of the collapsing bubbles increases as the 11th power of velocity.

Once material begins to be lost from the surface, the dependence of the rate of loss with respect to velocity becomes ambiguous. Some investigators claim the rate of loss varies with the 5th power of velocity, while others have found it varies with the 6th power. Undoubtedly, the variation is a function of the base material, the method of testing, and the damage phase.

Air Content Effect:

For low values of air concentration, damage has been found to vary inversely with the air concentration (Stinebring, 1976). The tests were conducted at air concentrations between 8×10^{-6} and $20 \times l0^{-6}$ moles of air per mole of water. At high air concentrations, of around 0.07 moles of air per mole of water, damage was found to be completely eliminated over a 2-hour test period in a Venturi-type test facility (Peterka, 1953).

In 1945, assumptions were that air injected under a water prism would “act as a cushion between the high-velocity water and the tunnel lining”. It was further reasoned that “the air would aid in relieving the sub atmospheric pressures”. Neither axiom is correct (Bradley, 1945).

Currently, two theories explain the mitigating effects of aeration on cavitation damage. One theory is based upon the presence of no condensable gases in the vapor pocket that cushion or retard the collapse process. The second theory is based upon the change in sonic velocity of the fluid surrounding the collapsing vapor bubble due to the presence of undissolved air.

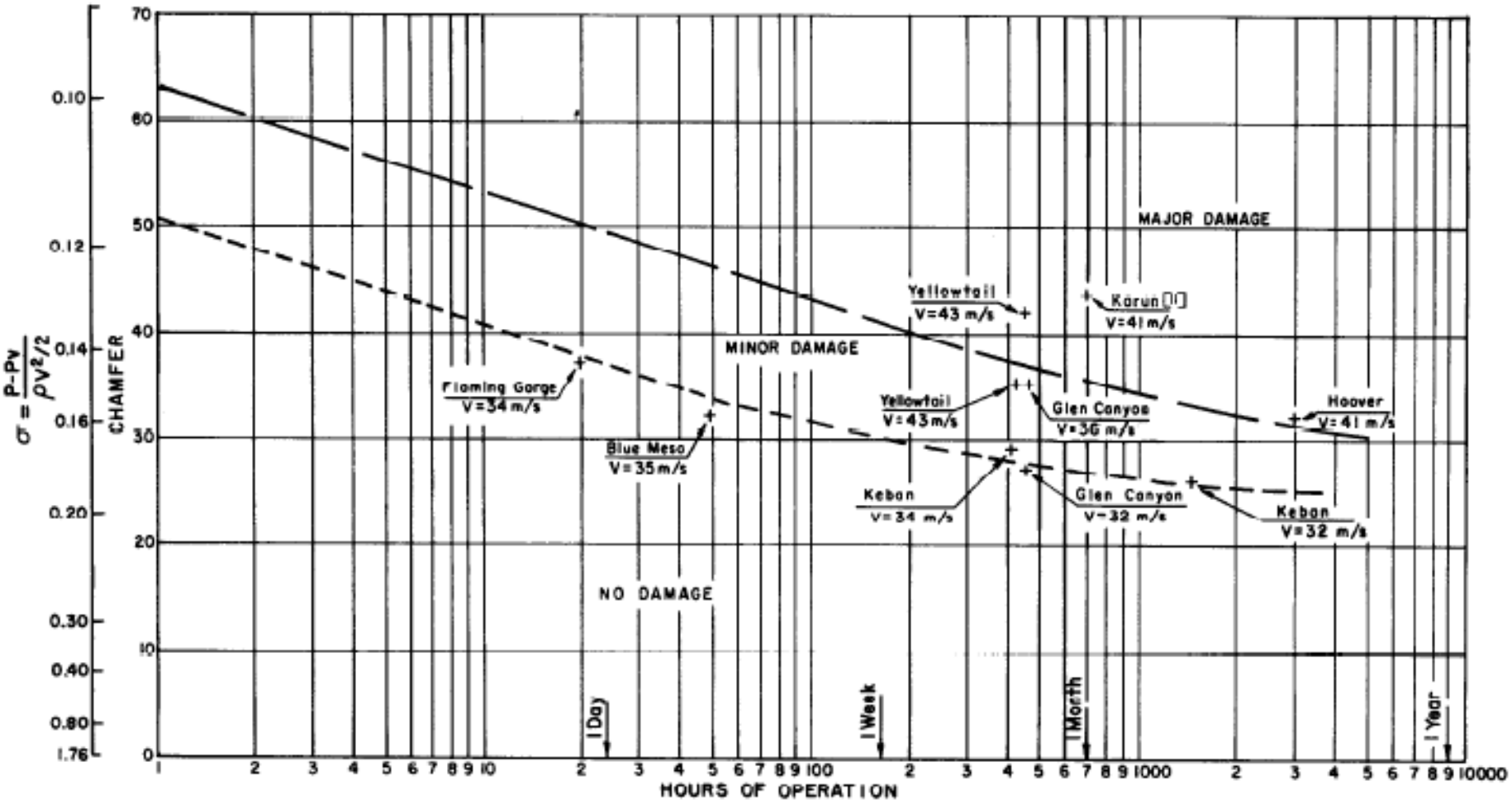

Figure 4.7: Damage experience in spillways (Falvey, 1990)

Of the two current theories, about the effect of undissolved air in water, the theory regarding the change in sonic velocity seems to be the most valid. Studies have shown that diffusion of undissolved gases into a vapor cavity proceeds at a very slow rate relative to the rate of vaporization.

Because the vapor cavity growth time is short, it seems unlikely for sufficient gas to be present (in the vapor cavity) to significantly affect the rate of collapse of the cavity or the pressures generated by the collapse (Falvey, 1990).

4.2.4. Effects of structure's surface resistance and material to cavitation damage

The resistance of a surface to damage depends upon several factors including the ultimate strength of the material, ductility, and homogeneity. It is not clear which strength characteristics of a material are significant when evaluating the surface resistance. With metals, surface deformation caused by the impact of collapsing bubbles produces tensile forces within the material. On concrete surfaces, tensile forces are also possibly the significant factor. Thus, tensile strength and not compressive nor shear strengths may be the more important parameter. The properties of strength and ductility can be combined into one parameter known as resilience (Rao et al, 1981). Resilience is defined as the area under the stress-strain curve of a material.

Presently, correlations have not been developed that quantify the amount of damage, of a given material, for a specified amount of cavitation. However, to express the resistance of a material relative to the resistance of other materials-for a given cavitation condition-is possible. For example, in a Venturi testing device, cavitation produced a hole 13 mm deep in concrete after 3 hours at a flow velocity of 30 m/s. The same size hole was produced in polymer concrete after 125 hours and in stainless steel after about 6,000 hours. Carbon steel was found to be damaged about 7 times faster than stainless steel; aluminum or copper is damaged about 25 times faster than stainless steel. Figure 4.8 shows a curve of relative damage developed for this and other data on materials conventionally used in construction of hydraulic structures. For the effect of velocity, an 11th power dependence on velocity was assumed (Colgate, 1977).

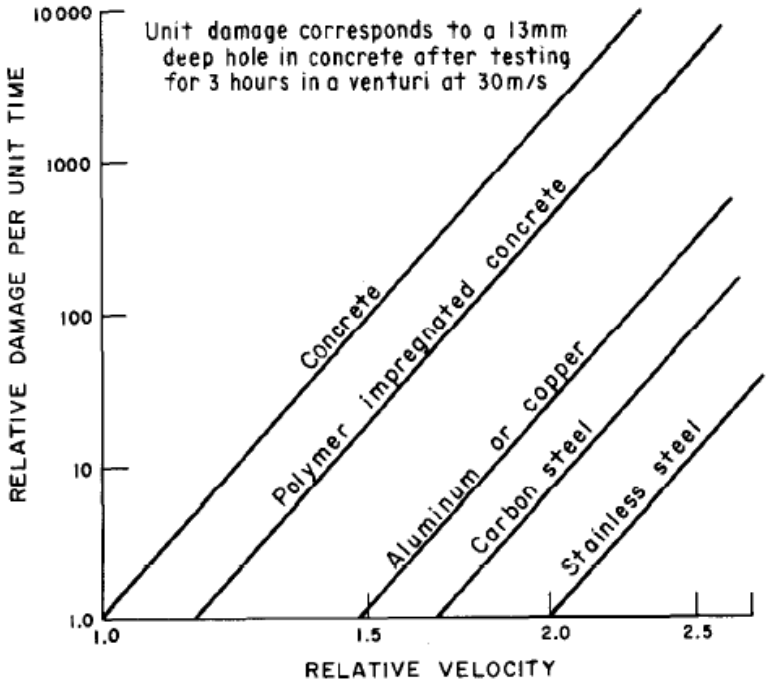

Figure 4.8: Comparative cavitation resistances of various materials (Colgate, 1977)

Exposure Time Effect:

The rate of erosion-of any surface-caused by cavitation is not constant with time. Observations have shown that several different rates actually occur. Each rate has been given a specific name, (Heymann, 1967), as noted on Figure 4.9.

At first, a period begins where loss of material does not occur. The period is known as the "incubation zone." In this zone, metal surfaces become pitted. Many investigators use data taken in the incubation zone as the most significant for damage correlations (Stinebring, 1980).

Following the incubation zone, the damage rate increases rapidly during a period called the "accumulation zone." This rate reaches a peak. Depending upon the type of testing facility, the damage rate follows one of two trends. The damage rate either decreases into an "attenuation zone"- which is followed by a constant damage rate plateau called a "steady-state zone," or the damage rate reaches a steady-state plateau-which is then followed by an attenuation zone, as shown on Figure 4.9. These damage rate characteristics have been explained using a statistical representation of the cavitation collapse mechanism (Heymann, 1967).

In hydraulic structures, which have irregularities on the boundaries, the location where cavitation bubbles collapse does not change significantly during the damage

process. This means that as damage increases, the distance between the collapsing bubble and the surface increases. Thus, it can be expected that the damage rate will tend to vary inversely with time. With increasing time, for a constant flow rate, the depth of damage downstream from an irregularity will appear to reach a constant value. This hypothesis has been verified in field investigations (Wang and Chou, 1979).

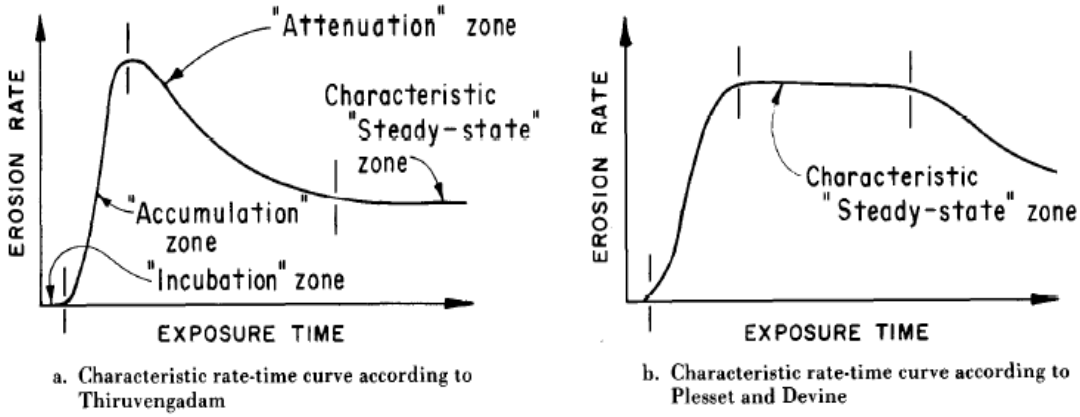

Figure 4.9: Cavitation damage rate (Heyman, 1967)

4.2.5. Short-Time cavitation erosion of concrete

The behavior of concrete under long-time cavitation erosion — several hours up to several years — has been an issue since concrete is used for dams, spillways, channels and other hydraulic structures. Some classical investigations have been performed by Price and Wallace.

A general review about this problem is given by (Graham et al, 1987). The results of these investigations can be summarized as follows:

- The cavitation resistance increases if the compressive strength increases.
- The cavitation resistance increases if the water–cement ratio decreases.
- The cement type does not influence the cavitation resistance.
- Coarse aggregates are more easily plucked away due to cavitation than small aggregate. Therefore, a maximum aggregate size of 20 mm is recommended.
- The bond between cement matrix and aggregate grains plays a major role. The better the bond, the higher the cavitation resistance.
- The aggregate material hardness is not critical for the cavitation resistance.

Short-time cavitation erosion is defined here as cavitation acting over a maximum duration of 10 s. Short-time cavitation is a phenomenon that could play a role during

water jet impact of solid materials. Especially in concrete hydro demolition (is a concrete removal technique which utilizes high-pressure water to remove deteriorated and sound concrete as well as asphalt and grout), which is one of the most important useful applications of water jet erosion, short-time cavitation erosion may occur. Scheuer (1985) investigated the influence of the surface profile and flow velocity on the introduction of cavitation on solid surfaces and found that, independent of the geometry, a disproportion 5 mm high introduces cavitation at a flow velocity as low as V=4.0m/s. This velocity will reliably be reached in any jet flow that develops a stagnation pressure of P=25 MPa on the solid surface. Therefore, short-time cavitation erosion, as an additionally contributing failure mechanism, seems to be very likely in concrete hydro demolition. Nevertheless, no investigation is known so far that deals with this very special issue.

Moreover, short-time cavitation erosion is a promising method to study the material removal mechanisms acting in the early stage of cavitation (momber, 2000).

To find out the short-time effect of cavitation, the study is done by two different aggregate type concretes under same cavitation situations:

Concrete No. 1 contains round quartz with Compressive strength 21 MPa; whereas, concrete No. 2 contains broken limestone with Compressive strength 39MPa.

With modeling the cavitation chamber, experiment is done and results are shown below on Fig. 4.10.

- The average mass loss after t =10s was 1.1 g for concrete 1 and 0.3 g for the concrete 2. The cavitation resistance increases as the compressive strength increases. This is in agreement with experience from long-time cavitation experiments on concrete.
- Short-time cavitation erosion may be a considerable erosion phenomenon that directly contributes to the material removal in concrete hydro demolition processes.
- Even a very short exposure time t=2s is sufficient to modify the surface topography of the investigated specimens.
- The material's behavior during cavitation erosion significantly depends on its capability to transfer local stresses and to locally deform. High stiffness and brittleness promote Trans granular fracture.

- The interfacial bond between aggregate and cement matrix is on decisive importance for the cavitation erosion resistance (Momber, 2000).

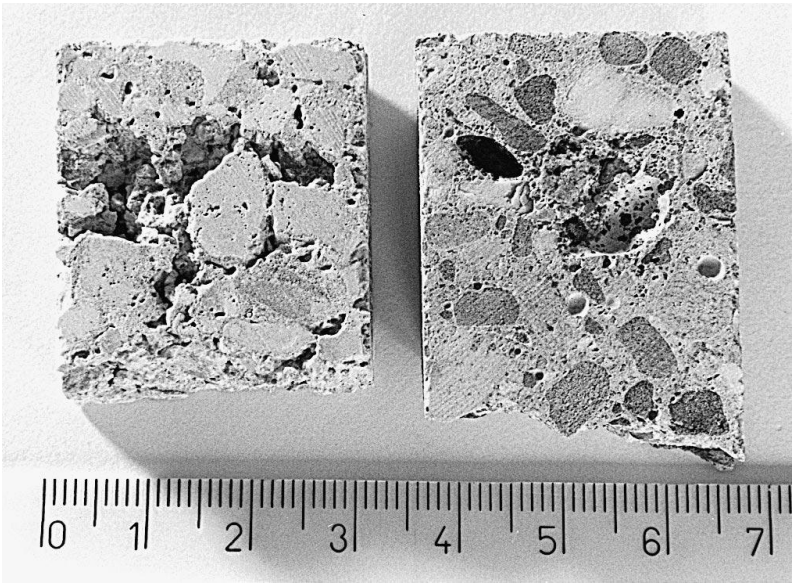

Figure 4.10: Macroscopic view on the cavitation damage for t_c = 10s Left: concrete 1. Right: concrete 2.

4.2.6. Effect of changes in liquid properties on damage

There have been reports from various hydraulic-turbine installations that the rate of cavitation damage varies with the season of the year even under the same operating conditions of head, loss, tail-water level, etc. The explanation for this seems to be connected with a change in the pertinent physical properties of the water and its contaminants. For example, temperature, dissolved-gas content, and size and concentration of the nuclei may vary with the season. Several of the physical properties of water change with the temperature. The vapor pressure increases as temperature increases, the density decreases, and the bulk modulus increases in the range of interest for hydraulic turbines. If the system head remains constant, velocities will also remain constant independent of changes in density. For the same initial cavity size and collapsing head, radiated collapse pressures should increase with density increase. Since the natural density changes are very small, this effect should not be important. The degree of cavitation will, of course, vary with changes in vapor pressure (Knapp et al, 1970).

4.2.7. Recognition of cavitation damage

When damage has occurred in the field, it is important to know the cause of the damage so that appropriate remedial action can be initiated. The following discussion is general observations, which will provide guidelines, for the recognition of cavitation damage.

Texture

It was mentioned that damage caused by a collapsing cavity is primarily caused by a pressure wave that travels at the speed of sound in the water. Since the speed of sound is between 10 and 40 times greater than the flow velocities, which are normally associated with damage, damage appears to be caused by a source perpendicular to the surface. This means the direction of flow cannot be determined by examining the damaged area. Also, this effect has an impact on the texture of the damage.

In steel, the effect of the collapse of the many minute cavitation bubbles perpendicular to the surface is to produce a grainy texture. The scale, of surface texture, depends upon the size of the cavitation bubbles which are produced. In a laboratory facility, the structure of the damage is fine grained as shown on Figure 4.11a because the bubbles are small. Whereas, in the liner of an outlet conduit the surface texture is much coarser grained because the cavitation bubbles are larger as shown on Figure 4.11b.

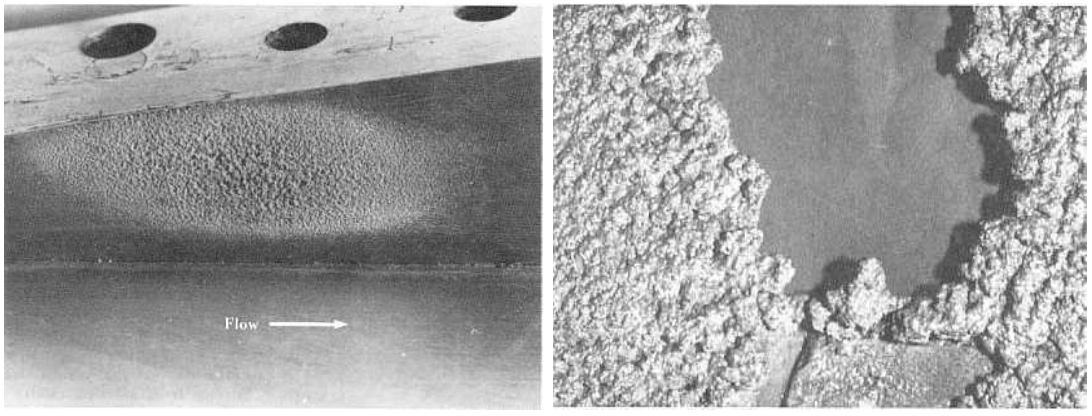

a. Venturi throat of cavitation test facility **b.** Ross Dam (Seattle, Washington) outlet works conduit

Figure 4.11: Texture of cavitation damage in steel (Falvey, 1990)

The effect of the collapse perpendicular to a concrete surface produces a surface in which the individual pieces of aggregate are cleaned of the cement which binds the

concrete. Deep crevices and holes can be found in the matrix. It almost appears as though worms bored into the concrete. The difference in appearance of laboratory and field produced damage is not significant as shown on Figure 4.13. None of the aggregate is broken.

The contrast between the texture of damage caused by cavitation and that caused by erosion, with sand-Laden water, is easily recognized in steel. With cavitation, direction cannot be detected and the surface has a grainy texture. With erosion by sand-laden water, flow direction is apparent and the surface is smooth and shiny.

Similarly, the difference between cavitation, freeze-thaw damage, and erosion by sand-laden water is apparent in concrete. With cavitation, individual, polished pieces of aggregate are exposed in the damaged zone as shown on Figure 4.13a.

Whereas, in the freeze-thaw zone, individual pieces of aggregate are broken and the profile through the damaged area is relatively flat as shown on Figure 4.12.

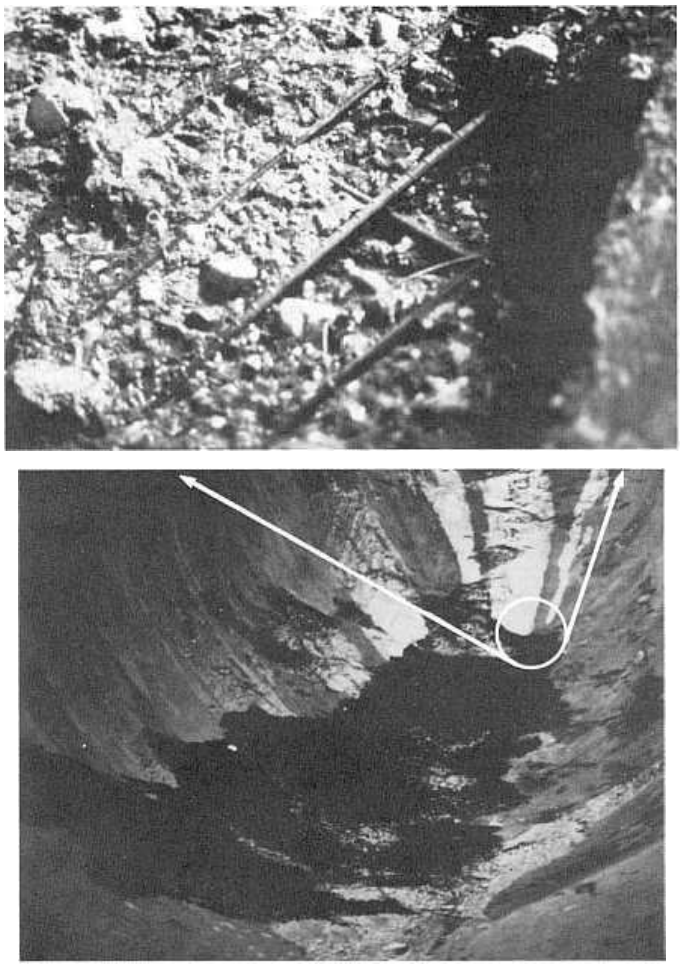

Figure 4.12: Kortes Dam, Wyoming, freeze-thaw damage.

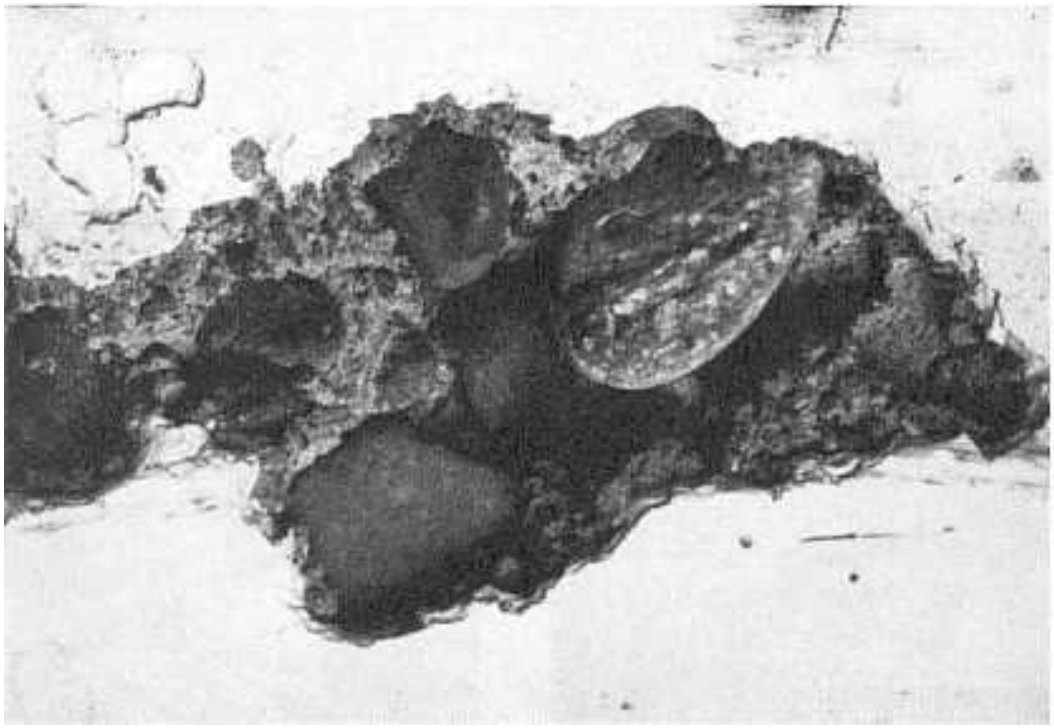

a. Cavitation damage produced in a Venturi cavitation test facility

b. hoover Dam, Nevada spillway tunnel - initiation of damage

Figure 4.13: Cavitation damage in concrete (Falvey, 1990)

Symmetry

If cavitation damage occurs on a structure, it will occur in similar locations elsewhere on the structure. For instance, if cavitation damage is observed on the conduit wall downstream of a gate slot, it will occur downstream of the opposite gate slot as shown on Figure 4.14.

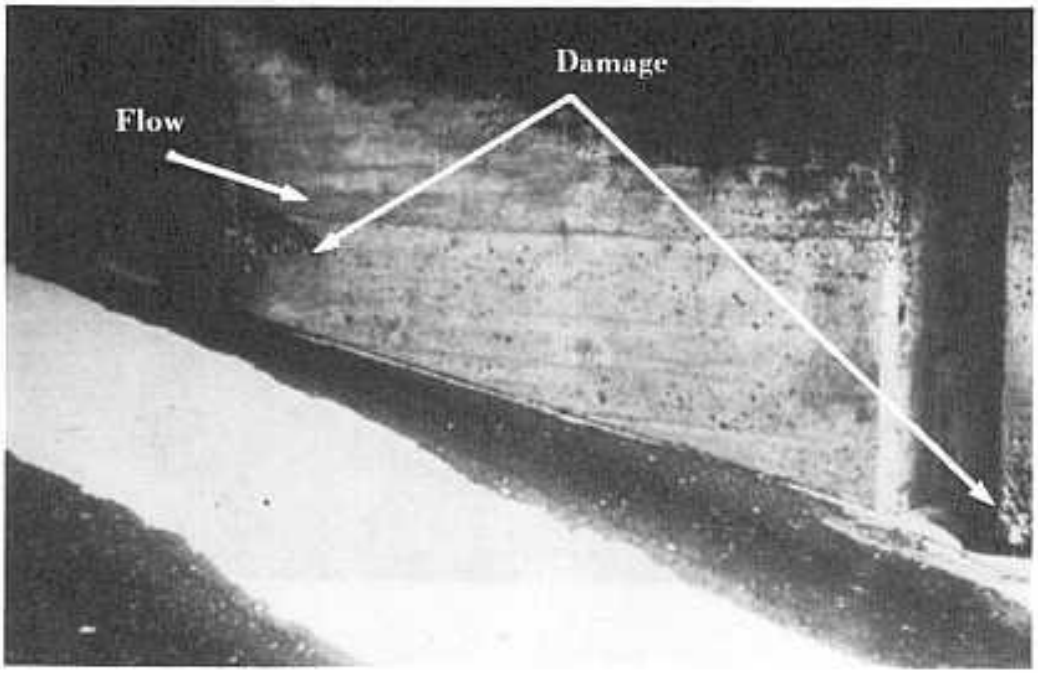

a. Left side of outlet

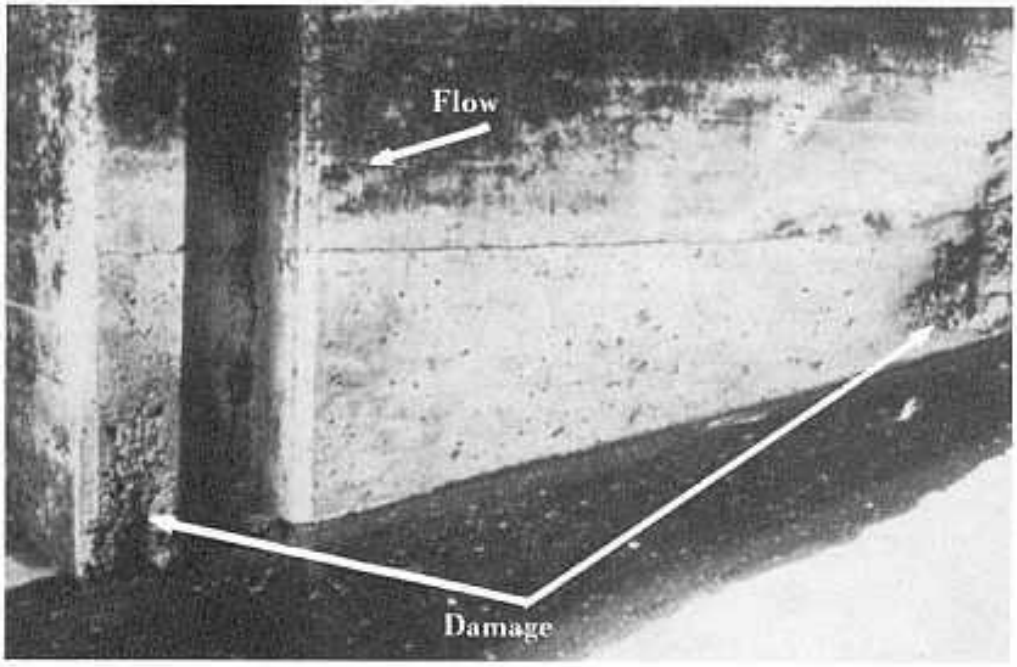

b. Right side outlet

Figure 4.14: Palisades Dam, symmetrical damage in outlet structure.

Origin

Cavitation damage always occurs downstream from its source. This has two important implications. First, there must be a source of the cavitation and secondly, the damage will not progress upstream of the source. Usually, the source is easily identified. Surface irregularities, calcite deposits, gate slots, and sudden changes in flow alignment are typical sources for damage.

Longitudinal vortices in the flow are known also to be sources of cavitation which have caused damage. Generally, the exact location of these sources cannot be accurately specified. A typical example of cavitation damage caused by longitudinal vortices in the flow through a slide gate is shown on Figure 4.15.

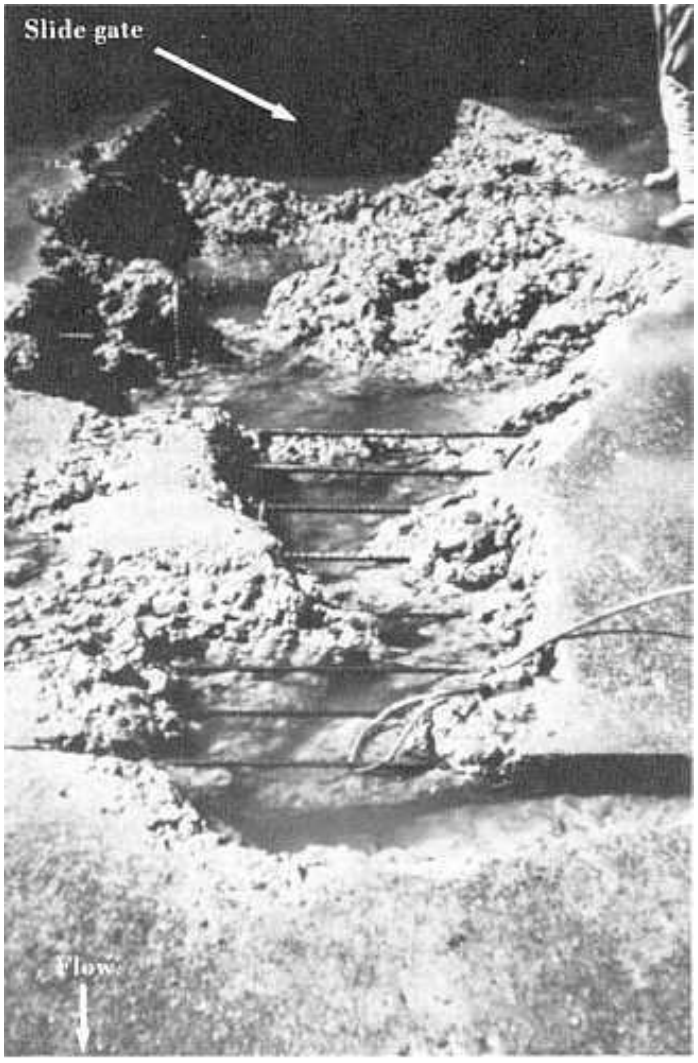

Figure 4.15: Palisades Dam, outlet works vortex caused damage downstream of slide gate (Falvey, 1990).

5. CAVITATION DAMAGE ON BIG SCALES OF SOME HYDRAULIC STRUCTURES AND TURBINES

Blue Mesa Dam is a part of the Bureau's Wayne N. Aspinall Storage Unit, Gunnison Division of the Colorado River Storage Project. The dam is located in mountainous country on the Gunnison River 40 km west of Gunnison, Colorado. The primary purpose of the unit is to develop the water storage and hydroelectric power generating potential along a 64-km section of the Gunnison River above the Black Canyon of the Gunnison National Monument. Other purposes of the unit are irrigation, recreation, and flood control.

The dam is a zoned earth fill structure 240 m long at the crest and 104 m high above the riverbed. The reservoir is 30-km long having a storage capacity of $1.2 \times l0^9$ m^3. A 60-MW power plant is located at the toe of the dam.

Figure 5.l shows the spillway on the right abutment (Beichley, 1964); its capacity is about $963 m^3/s$ at the maximum reservoir water surface elevation of 2292m. Water discharges through: a gate section a tunnel transition section, a tapering inclined tunnel, a vertical bend, a nearly horizontal tunnel, and a flip bucket. The flip bucket directs flow into the river channel about 150 m downstream of the power plant.

During construction, the nearly horizontal section of the tunnel and the flip bucket were used to pass diversion flows around the construction site.

The spillway operated several days in June and July 1970. On 2 days, the discharge reached $99 m^3/s$.

Upon inspection, an area of cavitation damage was discovered. At station 4+54.15, cavitation damage had begun downstream from a hole which was formed when a piece of wood popped out of the concrete liner. The pop out was 150 mm wide, 127 mm long and 25 mm deep. Cavitation damage began 63 mm downstream of the pop out. The damage-nearly circular-with a diameter of 76 mm was 13 mm deep. The cavitation index at this location is 0.19 at 10 percent of the design discharge. The spillway operating history is not known; therefore, the damage index could not he

calculated. Other pop outs and spalls had occurred throughout the tunnel. However, cavitation was not discovered at any of the other sites.

The analysis reveals that the lowest cavitation index occurs at the point of tangency of the vertical curve with the nearly horizontal tunnel (STA 4+73.88). The second lowest value occurs at the point of curvature of the vertical bend (STA 4+33.66). Cavitation indexes at these locations are 0.159 and 0.188 respectively, for a flow of $99 m^3/s$. The maximum values of the damage potential also occur at these locations.

The analysis indicated extensive damage could he expected if the spillway were to operate for periods of 1 week or more. The most susceptible location for damage to occur was immediately downstream of the vertical bend. Because of this potential for damage, an aerator was designed and constructed in the spillway tunnel.

The aerator was placed at station 4+16.05. At this location, the cavitation index is greater than a value of 0.218 for all discharges. Therefore, damage upstream of the aerator is extremely unlikely. At this location, the aerator is 54.3 m below the maximum reservoir elevation.

The aerator consisted of a ramp, a downstream aeration groove, and a concentric conical offset located downstream of the aeration groove as noted on Figure 5.1.

The aerator was completed in 1985. Following its completion, the spillway passed flow up to $56.63 m^3/s$. These flows occurred in the late summer of 1986 and lasted for several days. There have been no reports of damage to the tunnel.

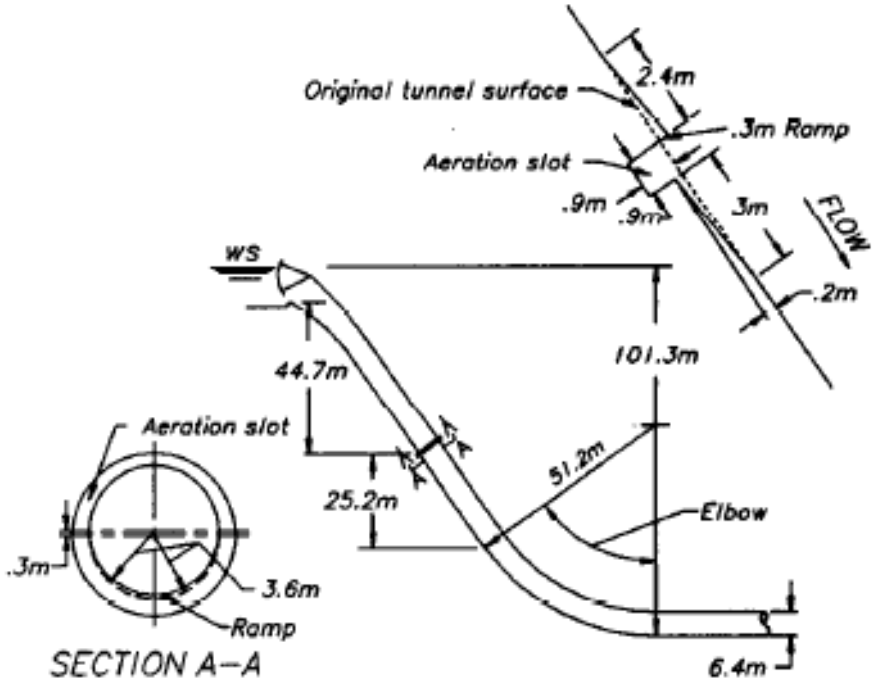

Figure 5.1: Blue Mesa Dam, tunnel spillway, aeration slot

Glen Canyon Dam is part of the Glen Canyon Unit, Middle River Division of the Colorado River Storage Project. The dam is located on the Colorado River in northeast Arizona 25 km upstream of Lee's Ferry.

The structure is a 216-m-high concrete arch dam having a crest length of 475 m. The reservoir has a storage capacity of 3.3×10^9 m^3. A 950 MW power plant is located at the toe of the dam. An outlet works, with four hollow jet valves; having a total capacity of $425 m^3/s$ is located on the left abutment of the dam.

The dam has an open-channel flow tunnel spillway on each abutment as shown on Figure 5.2. Each spillway is 12 500 mm in diameter and has a maximum capacity of $2900 m^3/s$. Flow to each spillway passes radial gates, a 55° inclined tunnel, a vertical bend (elbow), and 305 m of horizontal tunnel to a flip bucket.

Both spillways were operated for extended periods in 1980 (Burgi and Eckley, 1987). In 1981, an inspection revealed that deposits from cracks in the lining had initiated cavitation damage at several locations in the left spillway. Little damage had occurred in the right spillway. This was probably due to the shorter operating time. Following this inspection, a photographic survey of the tunnels was performed to document the damage.

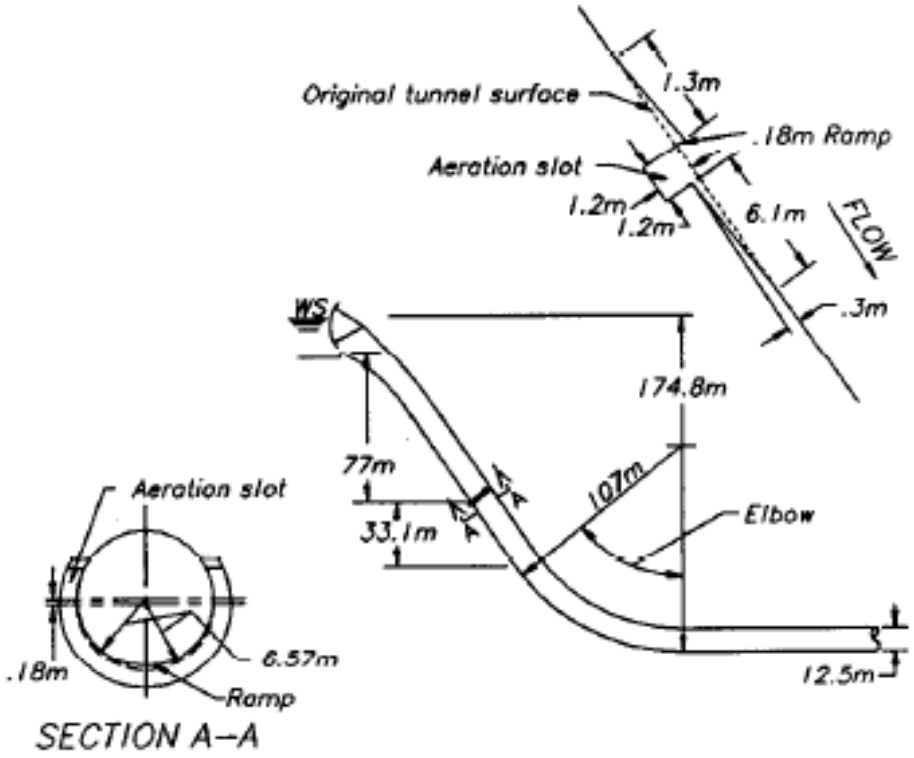

Figure 5.2: Glen Canyon Dam, tunnel spillways - aeration slots

Following the inspection, a study was made to identify the scope of work required to repair the damage and to prevent future occurrence. It was recommended the damage be repaired and aerators be installed near station 6+86.0. These modifications were planned to begin in 1984. Unfortunately, high flows in the Colorado River occurring in the spring of 1983 had to be passed through the spillways.

The first indication that damage was occurring to the left tunnel spillway (during the 1983 flood) came on June 6, when loud rumblings were heard from the tunnel (Burgi et al, 1984). Several large holes were found in the invert during an inspection in the afternoon of June 6. Flows were resumed through both tunnels. At the end of the flood, extensive damage had taken place in both tunnels as shown on Figure 5.3. Even though damage was extensive, it only excavated a hole whose depth was about equal to the spillway diameter. At this point, the eroded cavity was evidently large enough to dissipate the energy of the high velocity water. In the elbow portion of the tunnels, the depth of the damage as noted on Figure 5.4 was on the same order as the depth of the flow.

Even while the spillway flows were continuing, an emergency program was initiated to design, model test, and construct aerators in the inclined portions of the spillways

(Pugh, 1984). These aerators consisted of: a ramp, a groove or slot, a downstream offset, and a transition back to the original tunnel diameter as shown on Figure 5.2. The ramp is 1295 mm long and 180 mm high at the centerline of the invert. The groove is 1200 by 1200 mm. The downstream edge of the slot is offset 305 mm from the original tunnel diameter. The length of the transition to the original tunnel diameter is 6096 mm. The end of the ramp is at station 6+85.80 which is 96.2 m below the maximum reservoir elevation.

The tunnels were ready for service after finishing construction on October 10, 1984.

In August 1984, the left tunnel was tested to verify the operation of the aerator. Pressure measurements were taken in the invert to compare with model studies and air velocities were measured in the air groove to estimate the airflow quantities (Frizell, 1985). Flow rates up to 1416 m^3/s were passed through the spillway. This discharge was 40 percent greater than had previously passed through the spillways. In addition, a discharge of $566 m^3/s$ was maintained for 48 hours. This flow rate and duration had caused damage to the spillway during the 1980-81 flows.

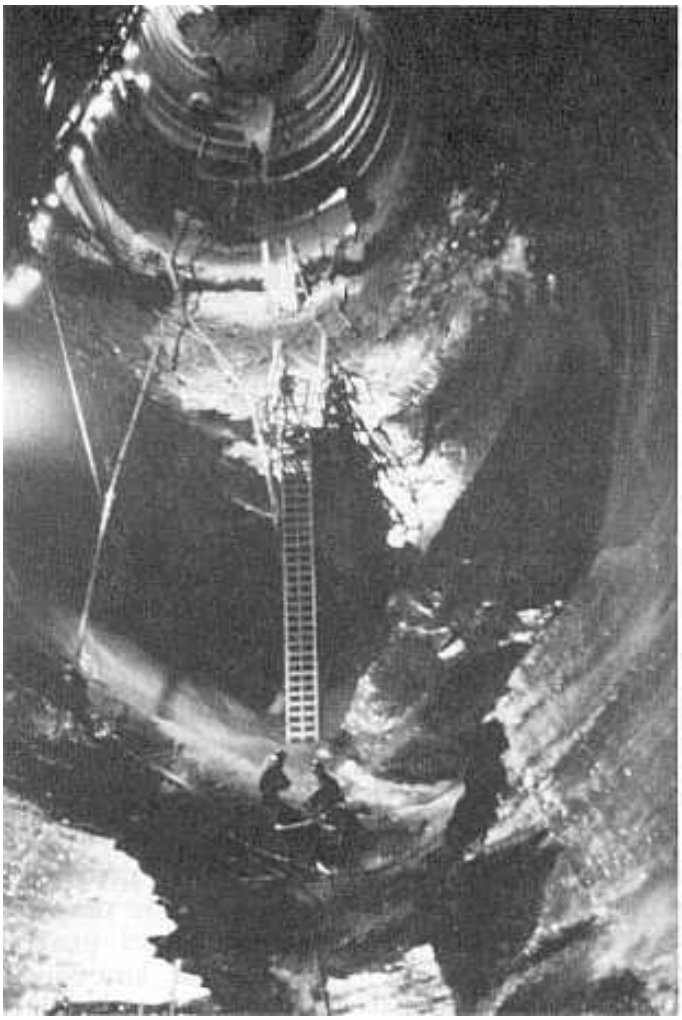

a. Left tunnel

b. Right tunnel

Figure 5.3: Glen Canyon Dam, tunnel spillways major damage (Falvey, 1990).

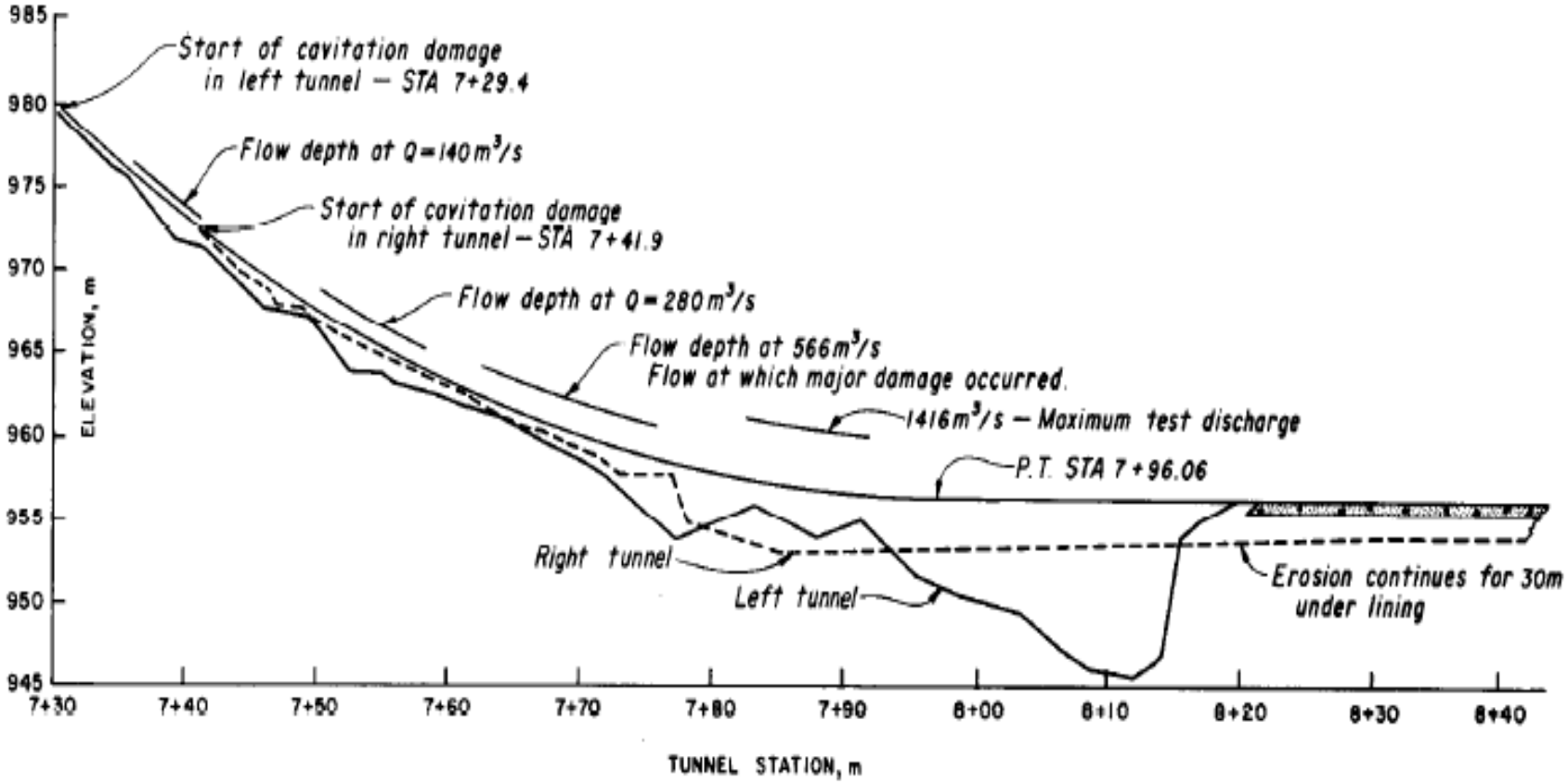

Figure 5.4: Glen Canyon Dam, tunnel spillways - damage profiles (Falvey, 1990).

Hoover Dam is a part of the Boulder Canyon Project. It is located on the Colorado River about 58 km from Las Vegas, Nevada. The purpose of the project is to: provide river regulation, flood control, storage for irrigation, and power generation.

The dam is a concrete gravity-arch structure 221 m high having a crest length of 373 m. The original reservoir had a storage capacity of 40 x 10^9 m^3. A survey in 1963-64 showed that the original capacity had been reduced by 12 percent since its dedication in 1935. The power plant has 14 hydro turbines with a combined capacity of 1344.8 MW. The combined output of the river outlet works is 1269 m^3/s.

The dam has an open-channel type tunnel spillway on each abutment of the dam as shown on Figure 5.7. Water enters each spillway by first passing through a gated, side-channel overflow weir. Then it flows over an ogee crest into an inclined tunnel.

A vertical bend connects the end of the inclined tunnel to an almost horizontal tunnel. The horizontal tunnel terminates in a flip bucket. The combined capacity of the tunnels is about 11300m^3/s.

The spillway tunnels operated for the first time in the winter of 1941. The Arizona spillway operated for 116.5 days at an average flow of 366m^3/s with a maximum flow of 1076m^3/s. The Nevada spillway operated for only 19.5 hours at an average flow of 227m^3/s and a maximum flow of 407m^3/s (Keener, 1943). At the conclusion of the spill, the Arizona spillway had suffered severe damage, but the Nevada spillway was essentially undamaged. Figure 5.5 shows the damage to the Arizona spillway consisting of a hole 35 m long, 9 m wide and 13.7 m deep. Evidently, the damage was caused by a misalignment in the tunnel invert (Warnock, 1945). The misalignment is shown on Figure 5.6.

Undoubtedly, the depth of the hole was influenced by the presence of a fault that passed obliquely across the tunnel. Hot water (32° C) flowed from the fault under a pressure of 895 kPa (Walter, 1957).

The Arizona tunnel was repaired by backfilling and compacting river rock and then covering with a thick layer of concrete. Finishing was done by bushing and wet sandblasting, followed by stoning, and finally, by grinding with a terrazzo machine.

This produced an exceptionally smooth and durable surface.

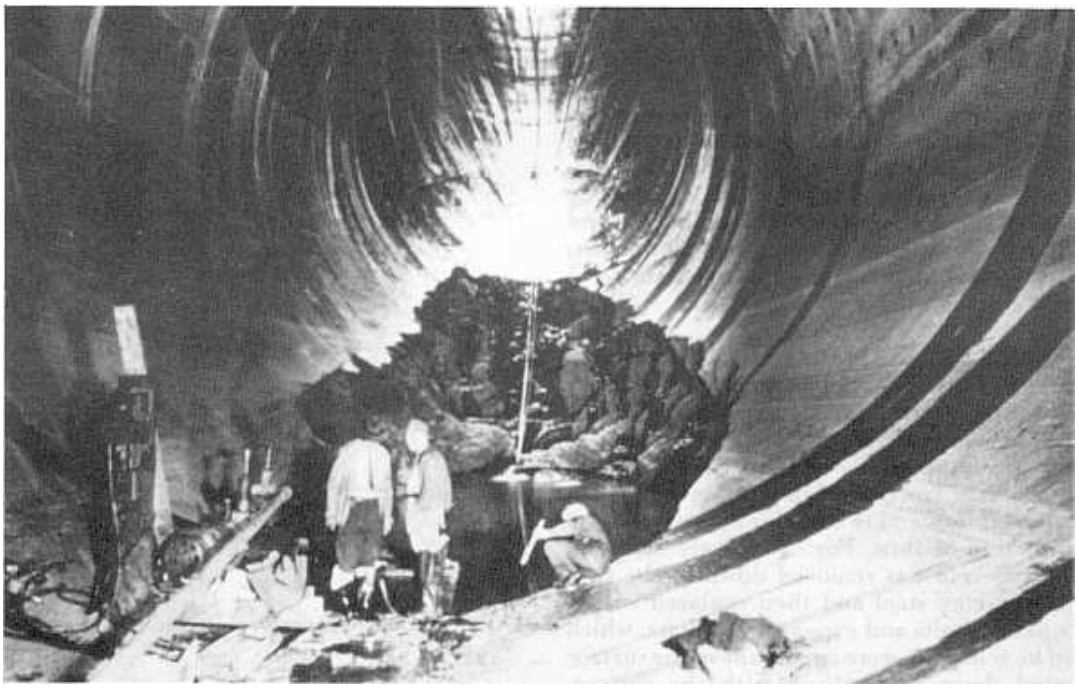

Figure 5.5: Hoover Dam, Arizona tunnel spillway-major damage (1942).

Figure 5.6: Hoover Dam, Arizona tunnel spillway-misalignment that caused major damage (Falvey, 1990).

In 1983, both tunnels operated for several hundred hours at discharges of about 283m^3/s. This time only minor damage occurred in the Arizona tunnel. However, in the Nevada tunnel the damage was on the verge of becoming severe.

The cause of this damage was a relatively insignificant pop out. The damage index, at the station where the damage began, is 6900 for a 10-mm sudden offset. This value compares favorably with the recommended range of design values for the description of damage.

Since damage occurred in both tunnels-even with exceptionally smooth surfaces-aeration devices were designed for each spillway (Houston et al, 1985) as shown on Figure 5.7. Each aerator consisted of a ramp and a downstream offset. The ramp is 900 mm high on the invert and feathers to zero height at 35° on each side of the tunnel crown. The offset is concentric with the original tunnel diameter. The 1500-mm offset transitions back to the original diameter in 7620 mm. Each aerator is located about 78 m below the inlet to the tunnel. The installation of both aerators was completed in June 1987.

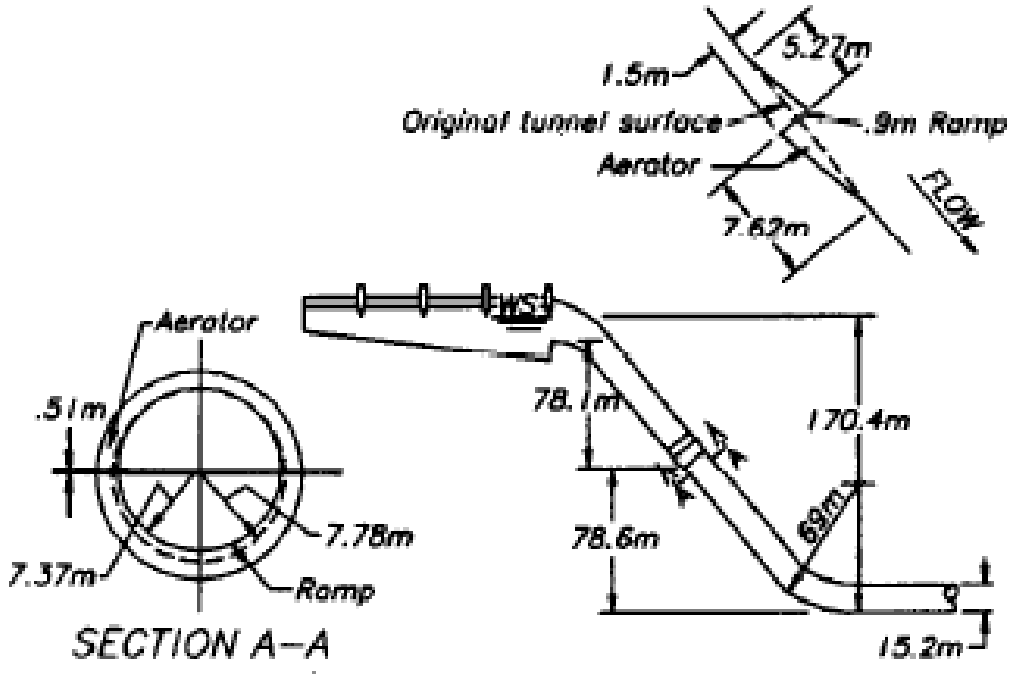

Figure 5.7: Hoover Dam, tunnel spillways-aeration slots (Falvey, 1990)

Yellowtail Dam is located 66 km southeast of Billings, Montana, on the Bighorn River. It is a part of the Pick-Sloan Missouri Basin Program. The purpose of the project is to: provide irrigation water, flood control, and power generation.

The dam is a concrete thin arch structure having a height of 151 m and a crest length of 451 m. The reservoir capacity is 0.32 X 10^9 m^3. The power plant contains four units with a combined nameplate capacity of 250 MW.

The spillway consists of: an approach channel, a radial gate controlled intake structure, a concrete lined tunnel, and a combination stilling basin-flip bucket (Beichley, 1964). The maximum capacity of the spillway is 2605 m^3/s.

Because of high inflows to the reservoir, the spillway began discharging for the first time on June 26, 1967 (Borden et al, 1971). On July 4, the flows were high enough to flip the water out of the bucket at the end of the spillway. The flows continued at a discharge of about 425m^3/s until July 14 when the flip suddenly stopped. The cessation of the flip indicated that energy dissipation was occurring within the spillway tunnel. The cause of the energy dissipation was discovered to be a large cavitation caused hole 2.1 m deep, 14.0 m long, and 5.9 m wide as shown on Figure 5.8. Downstream of this large hole, several smaller holes had developed. The large patch 6 mm deep, 152 mm wide, and 254 mm long at station 3+ 16. The damage index for this hole is 9600. The minimum cavitation index at station 3+16 is 0.15.

Higher up in the elbow of the tunnel, another damaged area was found at station 2+88 which was 9 m long and centered about 1 m to the right of the tunnel center line as shown on Figure 5.9. This damage was initiated by the failure of an epoxy mortar patch located within a 457-mm square dry patch. This damage formed five distinct teardrop shaped holes. The most upstream hole was 305 mm wide and 152 mm deep. The next downstream hole was 610 mm wide, followed by a hole 910 mm wide. The fourth hole was 1829 mm wide and the last about 1520 mm wide. The damage index for this damaged area is 3520. The minimum cavitation index at station 2+88 is 0.15.

Following this damage, one of the most ambitious repair procedures ever undertaken by the Bureau was begun. Borden et al. (1971) an aerator was designed for the tunnel, which was located 103 m below the maximum reservoir elevation (Colgate, 1971), as shown on Figure 5.10. The aerator consisted of a ramp 685.8 mm long and

76.2 mm high at the invert. Immediately downstream of the ramp, a 914-mm square aeration groove was located.

Figure 5.8: Yellowtail Dam, tunnel spillway-major damage downstream of elbow (Falvey, 1990)

Figure 5.9: Yellowtail Dam, tunnel spillway - damage in elbow (Falvey, 1990)

The downstream edge of the groove was connected to a 152-mm offset which transitioned back to the original diameter of the tunnel in 2635 mm. The transition had a 22.86-m radius of curvature in the flow direction.

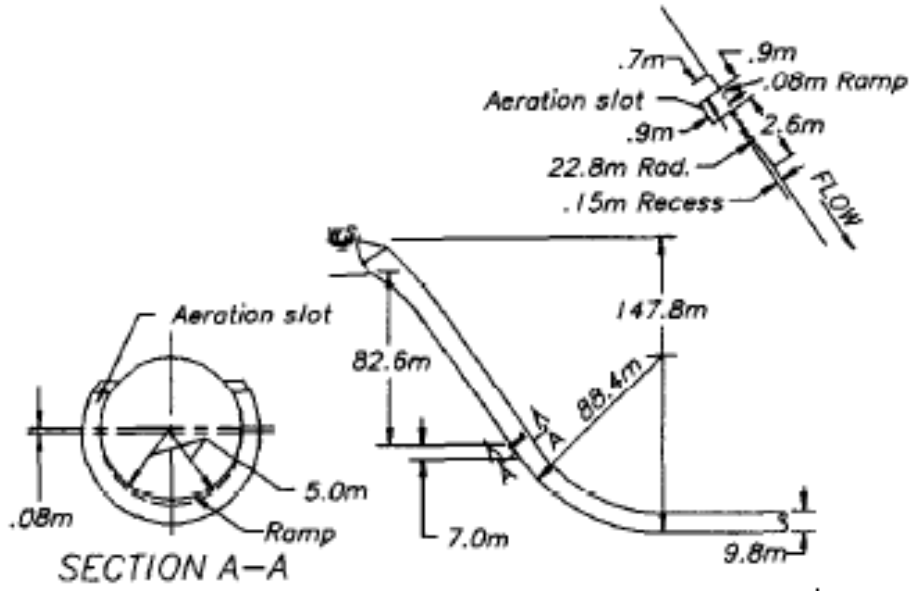

Figure 5.10: Yellowtail Dam, tunnel spillway - aeration slot (Falvey, 1990)

In addition to the aerator installation, large damaged areas were repaired with epoxy bonded concrete (Borden et al, 1971). Shallower damaged areas were repaired with epoxy-bonded concrete and epoxy bonded epoxy mortar. Irregularities in the epoxy bonded concrete were removed by grinding them to a 1:100slope. Finally, the tunnel surface below the springline (The springline is the generatrix for the tunnel roof arch) was painted with an epoxy-phenolic paint.

Following the 1969 repair, the spillway was operated at a discharge of 141m^3/s for 118 hours and at a discharge of 425m^3/s for 24 hours. In 1970, another spillway test was conducted. The test began with a flow of 141m^3/s for 11.5 hours; then the flow was increased to a discharge of 396 m^3/s and held there for 95.2 hours. This was followed by a release of 113m^3/s for about 18 hours. Following the test, an inspection of the tunnel revealed absolutely no damage. The damage index for the station at which the maximum damage occurred was 7690. Without an aerator or the extremely smooth surface treatment, moderate damage would have been predicted for a damage index this large.

Therefore, the tests at sufficiently high discharges and durations proved the effectiveness of the repair (Falvey, 1990).

Keban Hydroelectric Power Station

Keban hydroelectric power station first entered in service in 1974. Power plant has 4x157, 5 + 4x175 in overall 1330 MW installed power. Keban dam is third big power station in turkey, and each year it is producing around 6600000000 kWh energy, every year two of eight units are closed for cavitation repair, each turbine has 249.000 HP power and can get 135 m^3/s (discharge).

Keban's power station was repaired during 30.04.2007 to 29.06.2007 and procedure was at written below:

Units repair period was told to be 40 days, but it is extended to 61 days. Cavitation happened in wings of turbines and wheels.

The company made welding parts and renews the materials, and all the expenses are listed below:

Materials used: 11.205.25 TL

Workers expenses: 93.046.50 TL

Tenders expenses: 10.620 TL

Overall: 114.871.75 TL

The amount of stopping the units from working for 61 days was 3 million TL.

Kara Kaya Hydroelectric Power Station

The most serious cavitation damage was seen in Kara kaya power plant. Power station has 6×300 MW overall 1800 MW build power and with producing 7.500.000.000 kWh energy it is second big in turkey.

In 1987 when it was first in use, there were huge cavitation damages.

Each year two unit is closed for repair, the units which were closed for repair was worked for 22092.30 hours.

It was planned to finish repair in 60 days but it is done in 66 days.

They worked on welding with special Cr-Ni material to fix the problem, and because of this period of time not working the cost, is almost 7 million TL (Uni, 2010).

6. PREVENTION OF CAVITATION IN HYDRAULIC STRUCTURES

6.1. Structure Geometry and Flow Boundary Conditions Precautions

As water flow down a chute, its velocity increases and the flow depth decreases. This combined effect causes the cavitation index of the flow to decrease with the longitudinal distance along the chute. Eventually, a point is reached on the chute where normal surface irregularities will cause cavitation to begin.

Cavitation could be prevented from forming if it were possible to reduce the velocity or to increase the boundary pressure. For straight spillways, the pressure can be increased by increasing the flow depth through the use of convergent chute walls.

For spillways-composed of vertical curves-the boundary pressure can be increased by changing the curvature of the flow boundary.

Curvature on a spillway or chute can be manipulated to produce a profile having a constant cavitation index or it can be varied so as to control the pressure distribution in a prescribed manner.

The first technique produces a constant cavitation number spillway. The second technique produces a controlled pressure spillway. Both techniques use the same fundamental equations Named Equations of Motion.

Another method for reducing the flow velocity is to increase the boundary friction; that is, make the surface rougher. At first thought, this appears to be contrary to everything that has been published on the requirement of making boundaries smooth for high velocity flow. However, the real culprit in causing cavitation is not the roughness of the boundary, but the roughness of individual asperities. If making a surface uniformly rough is possible, then its cavitation characteristics will actually improve (Falvey, 1990).

Lin et al. (1982) proposed a method in which the vertical radius of curvature is varied to produce a constant cavitation index value over the length of the vertical

bend. The method is sufficiently general to include the effect of convergence of the sidewalls.

The resulting profile produces a gradually increasing pressure distribution through the vertical curve. If the vertical curve terminates at a chute or in a tunnel, a large pressure gradient is produced at the point of tangency. The large gradient may have an adverse effect on the flow conditions at this point. However, if the vertical curve terminates in a flip bucket, the method produces an excellent spillway profile that has the minimum potential for cavitation damage. The invert profile produced by this method is known as a constant cavitation number profile, Fig 6.1.

To eliminate the generation of large pressure gradients at the end of the vertical curve, Ku and Jin (1985) proposed an equation for the vertical curve which is tangent to the upstream and downstream slopes. In addition, the reciprocal of the radius of curvature varies uniformly from a value of zero, at the point of curvature, to a maximum value at the center of the curve and then back to zero at the end of the vertical curve. This method produces a triangular-shaped variation in the pressure distribution along the boundary. Although Ku and Jin used a linear variation for the radius of curvature, any shape of curve could be used. This method produces a controlled pressure profile.

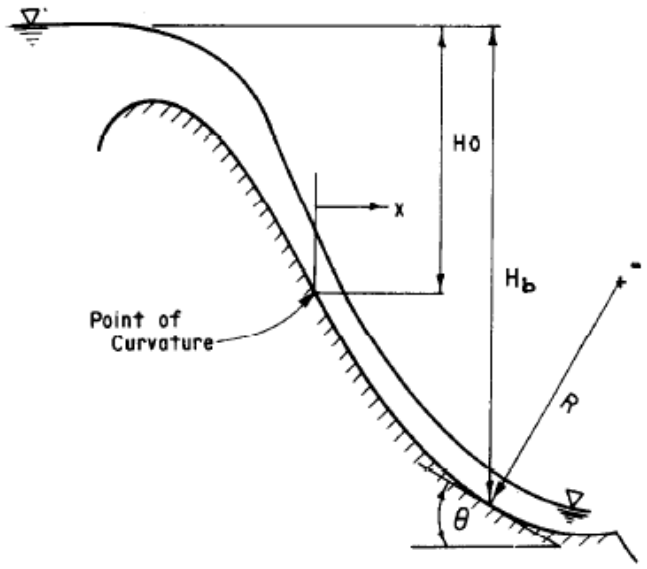

Figure 6.1: Definition sketch for geometry

Example of Changing Invert Curvature:

The techniques of designing with a constant cavitation number and a controlled pressure profile were applied to the Bureau's Glen Canyon Dam configuration to illustrate the methods and the potential benefits. The benefits are increased values of the cavitation index of the flow. Increasing the cavitation index reduces the potential for damage by cavitation. This implies that during construction surface tolerances might be relaxed. In addition, potentially dangerous conditions caused by growth of calcite deposits, after construction will not develop.

An analysis of the cavitation potential, of Glen Canyon Dam tunnel spillway, using the program HFWS (A program which is developed to calculate the hydraulic and cavitation properties of free water surface flow), showed the lowest values of the cavitation index occurred upstream of the point of curvature and downstream of the point of tangency of the vertical bend (see Fig. 6.2). The lowest values of the cavitation index for flow through the elbow occurred for a discharge of about 475m^3/s (Falvey, 1990).

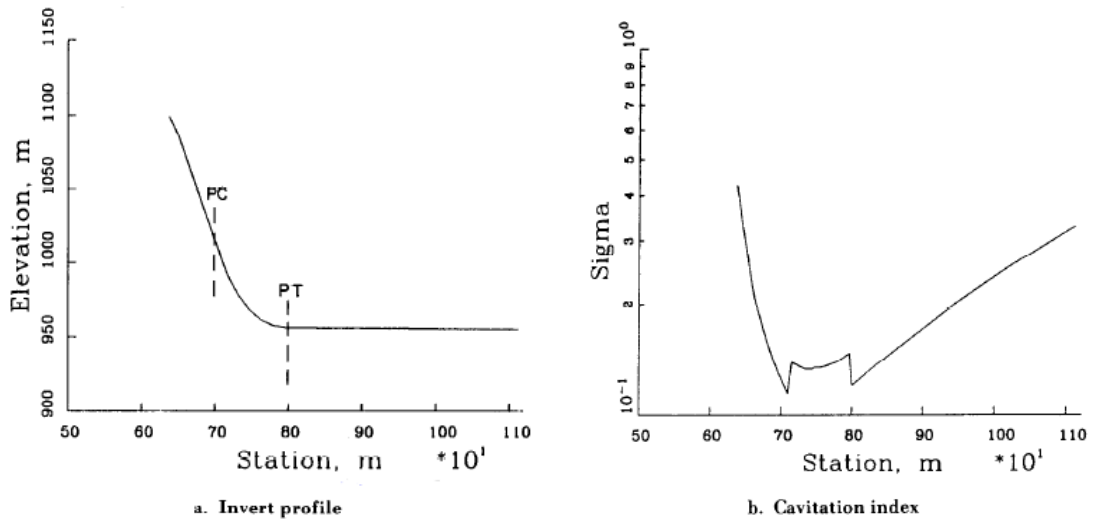

Figure 6.2: Glen Canyon Dam, left spillway tunnel-cavitation index for flow of Q =475m^3/s (Falvey, 1990).

Constant Cavitation Number Profile

With a constant cavitation number profile it is not possible to control the cavitation index downstream of the point of tangency. However, all of the spillway from the end of the crest profile to the point of tangency can be controlled.

The problem is to determine a constant cavitation number profile that is tangent to the spillway crest profile and that terminates at an elevation equal to the elevation of the point of tangency. To perform these computations, the following procedure was followed:

1. Variation in flow depth and velocity is determined along the spillway crest profile using the computer program HFWS.
2. A point is arbitrarily selected along the crest profile as the starting location for the constant sigma profile. This point should have a value of the cavitation index greater than or equal to 0.2. In some cases, this is not possible if the vertical drop to the lower tangent point is too great.
3. Initial conditions are calculated using equations for the definition of the unit discharge in a circular section and using the flow depth and invert slope at the selected starting location.
4. Constant cavitation number profile program is run.
5. If the final elevation of the constant cavitation profile does not match the desired elevation of the point of tangency, increase the value of the unit discharge and repeat steps 3 and 4. If the unit discharge gets so large that the radius of curvature becomes negative-somewhere on the profile-select, for the initial station, a location that has a lower elevation.
6. Flows conditions with the resulting profile are recalculated with program HFWS to investigate the effect of boundary friction.

The results of the analysis show that the cavitation index could have been increased from a minimum value of $\sigma = 0.104$ (shown on Fig. 6.2) to a minimum value of $\sigma = 0.115$ (shown on Fig. 6.3) for the portion of the tunnel between the spillway crest and the point of tangency at the end of the vertical curve.

This increase in the flow cavitation index would not have prevented the damage which occurred in the Glen Canyon spillways during the 1983 flood. However, the time of operation before damage occurred would have been extended.

The cavitation index of Figure 6.3 is not constant because the equal cavitation number profile was developed using rectangular sections. The conversion of the cavitation index from the rectangular to the circular section can be calculated by

equation. Also, the index is not constant because boundary friction is neglected in the development of the equal cavitation number profile, but is considered in the water surface profile program HFWS.

Two problems exist with the constant cavitation number profile: a large pressure gradient exists at the point of tangency, and the curve is too short.

The gradient will not induce cavitation, but it may cause rapid variations in the water level depth. The second problem is the most severe. Because the curve is too short, the cavitation index at the end of the curve is still very low-being about equal to 0.101.

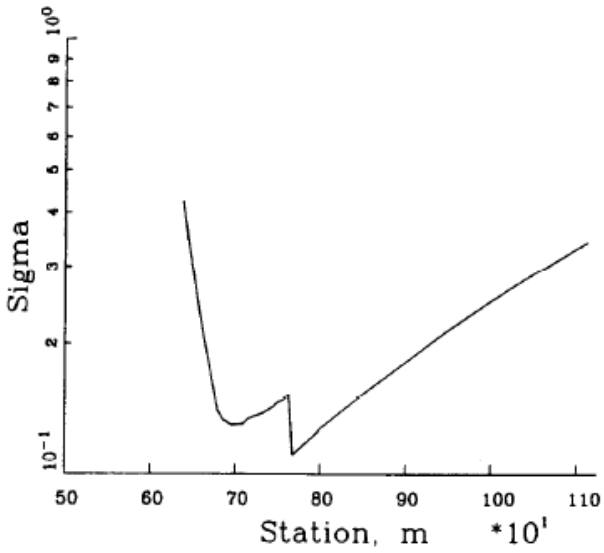

Figure 6.3: Glen Canyon Dam, equal cavitation number spillway profile – cavitation index for flow of Q = 475m^3/s (Falvey, 1990).

Controlled Pressure Profile:

With the controlled pressure profile, the radius of curvature at both the point of curvature and at the point of tangency is infinite. Therefore, large pressure gradients do not exist with these profiles.

A great difference between the cavitation indexes, with either the linear or the sinusoidal variation in pressure along the vertical curve, is not evident as noted on Figure 6.4. Because both curves are longer than the equal cavitation number profile, improvements in the cavitation index have been made at the point of tangency.

For Glen Canyon Dam, the controlled pressure profile resulted in the most favorable cavitation characteristics in the vertical bend. At station 720 the cavitation index reached a value of 0.20 as compared to a value of 0.14 in the existing design.

All of the controlled pressure profiles began at station 678.86 which is the location where the crest profile matches the equal cavitation number profile.

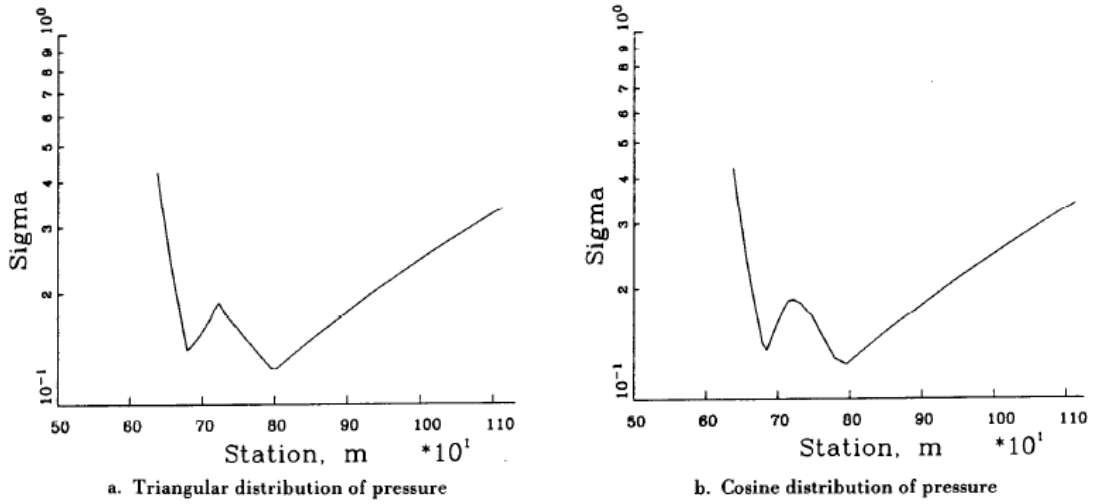

Figure 6.4: Glen Canyon Dam, controlled pressure spillway profiles - cavitation index for flow of Q = 475m^3/s (Falvey, 1990).

Example of changing surface roughness:

The beneficial effect of increasing the surface roughness on the cavitation index can be seen by examining the cavitation index of the flow for the Glen Canyon tunnel spillways having rugosities of 0.015 and 1.5 millimeters. The smaller value of the rugosity corresponds to new, unusually smooth, and concrete placed against steel forms having excellent workmanship. With this surface, construction joints are well aligned. The larger value of rugosity corresponds to an unusually rough surface placed against rough wood forms, where erosion at poor concrete and poor alignment of joints occurred.

These values represent the extremes of what actually will he achieved in the field.

As shown on Figure 6.5, increasing the rugosity results in an increase in the cavitation index from 0.091 to 0.118 at station 800 the site of the most severe damage during the 1983 spill. The damage potential also experienced significant decreases. For the larger rugosity value, the damage potential was 3.2 times smaller than for the smaller rugosity as shown on Figure 6.5.

These examples show that, on Glen Canyon Dam tunnel spillways, the effect of increasing the surface roughness is greater than the effect of changing the invert curvature.

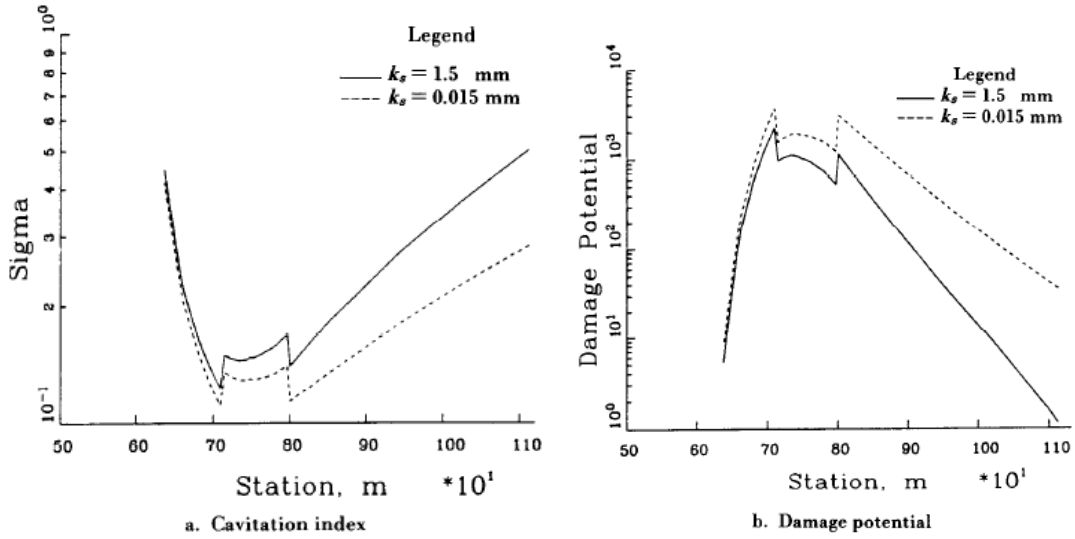

Figure 6.5: Effect of rugosity on cavitation characteristics (Falvey, 1990).

The effect of increased surface roughness has not been conclusively tested in the field. However, at Glen Canyon Dam, the left tunnel spillway invert was not repaired downstream of station 850. This area had suffered severe erosion during diversion; irregularities varied between 25 and 76 millimeters deep. During the 1984 tests, cavitation damage did not occur in this area. The air content in the water (from the aerator) probably had the greatest impact on this result. Similarly, the “rocky road” or “cobble stone” appearing surface of the invert (downstream of the vertical bend at the Nevada spillway of Hoover Dam) was not repaired when the aerator was installed. Nevertheless, all isolated irregularities on the otherwise smooth walls above the invert were removed (Falvey, 1990).

6.2. Flow Aeration and Aeration Design

6.2.1. Purpose and types of aerators

Damage experience, for flows in spillway tunnels and chutes, indicates that damage becomes significant when water velocities exceed 30 meters per second (Fig 4.7). This velocity corresponds to a head of about 45 meters. From cavitation damage viewpoint, this velocity or head can be considered as the borderline for high velocity or high head flows. Past practice recommended that surfaces exposed to high velocity flows be protected by strict attention to the surface tolerances. For new construction, this procedure may be acceptable. However, weathering of the concrete surface or the deposition of calcite through minute cracks in the boundary (after construction) can soon create a surface which is not within the specified or constructed tolerances. Therefore, other means of protecting the surface need to be considered.

It is known that extremely small quantities of air, dispersed through a water prism, will significantly reduce the tendency for cavitation to damage a surface. Peterka (1953) found that about 7.5-percent air was needed to stop damage in concrete having a 28-day compressive strength of about 17-megapascal. Semenkov and Lentiaev (1973) found that the quantity of air needed to protect a surface increased as the strength of the surface decreased. They found an air concentration of 3 percent was needed for 40-megapascal strength concrete and an air concentration of almost 10 percent is needed to protect 10-megapascal strength concrete. These values compare favorably with the experiments of Peterka.

Apparently, the first successful application of aerators in a hydraulic structure-to prevent cavitation damage-was at Grand Coulee Dam, (Colgate and Elder, 1961). In this case, excessive damage had occurred at the intersection of the river outlet tubes with the downstream face of the spillway. Previous attempts to protect the surface with epoxy coatings had been unsuccessful. After installing the aerators, reports of damage have stopped.

The first known installation of aerators in a spillway was at the Bureau's Yellowtail Dam following large discharges in June 1967, (Borden et al, 1971). The installation included not only the construction of an aerator, but careful attention was given to flow surface irregularities downstream of the aerator. For the first 7-meters

downstream from the vertical bend, all into-the-flow misalignments were removed by grinding to a 1:l00 chamfer. For the next 15 meters, a 1:50 chamfer was used. After all holes were patched and all misalignments were removed by grinding, the entire surface below the spring line was painted with a two-coat epoxy phenolic paint to provide a smooth surface and to cement particles of the epoxy mortar or concrete to each other. This work was one of the most difficult repairs undertaken by the Bureau. However, subsequent tests indicated that the repairs were completely successful.

Following the success at Yellowtail Dam spillway, aerators have been installed on spillways worldwide. Although much theory has been developed, aerator design is still somewhat of an art. The following sections summarize the present theory and design methods that can be used to size aerators. However, the results should be regarded as preliminary subject to verification by model testing.

Types of Aerators:

The principal types of aerators shown on Figure 6.6 consist of deflectors, grooves, offsets, and combinations of these, (Vischer et al, 1982). The purpose of the deflector is to lift the flow from the boundary so that air can be entrained underneath the flow surface. In this manner, air enters the flow without using mechanical methods like air pumps-which require energy. Aeration grooves, slots, or air ducts are used to distribute air across the entire width of the aerator. Finally, an offset is used on flat slopes to prevent the aerator from being submerged by a portion of the flow from the jet as it strikes the downstream boundary.

The design of an aerator consists of:

- Locating the aerator
- Proportioning the ramp or deflector
- Sizing the air supply duct and air groove
- Dimensioning the downstream offset

The goals of the aerator design are to construct a device that will protect the flow surface and not self-destruct if the aerator happens to fill with water.

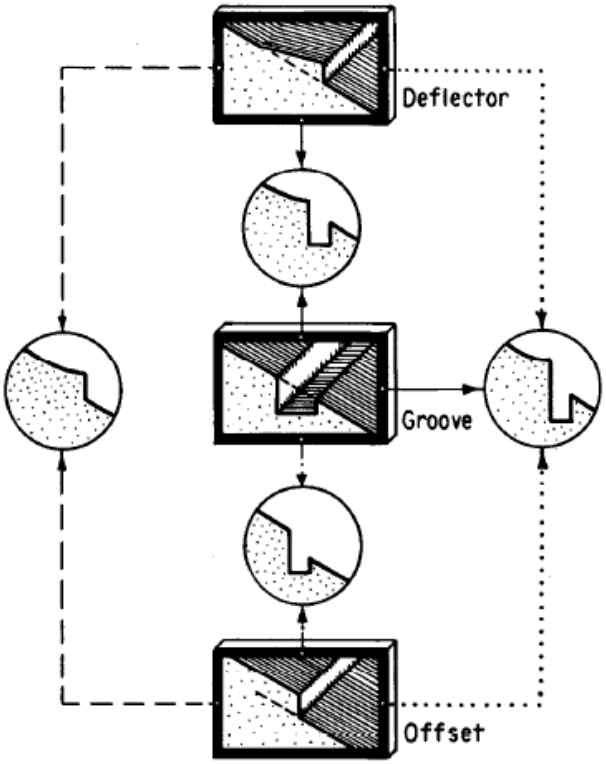

Figure 6.6: Types of aerators.

6.2.2. Aeration techniques and some installing examples

Location of aerator:

Significant damage on spillways has been observed to occur when the cavitation index of the flow is less than 0.20 (see Fig 4.7). Minor damage can occur for indexes greater than 0.20, but the extent of the damage generally has not required repair. Therefore, from a design viewpoint, flow boundaries exposed to flows that have cavitation indexes greater than 0.20 will be essentially safe from damage. Obviously, the strength of the concrete and the surface tolerances will influence this assumption.

In actual practice, this criterion is difficult to achieve. Placement of an aerator high enough on a chute or spillway to keep the cavitation index greater than 0.20, may require the use of excessively large ramp heights. The large ramps can cause the jet to touch the crown of a tunnel spillway or to overtop the walls of chute spillways. Placement of the aerator in areas where the cavitation index is less than 0.20 requires careful consideration of the flow tolerances upstream of the aerator.

The maximum discharge is not necessarily the flow rate that produces the lowest values of the cavitation index of the flow. This can be rationalized in the following manner.

- For low flow rates, friction dominates. Although flow depths are small, velocities are also small. Therefore, the cavitation index of the flow can be large.
- As the flow rate increases, the relative effect of the boundary friction decreases and the flow velocity increases. This causes the cavitation index of the flow to decrease.
- Finally, at much higher flow rates, the increase in flow velocity is small. Hence, flow depths are increasing and the cavitation index of the flow increases.

The cavitation index at the aerators and the critical discharge (as a percent of the design discharge) for a variety of tunnel spillways -constructed by the Bureau- are given in Table 6.1.

Table 6.1: Location of aerator and critical discharge (Falvey, 1990)

Spillway	Cavitation index at aerator	Critical discharge (Percent of maximum)
Blue Mesa	0.22	30
Flaming Gorge	0.19	52
Glen Canyon	0.14	14
Hoover	0.18	19
McPhee	0.19	100
Yellowtail	0.13	16

With respect to the cavitation index, Yellowtail and Glen Canyon spillways have the lowest values. However, at both of these spillways, special care was given to the tolerances of the flow surface upstream of the aerator. For other spillways, the required construction tolerances were relaxed due to the higher values of the cavitation index of the flow.

With exception of McPhee, all spillways shown in Table 6.1 are tunnel spillways having vertical bends that are concave upward. McPhee is a chute spillway having vertical bends that are concave downward.

In addition to consideration of the cavitation index of the flow, curvature of the boundary should be considered. In particular, aerator installation in vertical bends which are concave upward should be avoided. Normally, the range of flow rates over which aerators in vertical bends will function satisfactorily is severely limited. For flows outside this range, grooves will fill with water or the underside of the jet will not remain aerated.

Ramp Design:

The purpose of the ramp is to lift the flow away from the lower boundary of the chute or spillway. By lifting the flow away from the boundary, it forms a free trajectory allowing the underside of the nappe to become aerated. When flow once again rejoins the boundary, it should have entrained enough air to protect the downstream flow surface from cavitation damage.

The water trajectory is a function of the:

- Height of the ramp
- Depth of flow at the ramp
- Slope of the ramp
- Length of the ramp
- Pressure underneath the nappe
- Average velocity at the ramp
- Transverse turbulent velocity component at the ramp

Several methods are available to determine the jet trajectory. Wei and DeFazio used a finite element method to solve the Laplace equation for flow over the ramp. This method produces excellent results for both ramps and free over falls. In addition to solving for the jet trajectory, the pressure distribution around the ramp is determined. Knowledge of the pressure distribution is valuable for design of chute training walls in the vicinity of the ramp.

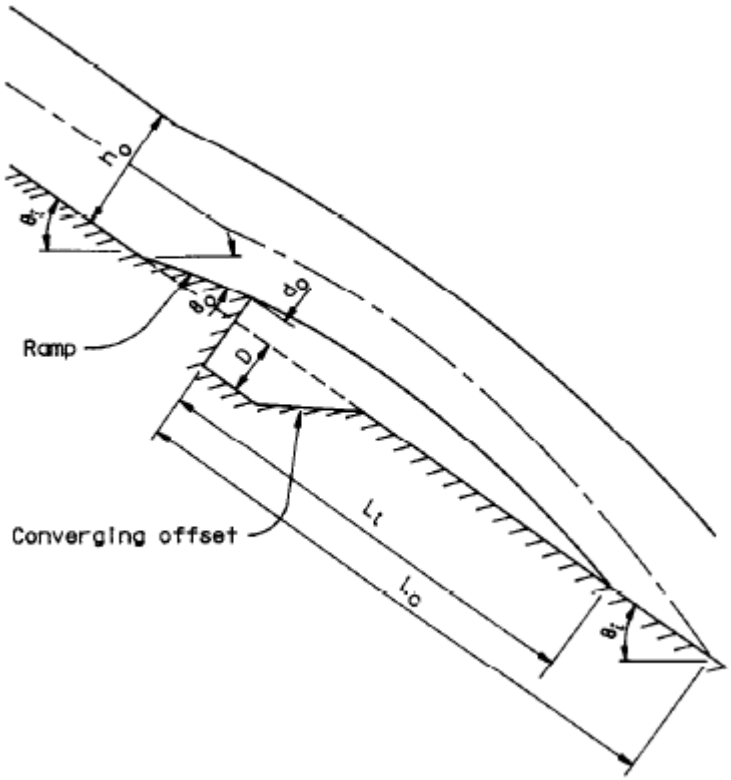

Figure 6.7: Length of jet trajectory.

Through the proper choice of ramp angle and height, it is possible to cause the trajectory to impact the downstream chute at any desired location.

Generally, the trajectory should impact downstream of the area that has the smallest value of the cavitation index of the flow. In some cases, this is impossible because the smallest values occur downstream of the vertical bend of a tunnel spillway.

The trajectory should be chosen so it does not impact within the vertical bend because this usually causes the formation of fins which lead to poor downstream flow conditions. An impact location in an area having an extremely small cavitation index is acceptable because the surface downstream of the impact area will be adequately aerated.

In circular tunnels, the ramp height must be tapered around the circumference from a maximum value at the invert to zero at or above the point where the free water surface, at maximum discharge, intersects the tunnel wall. This is done to prevent a fin from forming where the jet impinges on the tunnel wall. Without the taper, the fin size increases as the discharge increases. At large enough flow rates, the fin can fold over and choke the tunnel.

With a tapering ramp, the upper portion of the jet is subjected to less contraction than the lower portion of the jet. Because of this, the angle where the jet impinges on the tunnel wall decreases as the flow rate is increased. A disadvantage of tapering is that the jet impinges closer to the ramp at the water surface than at the invert. Model studies are usually required with aerators in circular tunnels to verify proper design of the downstream offset for all discharges (Falvey, 1990).

Air Vent Design:

Several methods have been devised to vent air from the atmosphere to the underside of the nappe as shown on Figure 6.8. These include the following:

- Ramps or deflectors on sidewalls
- Offset sidewalls
- Piers in the flow
- Slots and ducts in sidewalls
- Duct system underneath the ramp
- Duct system downstream of ramp

Ramps or deflectors, offset sidewalls, and piers in the flow are frequently used to supply aeration downstream of control gates. Normally, these air vent types are not used on wide chutes because the required offsets are impractical from a construction or structural point of view.

Slots in walls are used in control gate structures. This solution lends itself to cases where installation in an existing structure is required. The downstream end of the slot may be offset in conjunction with deflectors to keep water from entering the slot. If the cross-sectional area of the slot is too small, water and spray will he pulled into the high velocity airstream flowing in the slot. The result will be insufficient air to protect the flow surface on the chute floor.

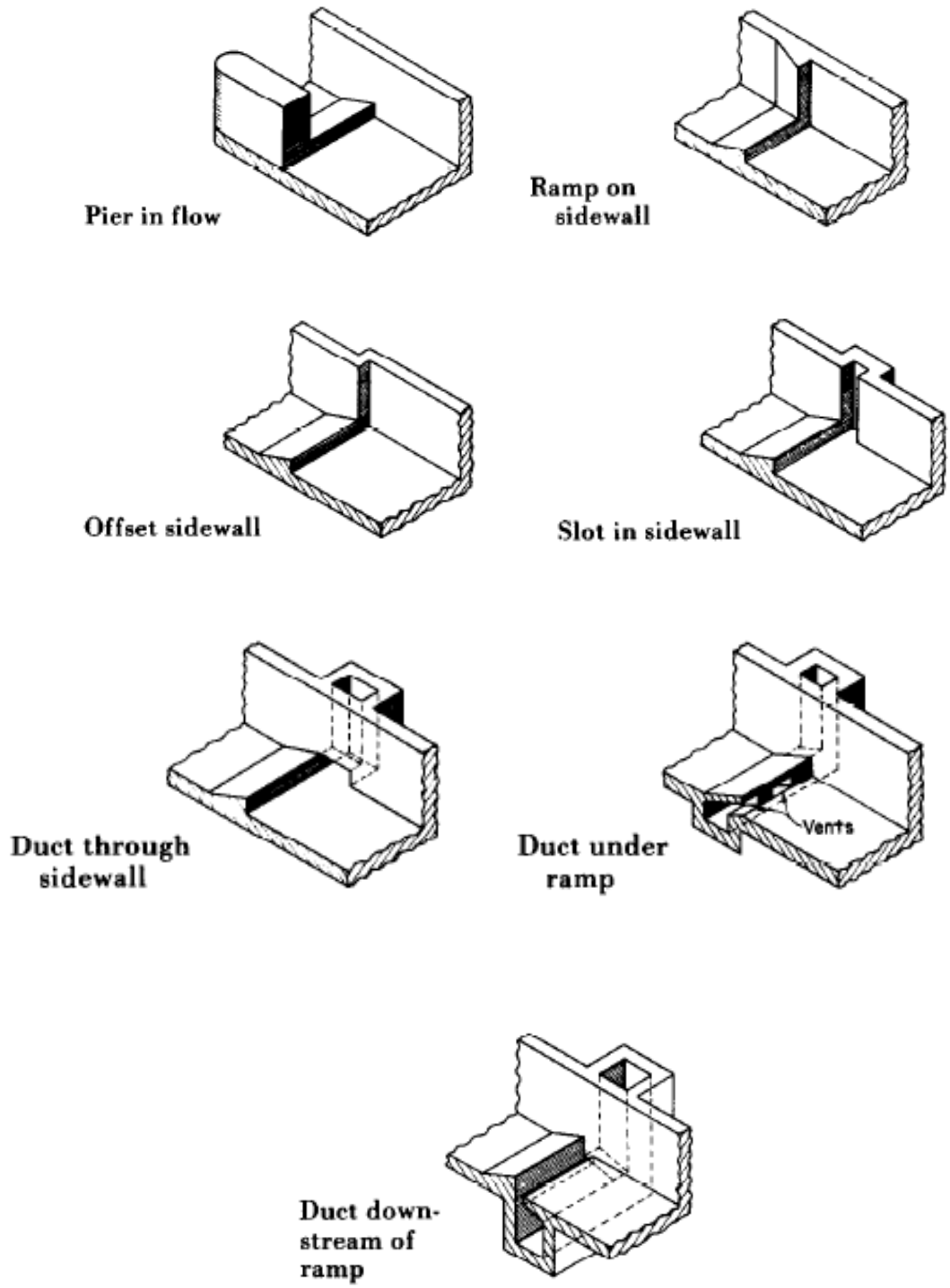

Figure 6.8: Air supply to aerator

Ducts through the sidewall are used on wide chutes when the required slot size or sidewall offsets are excessive. A duct is a closed conduit which may have a rectangular or circular cross section. In areas where freezing is a problem, ducts are routed through an embankment. This prevents the formation of ice plugs in the duct during times when water may be standing in the chute area (Fig. 6.8 Duct through sidewalls).

A duct, under the ramp, is used on wide chutes or in installations where a hydraulic jump may cover the ramp. In both cases, the system of ducts and vents ensures adequate aeration of the jet under nappe (Fig. 6.8 Dust under the ramp).

A duct-downstream of the ramp or offset-is used when the ramp height is too small to allow adequate venting. This scheme also simplifies construction. However, a drain for the duct must be provided to keep the duct free of water. Leakage and extremely low flow would tend to fill the duct on flat chutes if drainage is not provided. When operating the chute or spillway, air will enter the aerator not only through the duct but also through the drainage gallery (Fig.6.8 Duct downstream of ramp or offset).

In circular conduits on steep slopes, filling of the duct is not normally a problem because only a small portion of the duct can contain water. The air duct for circular conduits is commonly called an aeration groove or air slot.

In some cases, an air duct design having a direct connection to the atmosphere is not feasible. This is true especially with tunnel spillways and control gates located in outlet-works tunnels. For these structure types, ventilation is supplied to the duct above the flowing water. If space above the free water surface is too small, pressures under the nappe may begin to fluctuate. Criteria for the air space above the flowing water have not been established, Fig 6.9

Presently, physical model studies must be used to investigate ventilation adequacy.

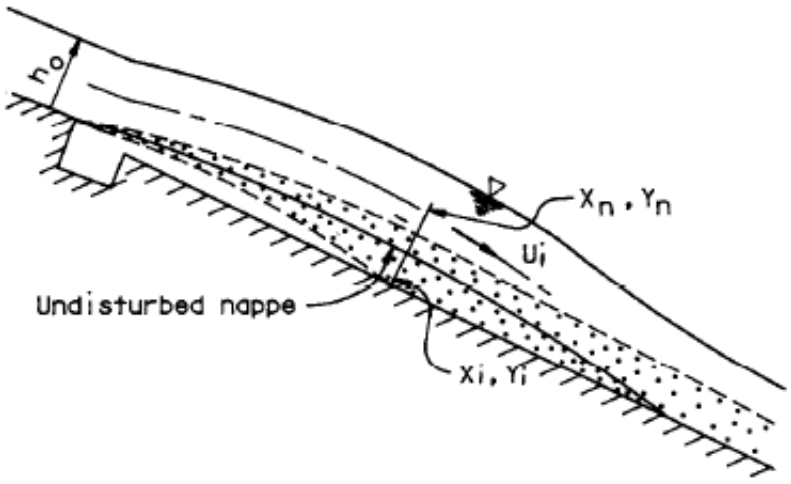

Figure 6.9: Air entrainment under nappe.

Aerator Spacing:

Aerators produce an air-water mixture at the flow boundary. If the concentration of the mixture is large enough, cavitation damage will be prevented.

As flow progresses downstream from an aerator, the air concentration decreases because of buoyancy of the air bubbles. However, the bubbles' tendency to rise is opposed by diffusive effects of turbulence which is generated at the boundary. If the concentration at the boundary becomes too small, another aerator would be needed. Therefore, a means of predicting the air concentration near the boundary, as a function of distance, is needed.

Spillway tests have shown air concentration decreases in the following manner:

Straight section . . . . . 0.15 To 0.20% per meter

Concave section . . . . . 0.50 to 0.60% per meter

Convex section . . . . . 0.15 To .20% per meter

Instead of a linear decrease in air concentration, it has been proposed that the air concentration decreases in proportion to its local value.

For this assumption, air concentration is given by:

$$\frac{C_x}{C_0} = e^{-0.017\,(L_x - L_i)} \qquad \textbf{(6.1)}$$

Where:

C_x = mean air concentration at distance X

C_0 = mean air concentration at beginning of aeration

L_x = slope distance downstream from aerator

L_i = slope distance downstream from aerator to beginning of aeration

0.017 = dimensional constant per meter, 0.017 m^{-1}

None of these methods considers the process of self-aeration of flow in a chute or spillway. The development of self-aerated flow consists of three zones as shown on Figure 6.10:

- A developing, partially aerated flow
- A developing, fully aerated flow
- A fully developed, aerated flow (equilibrium state)

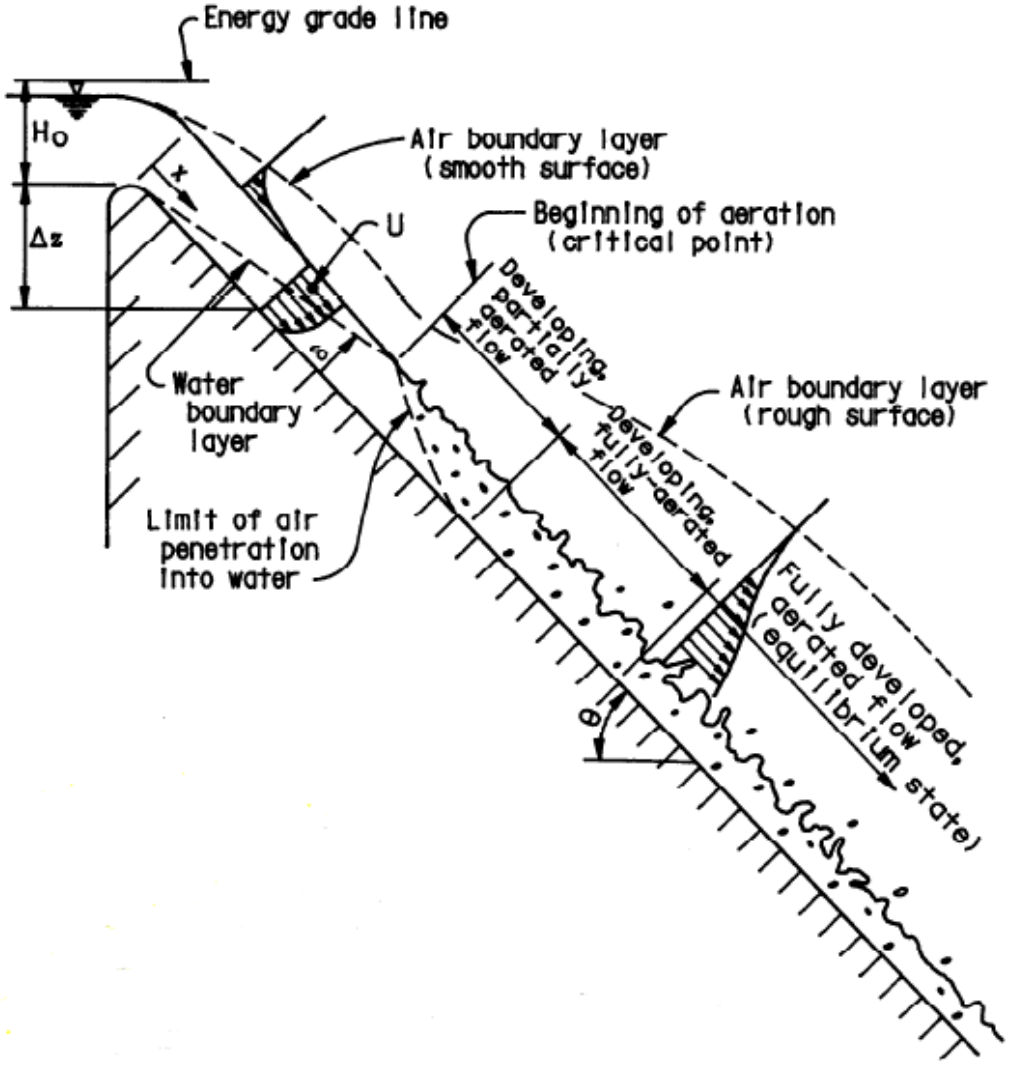

Figure 6.10: Development of self-aerated flow (Falvey, 1990).

A well designed aerator will produce, locally, higher air concentrations than those associated with the equilibrium state of aeration. Therefore, downstream of the aerator, the air concentration will decrease to that of the equilibrium state and not to zero as predicted by Equation (6.1).

Air concentration in the equilibrium state is governed by:

- Surface roughness
- Surface tension effects
- Flow velocity
- Turbulent energy at the air-water interface
- Gravity

Therefore, correlations of air concentration should include terms that contain a friction factor, a Boussinesq number, and an Eotvos number. Yevdjevich and Levin (1953) proposed a correlation of the form:

$$\frac{C_a}{1-C_a} = \beta = 0.062\, B^2 \alpha_0 f^{1/2} \qquad \textbf{(6.2)}$$

Where:

B= Boussinesq number of flow = U/ (g R_h)

C_a= mean air concentration of developed aeration

F= Darcy-Weisbach friction factor

G= gravitational constant (acceleration)

Q_e= entrained air flow rate

Q_w= water flow rate

R_h= hydraulic radius

U= mean flow velocity

α_0 = velocity distribution coefficient (kinetic energy coefficient about equal to 1.1)

β =Q_e /Q_w

Finally, Falvey (1990) proposed an equation accounting for surface tension.

$$C_a = \frac{\beta}{1+\beta} = 0.05\ B - \frac{(E \sin\theta)^{0.5}}{63} R_h^2 \quad \textbf{(6.3)}$$

Where:

E= Eotvos Number = (gR_h^2)/ (**ρ**ε)

ε= interfacial surface tension

Obviously, none of these equations consider all the pertinent parameters. However, Equation (6.3) tends to predict the same air concentration values; whereas, Equation (6.2) is somewhat high for high velocity flows.

Using the concept of self-aerated flow, change in mean air concentration, C_x, as a function of distance can be written (using the form of Equation (6.1)) as:

$$C_x = (\ C_0 - C_a) e^{-0.017\ (L_x - L_i)} \quad \textbf{(6.4)}$$

Where:

L_i = slope distance downstream from aerator to beginning of aeration

L_x = slope distance downstream from aerator

For cavitation damage on a flow surface, the air concentration at the wall-and not the mean air concentration-is the important factor. For the wall air concentration, C_w, Rao, and Gangadharaiah (1971) derived the following expression, in terms of the mean air concentration, C_a:

$$C_w = 1.17 C_a^{3.3} + \frac{(1-1.11 C_a^{2.18})^3\ (4.2\times10^{-4} - 0.1 C_a^{6.5})}{C_a^{6.5}} \quad \textbf{(6.5)}$$

The mean air concentrations in Equation (6.5) are determined from any of Equations (6.2) and (6.3).

For example as an experiment in China University of technology, the following procedure is followed:

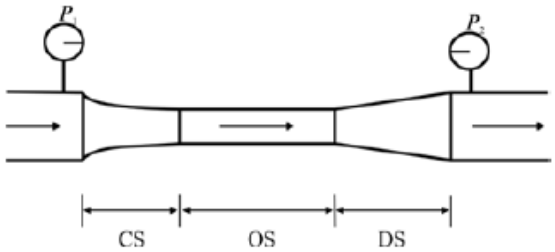

The distances of measuring points from the entrance in observation section are x=0.02 m, 0.045 m, 0.07 m, 0.095 m and 0.12 m, and the air concentration near wall C=4.1, 6.5, 8.8, 10.0, 12.0, 14.1. It can be seen from the Fig.6.11 that the pressure at each point increases with increasing air concentration.

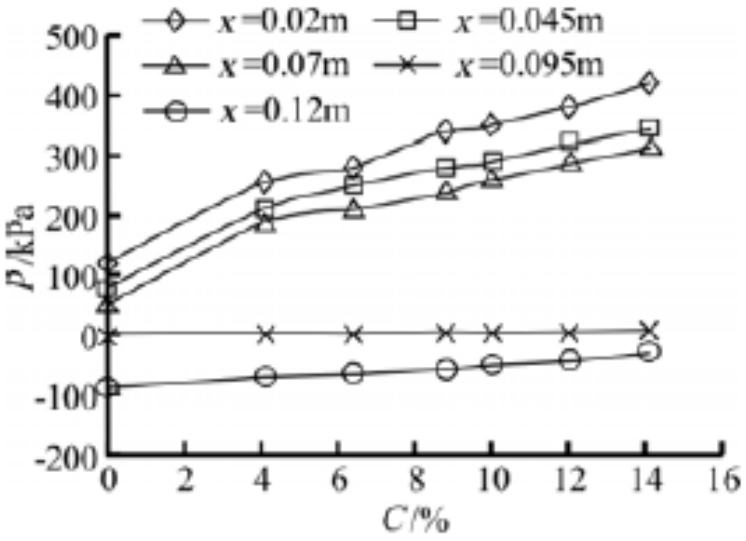

Figure 6.11: Variation of pressure with air concentration at V=49.6m/s (Dong and Cheng, 2007).

It can be seen from Fig.6.12 that the cavitation number increases also with increasing air concentration.

As it can be seen in Fig.6.13 sudden reduce in pressure due to removing the aerator was really big.

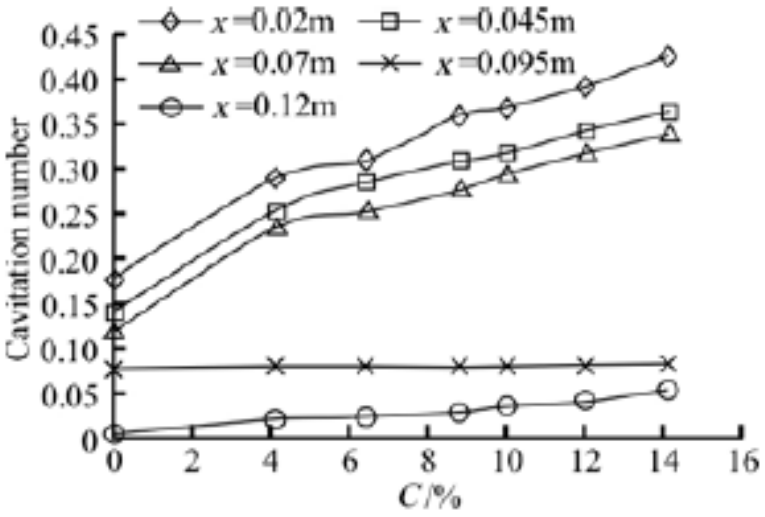

Figure 6.12: Variation of cavitation number with air concentration at V=49.6m/s (Dong and Cheng, 2007).

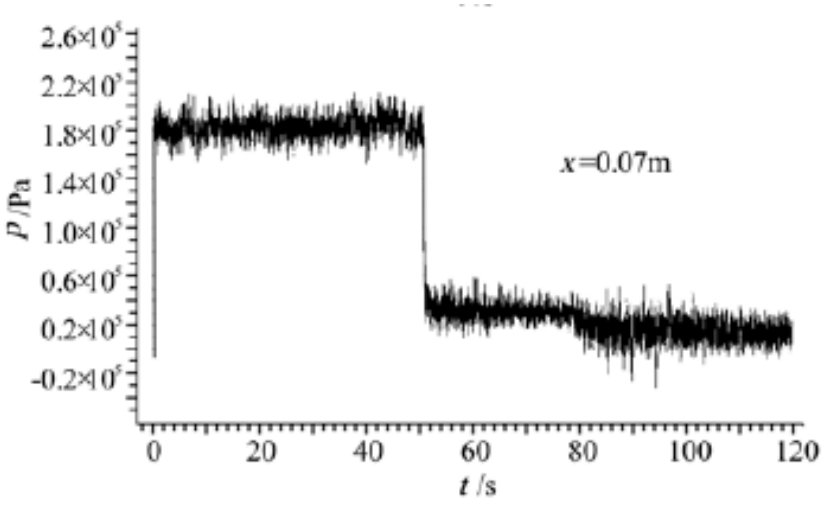

Figure 6.13: Pressure waveforms with and without aeration (*C*=6.4%) at *V*=49.6m/s (Dong and Cheng, 2007).

Through the above-mentioned experimental study at flow velocity 50 m/s, some conclusions can be drawn as follows:

The pressure and cavitation number in the cavitation region increase with the rising in air concentration. The pressure waveforms with and without aeration exhibit a stepped characteristic that suggested an abrupt change of pressure, in the absence of aeration, the concrete specimen was quickly eroded and flushed away due to the strong cavitation in a very short period. In the presence of aeration, the cavitation erosion level of concrete specimen was considerably reduced, decreasing with increasing air concentration. However, the phenomena of cavitation erosion still occur when air concentration would not reach the least air concentration to prevent cavitation control, which will not disappear until the air concentration reaches the least air concentration. Aeration was still effective to control cavitation erosion in flows at the velocity of the order of 50m/s (Dong and Cheng, 2007).

6.3. Operation of Structures

Structures that are not operated in accordance with the assumptions made in the design are likely to be damaged.

Here are some damage cases due to Operational disorders.

The studies conducted by Kenn and Garrod (1981) investigating the cause of cavitation damage to Tarbela tunnel indicated that it could have occurred due to the presence of severely sheared flows with a velocity exceeding 30 m/s in a stagnant or slowly moving water pool. As shown in Figure 6.14, the central intake gate to tunnel 2 was for some time open (at first fully, later partly) while both side gates were closed. The evidence suggests that during this time, intense vortices- induced cavitation was generated in the two essentially vertical planes of severely sheared flows leaving the inner walls of the adjacent piers. These cavities collapsed in the regions of high pressure further downstream and caused severe erosion of the concrete lining of the tunnel.

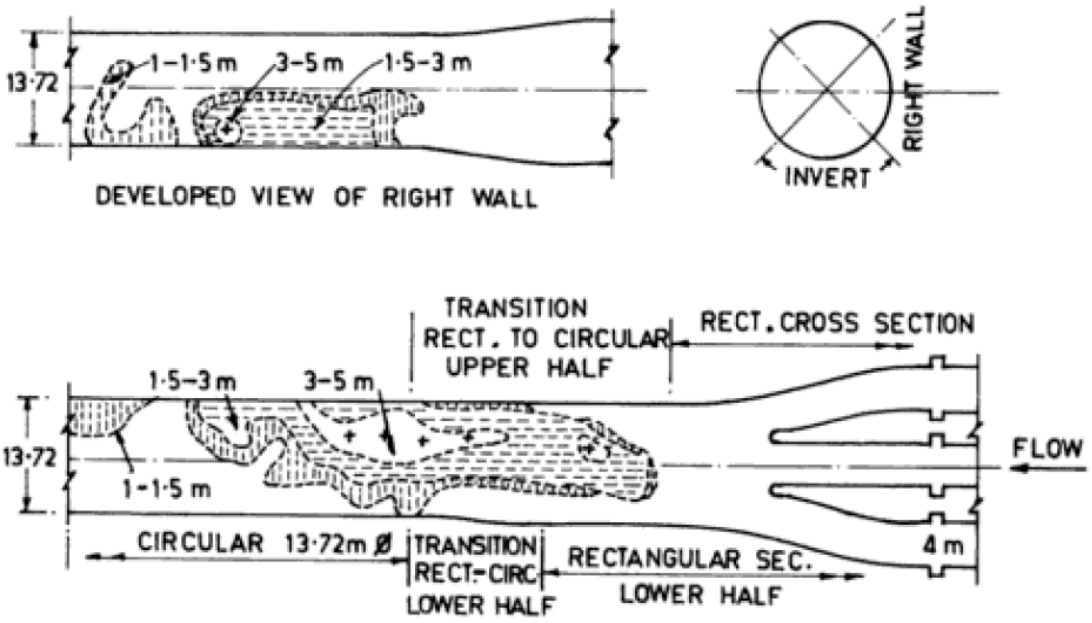

Developed View of Invert

Figure 6.14: Cavitation damage to concrete lining-Tunnel 2, Tarbela Dam, Pakistan. (Kenn et al.1981)

Asymmetrical operation of spillway gates and sluice gates can result in a condition conducive to the formation of shear layers and cause cavitation. It is well known that equal and simultaneous opening of all the gates ensures better hydraulic conditions in

the stilling basin and downstream. However, operating staff often prefer to open a single gate, starting from central gate, adding on other gates as the discharge level increases. Conditions resulting from such operations-with potential to cause cavitation- are illustrated in Figure 6.15.

Burgess (1981) has described cavitation damage to the concrete floor and kicker block of the deep sluice-stilling basin of the Roseires Dam, Sudan, Also believed to be a vortex-induced cavitation.

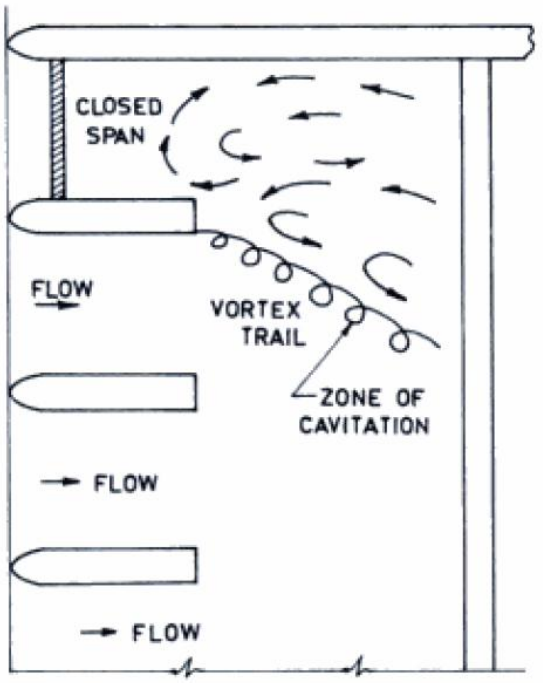

Figure 6.15: Flow separation and vortex trail due to asymmetrical operation of gates.

The deep-seated sluice structure consists of five sluices 10.5 m high by 6.0 m wide equipped with radial gates. The overall head on the sluices is 44 m, resulting in a velocity of about 29 m/s. the basin floor and the kicker block (a high-end sill) in front of sluice number five were repeatedly damaged, as shown in Figure 6.16.

It was found that sluice number 5 was operated most of the time while the other sluices were kept closed. Hydraulic model studies were conducted to study pressures at strategic locations in the damaged regions-also shown in Figure 6.16.

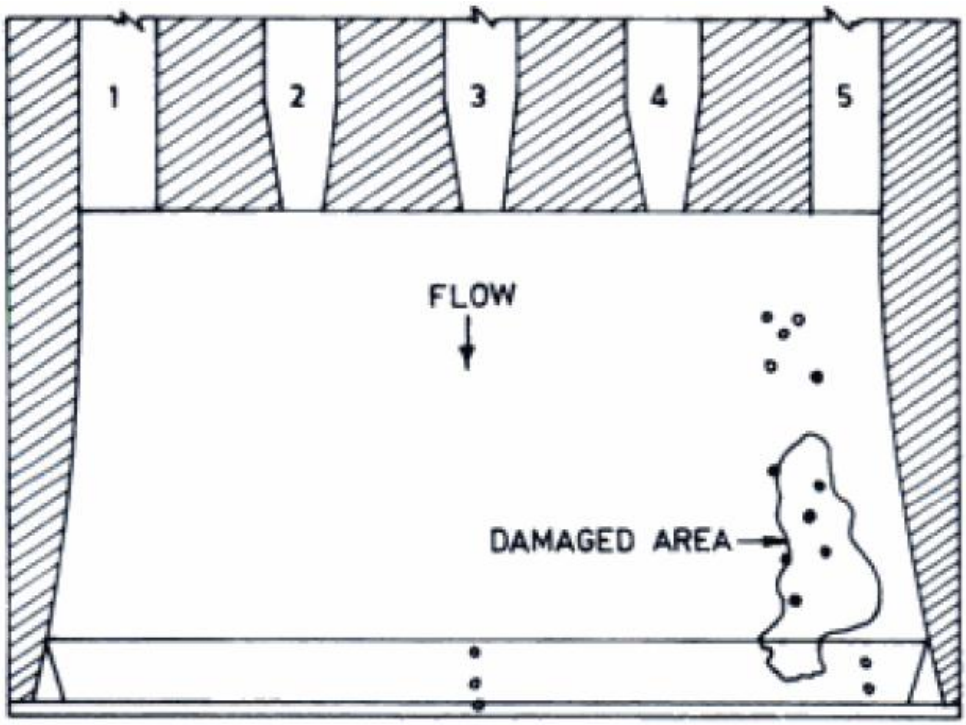

Figure 6.16: Damage to the basin floor and kicker block-Roseires dam, Sudan. (Burgess 1981)

- In all tests, pressures remained above the equivalent prototype vapor pressure
- Potential cavity formation and collapse condition recorded at least in one test

6.4. Other precautions and Design Recommendations

The first known major cavitation damage in a tunnel spillway occurred at the Bureau's Hoover Dam. After investigation and research, it was concluded the damage was initiated by a misalignment in the spillway invert. This resulted in an intensive period of investigations of surface irregularities and flow alignments. The tendency was to specify more stringent design tolerances in, hydraulic structures, (Ball, 1960). The only way to achieve rigorous tolerances was by careful attention to the methods used in finishing concrete. As a result, the concept of surface tolerance and surface finish became intertwined. As late as 1981, surface finishes to be used with high velocity flow had separate requirements (Concrete Manual, 1981).

In 1981, the Concrete Manual specified that a stoned finish should be provided for all spillways having flow velocities greater than about 23 meters per second. The technique needed to produce the surface is quite intricate:

The surface to receive the special finish should be thoroughly cleaned with high-velocity water jets to remove loose particles and foreign material and then brought to a surface-dry condition, as indicated by the absence of glistening-free water, by clean air jet. A plastic mortar consisting of 1 part of cement and 1 to l-1/2 parts of sand, by weight, which will pass a No. 16 screen, should be rubbed over the surface and handstoned with No. 60 grit Carborundum stone, using additional mortar until the surface is evenly filled. Stoning should be continued until the new material has become rather hard. After moist curing for 7 days, the surface should be made smooth and even by use of a No. 50 or No. 60 grit Carborundum stone or grinding wheel. A flexible disk power sander may produce an acceptable surface. After final stoning, curing is continued for the remainder of the 14day curing period, Fig 6.17.

After the surface was finished, it was inspected to determine adherence to specified tolerances. If an into-the-flow offset greater than 3 millimeters high was found, it was to be eliminated using bevels given in Table 6.2.

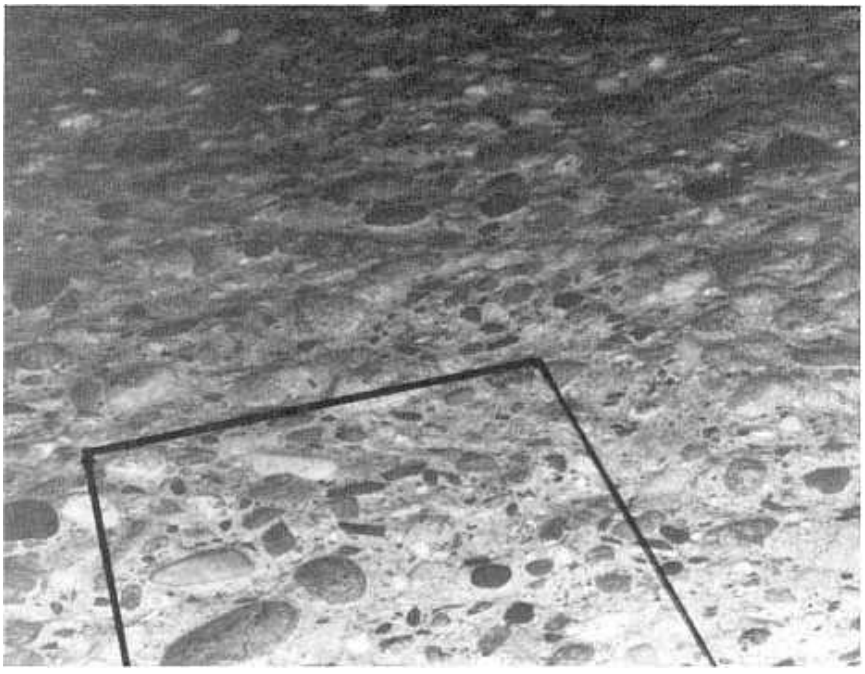

a. View of invert

Figure 6.17: Hoover Dam, Nevada spillway. Concrete surface near station 994.00

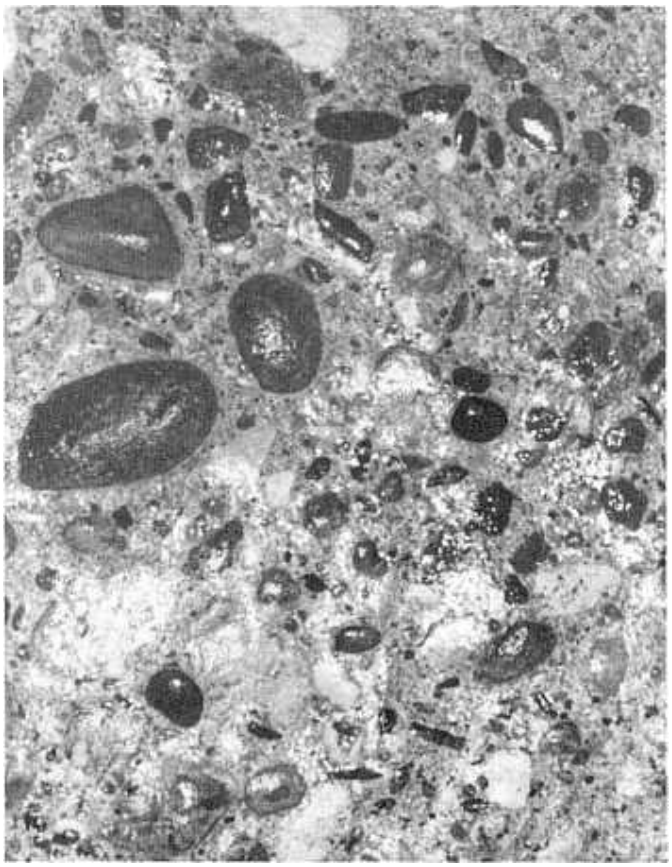

b. Invert close-up

Figure 6.17: Hoover Dam, Nevada spillway. Concrete surface near station 994.00

Table 6.2: Grinding tolerances for high velocity flow (Concrete Manual, 1981)

Velocity range m/s	**Grinding level, height to length**
12 to 27	1 to 20
27 to 36	1 to 50
Over 36	1 to 100

The tolerances were in perfect agreement with the current theory and reflected the best efforts of concrete specialists to accomplish the exacting requirements. However, from a practical aspect, these specifications were too exacting. Even if a structure was constructed according to rigid specifications, deposits left by moderate seepage could create local irregularities which would be out of the specified tolerances-within a short period.

For instance, at Glen Canyon Dam, within one month following the reconstruction and installation of the spillway aerators, calcite deposits-up to 10 millimeters high-had formed on the invert. Therefore, to maintain the exacting tolerances for

preventing cavitation damage, an extensive maintenance program would have to be initiated before each expected spill.

Specifications of Surface Tolerances

Tolerance is defined as the range of variation allowed in a constructed dimension from the design dimension. A tolerance can refer to either a structural feature or to a flow surface feature. Structural tolerances include specifications of line, grade, length, width, and plumb. Although these specifications are important, they do not have a significant effect on the cavitation characteristics of a hydraulic structure.

The following three basic types of flow surface variations are present in hydraulic structures.

Offset

Offset tolerances refer to variations caused by isolated abrupt surface irregularities where the dimension of the irregularity perpendicular to the flow is large relative to its dimension parallel with the flow. Normally, offset tolerances are the most critical. A smooth surface containing an offset is the most susceptible surface to being damaged by cavitation.

Slope

Slope tolerances refer to variations caused by surface irregularities where the dimension parallel with the flow is large relative to the variation perpendicular to the flow. The specifications of the slope tolerances ensure that variations will be gradual enough to prevent the irregularity from causing cavitation damage.

Uniformly Distributed Roughness

Uniformly distributed roughnesses refer to variations that occur over a relatively wide area. This type of irregularity is caused by erosion of a concrete surface by sand or gravel in the water passing over the surface. Another example is the rough surface left by poorly consolidated concrete which has been placed against a form. In most cases, the absolute height of uniformly distributed roughnesses can be much larger than offsets on a smooth surface without initiating cavitation damage. The critical element is the uniformity of the surface roughness.

Flow Surface Tolerance: Definition and Specifications

Flow surface tolerances for offset and slope variances, as shown in Table 6-2, have been quantified.

Table 6.3: Flow surface tolerances

Tolerance, T	Offset, mm	Slope
T1	25	1:4
T2	12	1:8
T3	6	1:16

The tolerances (see Table 6-3) can be associated with the cavitation index of the flow. The effect of aerated flow is included in the specifications of the required tolerance as shown in Table 6-4.

Table 6.4: Specification of flow surface tolerance

Cavitation of the flow	Tolerance without aeration	Tolerance with aeration
> 0.60	T1	T1
0.40 to 0.60	T2	T1
0.20 to 0.40	T3	T1
0.10 to 0.20	Revise the design	T2
< 0.10	Revise the design	Revise the design

Flow surface tolerances for uniformly distributed roughnesses have not been developed. Generally, cavitation characteristics of a uniformly rough surface are much better than for an isolated surface roughness element on a smooth surface. If uniformly rough surfaces could be created in the field, they would perform much better than the very smooth surfaces with isolated irregularities. However, a uniformly rough surface is difficult to construct. Research studies in this area will have to concentrate on the area1 statistical properties of the roughness. One useful parameter might be the ratio of the standard deviation of the surface roughness to the 90-percent size of the roughness elements. When this parameter is developed, Table 6.2 will require another column to show the allowable variation of a rough surface for each of the tolerance specifications.

Geometric Considerations:

Few structures have been designed in which the cavitation characteristics were the overriding consideration; one exception was the Aldeadavila Dam in Spain, (Galindez et al, 1967). Over 800 hydraulic tests on models of the spillway were performed to develop the spillway shape. After a few years of operation with large flows, some cavitation damage appeared at the end of the chutes caused by irregularities in the surface. The irregularities were repaired and damage stopped.

As water flows down a chute or through a tunnel spillway, flow velocity increases; hence, the flow depth decreases. Both effects lead to low cavitation indexes and potential cavitation damage. If the structure does not have a vertical curve, which can be used to control the cavitation index, then the flow depth can be controlled by decreasing the width of the chute or diameter of the tunnel. The change in cross section must be done carefully so that the chute walls are not overtopped or the tunnel does not fill with water. The decrease in the cavitation index through rougher surfaces is accomplished primarily as the result of increased flow depth.

Control of pressures in the chute downstream of the spillway crest can be accomplished through variations in both the invert curvature and chute width. For example, a crest having both inverts curvature and converging sidewalls was designed by G. Lombardi of Locarno, Switzerland, as shown on Figure 6.18, (Colgate, 1976). This spillway profile consists of a conventional spillway crest, a transition section having a constant slope invert, and a flip bucket. The invert profile of the bucket obeys a power law. In plan, the sidewalls converge uniformly at an included angle of approximately 3.3°. Both of these variations in geometry (invert curvature and convergent sidewalls) were not sufficient to prevent the cavitation index of the flow from being less than a value of 0.2. Therefore, damage probably would be expected to occur with the profile if the flow is not aerated.

Information on critical values of σ for different types of appurtenances is scanty. A summary of literature on typical values of σ for various structures is summarized in Table 6.5. It is, however, suggested that the designer may use these numbers only after studying the relevant references. Some reasons for this are: the exact geometry and test conditions must be understood, authors use different locations for determining reference parameters and similitude in the model is difficult to achieve.

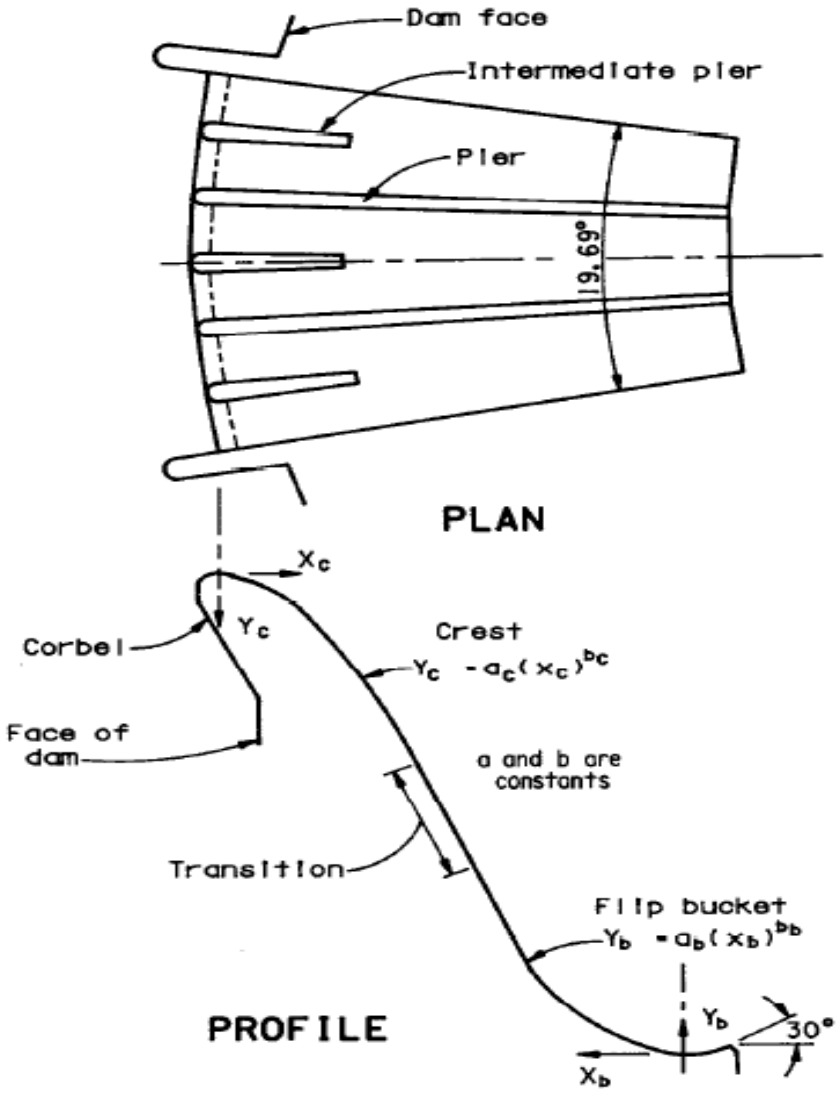

Figure 6.18: Lombardi crest

Table 6.5: Values of Ϭ at the Beginning of Damage

Structure or type of irregularity	Ϭ	Reference
Tunnel inlet	1.5	Tulis (1981)
Sudden expansion in tunnel	1.0-0.19	Russel; (1967)
Baffle pier		
Pyramidal shape	1.4-2.3	
Triangular (USBR basin III)	0.33	Khatsuria;
T-shaped baffle blocks	0.68	Kuttiammu
Spillway surfaces	0.20	Falvey (1982)
Gates and gate slots	0.20-3.0	Wagner; (1967)
Abraded concrete-20 mm max depth of	0.60	Arndt; (1977)
Slope into the flow	0.20	Ball; (1976)

7. CONCLUSION

To have an overview about cavitation prevention and effects, we can gather information in a chart like Fig 7.1. It has detailed information under the chart.

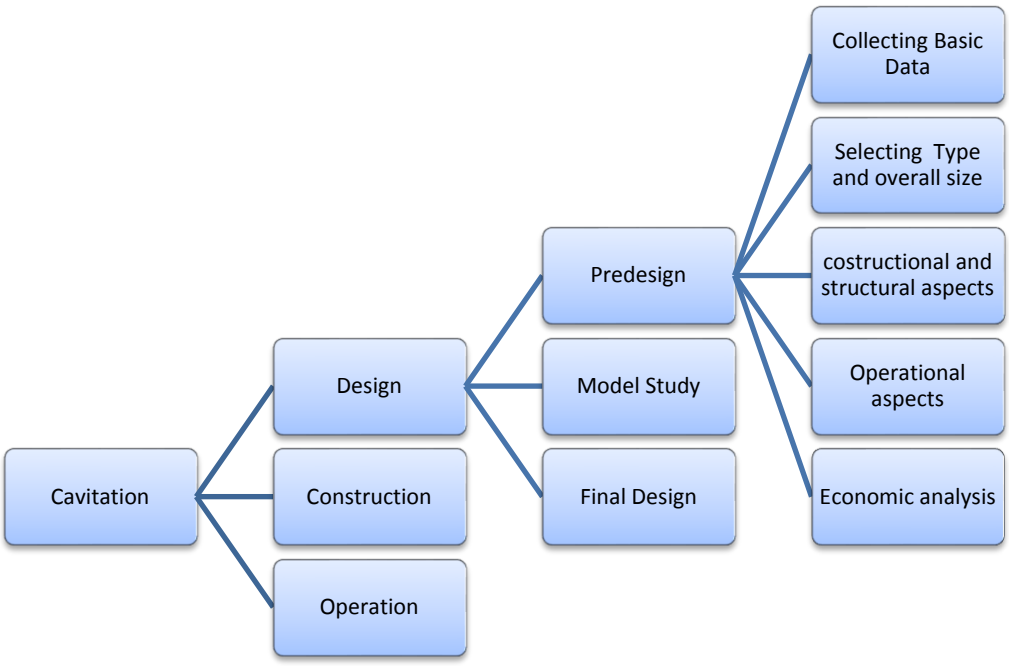

Figure 7.1: Schematic view of cavitation prevention period

Design:

Designs that are conducive to separation of the flow and creating zones of negative pressures are under designed crest profiles, gate grooves, and inadequate curvatures and transitions. Generally, the crest profiles should not be designed for heads less than 75% of the maximum depth of overflow. Sometimes, the portion of the crest upstream of the crest axis is widened in order to accommodate stop-log gates. However, such features have a detrimental effect on performance in terms of negative pressures and loss of discharging capacity. If, for any reason, such an arrangement is unavoidable, the design should be thoroughly studied in a model. Spillway crests normally have radial gates obviating the need for gate grooves. If vertical gates are to be adopted, the gate grooves should be designed with a recess on the downstream as recommended by Ball (1959) and (1979) Ethembabaoglu.

Abrupt grade-change transitions should be avoided, and the profile corresponding to the trajectory (As shown in Thesis) should be provided. In fact, a safety factor of 1.25 multiplied to the velocity has been suggested to prevent separation of the flow from the invert. (Regan et al. 1979)

It is generally recognized that, beyond a flow velocity of about 30 m/s and discharge intensity of 20 cumec/m, the surface finish required to withstand cavitation in not compatible, even with the best concrete finish and with all possible care taken. Therefore, use of cavitation-resistant liners and special materials like epoxy, fiber-reinforced concrete, etc., or provision of aerators is necessary in such situations.

Hydraulic-jump stilling basins and energy-dissipating appurtenances, like chute blocks, baffle piers, etc., are the most vulnerable to cavitation. Such appurtenances should not be used beyond the recommended velocity limit of 15-20 m/s or for cavitation indices smaller than that borne out by experience (Khatsuria, 2000). Alternatively, damage can be prevented by arranging the cavity's collapse well away from the boundary, as in the case of wedge-shaped supercavitating baffle piers.

Jet splitters at the end of the buckets have been damaged due to cavitation. Galperin et al. (1979) suggest that considerable improvement can be achieved by converging the two splitters instead of placing them parallel. This would create backpressure that can eliminate separation of the flow at the flow at the entrance to the splitters.

Model Studies:

Studies on a physical hydraulic model are almost indispensable for a major spillway project. Although designs of various elements of spillway and energy dissipation structures have evolved through generalized model studies associated with theoretical analysis, specific model study may still become necessary because of some uniqueness in the design, layout, or operational aspect. Despite the advent of mathematical and numerical modeling, which is aided by high-speed computers and computational techniques, studies on physical models continue to be undertaken for the solution of problems, which are presently not amenable to other approaches.

In the case of spillways, etc., at least two requirements are mandatory between the prototype and its model: similarity of geometric form and the equality of Froude number. With the same fluid (i.e., water) in the prototype and model, equality of other numbers is not possible. In such a situation, a correction is made for those

forces considered important, while those that are considered less important are ignored. This is the origin of the so-called "scale effect," although, more appropriately, this should be termed effect"! Which forces are correctable and which ones are negligible? This depends on the situation being considered and relies heavily on the modeler's experience and judgment.

The most important scale effects encountered in the modeling of spillways and energy dissipaters are those phenomena that cannot be adequately simulated in models:

- Friction
- Turbulence
- Cavitation
- Air entrainment and release
- Fluid-structure interaction
- Local scour below energy dissipaters

A useful approach in the study of cavitation potential is to use cavitation index, б, given by:

$$\sigma_i = \frac{P_0 - P_v}{\rho V_0^2/2}$$

Cavitation index obtained from the measurement of mean pressures and velocities with reference to the altitude of the prototype is compared to the incipient cavitation indices from Table 6.5 in chapter 6.

Cavitation tests may also be carried out using special equipment in which the ambient pressure is reduced below atmospheric pressure, thus encouraging cavitation to occur in the model. The special equipment for cavitation tests of this type (i.e., a cavitation tunnel) is elaborate, expensive to construct and maintain, and, hence, restricted to the problems of industrial applications, such as turbines, pumps, etc.

Construction:

The precautions to be taken during construction pertain to:

- Monitoring the progress of construction as per design profile, avoiding misalignments and large scale irregularity such as undulating or wavy surface finish, etc.

- Controlling surface finish within the permissible tolerances specified in relevant standards

While the former could be accomplished by proper supervision during construction, the latter requires careful and extensive review.

A tolerance is defined as the range of variation allowed in a constructed dimension from the design dimension. The following three basic types of flow surface variations are present in hydraulic structures:

- Offset: dimension of surface irregularities perpendicular to the flow is large relative to its dimension parallel to the flow
- Slope: dimension of the surface irregularities parallel with the flow is large relative to the variation perpendicular to the flow
- Uniformly distributed roughness: variation over a relatively large area. Absolute dimension of roughness element much larger than offset

For tolerances allowed USBR has designated three levels which mentioned in Table 6.3, Table 6.4 in chapter 6.

The significance of the close tolerances can be best illustrated by the example of the Fontana Dam spillway tunnel, USA. Even with the flow velocity as high as 48 m/s, no cavitation damage has taken place, presumably due to the close tolerances in the surface finish and to correct alignments.

Operation of structures:

Structures that are not operated in accordance with the assumptions made in the design are likely to be damaged. A common example is the hydraulic jump stilling basin for a spillway having a number of gates. The design presupposes equal opening of all the gates; hence, the invert elevation of the basin is determined on this condition. A number of stilling basins have suffered damage due to abrasion cavitation, and uplift as a result of asymmetrically operating the crest gates.

As shown in the cases from chapter, asymmetrical operations might induce shear cavitation in addition to producing flow conditions that are conducive to abrasion damage.

Asymmetrical operation of spillway gates and sluice gates can result in a condition conducive to the formation of shear layers and cause cavitation. It is well known that

equal and simultaneous opening of all the gates ensures better hydraulic conditions in the stilling basin and downstream. However, operating staff often prefer to open a single gate, starting from central gate, adding on other gates as the discharge level increases.

Prediction of such flow conditions and remedial measures can be best studied in hydraulic models.

Remedial measures and repairs

For existing structures that suffer repeated cavitation damage, the cause of cavitation must be ascertained in order to determine remedial measures. Misalignments and surface irregularities can probably be rectified; such a design profile deviation, which can be corrected, or roughness, such as offsets, which can be grinded to permissible values. However, inadequacy in design and certain types of irregularities cannot be rectified. In such cases, aeration is the best remedial measures. Karun spillway, Iran, is as example where aerators have been used after experiencing cavitation damage. Aerators that can be utilized on existing spillways are discussed in Chapter 6.

Conventional concrete typically performs poorly where the property of resistance against cavitation, abrasion, fatigue, and impact is important. Therefore, a variety of material and material combinations is used for the repair of concrete.

Installing stainless steel liner plates on concrete surfaces subject to high velocity flows has been a generally successful method for protecting against cavitation erosion. Stainless steel is found to be about four times more resistant to cavitation damage than ordinary concrete. The most preferred material is ASTMA 107 and S30403, due to its excellent corrosion and cavitation resistance and weld ability. Its drawbacks are high cost, sensitivity to vibration, and fatigue breakdown. There are several instances where steel plates have been ripped off, adding to the severity of the problem. Therefore, this alternative is gradually being replaced by special concretes such as epoxy, fiber-reinforced concrete, etc.

A major factor that is critical to the success of a repair is the relative volume change between the repair material and the concrete substratum. Many materials change volume as they initially set or gel; others change volume due to changes in moisture content or temperature. If a repair material’s volume relative to the concrete decreases sufficiently, cracks perpendicular to the interface will develop.

In such situations, epoxy compounds that provide a durable bond between the fresh concrete and epoxy concrete are generally used. Epoxy compounds have been recently developed that bond to damp concrete, even to concrete under water. However, there is no unanimous opinion regarding the effectiveness of epoxy treatment against cavitation damage. For example, Lowe et al. (1979) reported unsatisfactory results from the application of epoxy mixes on the Tarbela spillway structure, yet they reported positive results from the application of fibrous concrete and polymerized fibrous concrete. Meanwhile, Corlin et al. (1979) reported that epoxy coating on the stilling basin of Morforsen Dam, Sweden, had a satisfactory performance.

Fiber-reinforced concrete (FRC) utilizes randomly oriented, discrete fiber reinforcement in the concrete mixture. The superiority of FRC in comparison to conventional and polymerized concretes has been demonstrated by Lowe et al., (1979) with the help of erosion tests on concrete specimen. It is claimed that FRC is resistant to the combined effects of cavitation and abrasion erosion.

Polymers are also incorporated into concrete to produce a material with improved properties. These are polymer-impregnated concrete (PIC), polymer-Portland cement concrete (PPCC), and polymer concrete (PC). PIC is a hydrated Portland cement concrete that has been impregnated with a monomer, which is subsequently polymerized in situ. PPCC is made by adding water-soluble polymer to fresh, wet concrete. PC is a mixture of fine and coarse aggregate with a polymer used as the binder. These materials are used as concrete repair materials for damaged surfaces.

ALAG anti-abrasion concrete is a recent advancement. This is a special concrete made of calcium aluminate cement and calcium aluminate reactive synthetic aggregate. Because both the cement and the aggregates have the same physical and mineralogical characteristics, two types of bonds, i.e., physical bonds as well as chemical bonds, are ensured to give it mechanical strength to resist abrasion. It has also been tested with velocities up to 110 m/s in cavitation conditions. However, more study is required to ascertain its suitability for protection against cavitation damage.

REFERENCES

Aksoy, S.; Ethembabaoglu, S., 1979: Cavitation damage at the discharge channels of Keban dam, 13th ICOLD, Q 50, R 21.

Andreas W. Momber, 2000: Short-time cavitation erosion of concrete, accepted paper in Elsevier.

Ball, J. W., 1960: "Why Close Tolerances Are Necessary Under High-Velocity Flow," Bureau of Reclamation Report No. HYD- 473, October.

Ball, J. W., 1959: Hydraulic Characteristics of Gate Slots. ASCE jnl of Hyd Div. 85(HY 10), October.

BAŞEŞME H. 2003: Hidroelektrik Santraller ve Hidroelektrik Santral Tesisleri, EÜAŞ Ankara.

Beichley, G. L., 1964: "Hydraulic Model Studies of Yellowtail Dam Spillway - Missouri River Basin Project, Montana," Bureau of Reclamation Report No.HYD-483, August.

Beichley, G. L., 1964: "Hydraulic Model Studies of the Blue Mesa Dam Spillway," Bureau of Reclamation Report No. HYD-515, July.

Borden, R. C., Colgate, D., Legas, J., Selander, C. E., 1971: "Documentation of Operation, Damage, Repair, and Testing of Yellowtail Dam Spillway," Bureau of Reclamation Report No. REC-ERC-71-23, 76 pp., May**.**

Borden, R-C., Colgate, D., Legas, J., Selander, C.E., 1971: "Documentation of Operation, Damage, Repair, and Testing of Yellowtail Dam Spillway," Bureau of Reclamation Report REC-ERC-71.23,76 pp., May.

Bradley, J. N., 1945: "Study of Air Injection into the Flow in the Boulder Dam Spillway Tunnels - Boulder Canyon Project, "Bureau of Reclamation Report No. HYD-186, October.

Burgess, J. S., Nov, 1981: Discussion on the paper-Cavitation damage and the Tarabela tunnel collapse of 1974, Proc Institution of Civil engineering, Part I.

Burgi, P. H., Eckley, M. S., 1987: "Repairs at Glen Canyon Dam," Concrete International, pp. 24-31, March.

Burgi, P. H., Moyes, B. M., Gamble, T. W., 1984: "Operation of Glen Canyon Dam Spillways- summer 1983," Proceedings of the Conference on Water for Resource Development, American Society of Civil Engineers, pp. 260-265, Coeur d'hlene, Idaho, August 14-17.

Corlin, B.; Larsen, P. 1979: Experience from some overflow and side spillway, 13th ICOLD, Q 50, R37.

Colgate, D., Elder, R., 1961: "Design Considerations Regarding Cavitation in Hydraulic Structures," Tenth Hydraulics Division Conference, American Society of Civil Engineers, Urbana, IL, August 16-18.

Colgate, D., 1977: "Cavitation Damage in Hydraulic Structures," International Conference on Wear of Materials, St. Louis, MO, pp. 433-438, April 25-28.

Colgate, D., 1976: "Hydraulic Model Studies of Amaluza Dam Spillway," Bureau of Reclamation Report No. GR-25-76, 65 pp., December.

Colgate, D., 1971: "Hydraulic Model Studies of Aeration Devices for Yellowtail Dam Spillway Tunnel, Pick-Sloan Missouri Basin Program, Montana," Bureau of Reclamation Report No. REC-ERC-71-47, 13 pp., December.

Concrete Manual, 8th ed., 1981: Bureau of Reclamation, U.S. Government Printing Office, stock No. 024-003-00092-2, Washington, D.C.

DONG Zhi-yong, CHEN Lei, JU Wen-jie, 2007: Cavitation Characteristics of High Velocity Flow With and Without Aeration on The Order Of 50 m/s.

Dr., Fırat Üni. 2010: Fırat Havzası Hidroelektrik Santrallerinde Kavitasyon Olayı ve Onarımı (Keban-Karakaya-Atatürk Hes)

Falvey, Henry T. 1990: Cavitation in chutes and spillways. A water resources technical publication. Engineering monograph report no 42.

Frizell, W. K., 1985: "Spillway Tests at Glen Canyon Dam," Bureau of Reclamation, 52 pp., July.

Fujikawa, S., Akamatsu, T., 1980: "On the Mechanisms of Cavitation Bubble Collapse," International Association for HydraulicResearch, 10th Symposium of Section for Hydraulic Machinery, Equipment and Cavitation, Tokyo, pp. 91-102.

Galindez, A., Guinea, P. M., Lucas, P., and Aspuru, J. J., 1967: "Spillways in a Peak Flow River," Transactions of the 9th International Congress of Large Dams, vol. 2, Q33, R22, pp. 365-389, Istanbul, Turkey, September.

Galperin R S et al., 1979: Cavitation in Hydraulic Structures. Energiya publishing House, Moscow (in Russian).

Hammitt, F. G., 1979: "Cavitation Erosion: The State of the Art and Predicting Capability," Applied Mechanics Reviews, vol. 32, No. 6, pp. 665-675, June.

Heymann, F. J., 1967: "On the Time Dependence of the Rate of Erosion Due to Impingement or Cavitation," Erosion by Cavitation or Impingement, Special Technical Publication. No. 408, American Society for Testing and Materials, pp. 70-110.

Hickling, R., Plessett, M. S., 1964: "Collapse and Rebound of a Spherical Bubble in Water," Physics of Fluids, vol. 7, pp. 7-14.

Houston, K. L., Quint, R. J., Rhone, T. J., 1985: "An Overview of Hoover Dam Tunnel Spillway Damage," Waterpower 85, Proceedings of an International Conference on Hydropower, American Society of Civil Engineers, pp. 1421-1430, Las Vegas, Nevada, September.

J.R. Graham, W.S. Hamilton, J.G. Hendrickson, R.A. Kaden, J.E. McDonald, G.E. Noble, E.K. Schrader, 1987: Erosion of concrete in hydraulic structures, ACI Materials Journal 3r4

K. Warren Frizell and Nathan C. Cox, 2009: Studies Evaluate Cavitation Potential of Baffle Blocks within a Stilling Basin on a Novel Stepped Spillway Design, Presented at: 33rd IAHR Congress August 9-14, Vancouver, British Columbia, CANADA.

Katz, J., 1984: "Cavitation Phenomena within Regions of Flow Separation," Journal of Fluid Mechanics, vol. 140, pp. 397-436.

Keener, K. B., 1943: "Erosion Causes Invert Break in Boulder Dam Spillway Tunnel," Engineering News Record, pp. 763-766, November.

Kenn, M. J.; Garrod, A. D., 1981: Cavitation damage and the Tarbela tunnel collapse of 1974. Proc Instn of Civil Engrs, Part I. Feb 1981, 70.

Knapp, R. T., Daily, J. W., Hammitt, F. G., 1970: Cavitation, McGraw-Hill, Inc., New York.

Ku, C. H., Jin, Z.,1985: "The Investigation of a More Rational Configuration of the Invert Curve of a Spillway," Joint American Society of Mechanical and American Society of Civil Engineers Symposium, Alburquerque, NM, pp. 143-148, June.

Khatsuria, R. M. 2005: "Hydraulics of Spillways and Energy Dissipators" New York , Marcel Dekker Publication

Khatsuria, R. M.; Deolalikar, P. B.; Bhosekar, V. V.; Sridevi, M. I. 2000: Energy dissipator for a low head high discharge intensity spillway, 3rd Intnl R&D Conf; CBIP, Jabalpur, India, March.

L. Scheuer, 1985: Theoretische und experimentelle Untersuchungen zum Kavitationsbeginn an Oberfl¨achenrauheiten, PhD Thesis, RWTH Aachen, Aachen.

Lesleighter, E., 1983: "Cavitation in High-Head Gated Outlets - Prototype Measurements and Model Simulation," International Association for Hydraulic Research, 20th Congress, Moscow, vol. 3, sec. b., pp. 495-503, September.

Lin, B., Gong, Z., Pan, D., 1982:"A Rational Profile for Flip Buckets of High Head Dams," Scientia Sinia, series A, vol. 25, No. 12, pp. 1343-1352, China, December.

Liu C, 1983: A Study on cavitation inception of isolated Surface irregularities. Collected research papers, IWHR, Beijing, vol. XIII, pp. 36-56 (in Chinese).

Lopardo R A et al 1982: Physical modeling on cavitation tendency for macro turbulence of hydraulic jump. Intern conf on Hydraulic modeling of civil engineering structures, BHRA, Coventry, PP. 109-121.

Lopardo R A et al 1985: Modeling the behavior of high head hydraulic jump energy dissipaters under flood conditions. 2nd Intern Conf. on Hydraulics of floods and Flood control, BHRA, Cambridge, England. PP. 313-324.

Lowe III, J.; Bangash, H. D.; Chao, P. C., 1979: Some experiences with high velocity flow at Tarbela dam project, 13th ICOLD, Q 50, R 13.

May RWP 1987: Cavitation in hydraulic structures, occurrence and prevention. Hydraulic research Wallingford, report SR 79.

Oskolkov A G & Semenkov V M 1979: Experience in designing and maintenance of spillway structures on large rivers in the USSR, 13th ICOLD Congress, New Delhi Vol. III, Q50, R46, PP. 789-802.

Peterka, A. J., 1953: "The Effect of Entrained Air on Cavitation Pitting," Proceedings of the Joint Meeting of the International Association for Hydraulic Research and the American Society of Civil Engineers, Minneapolis, MN, August.

Peterka, A. J., 1953: "The Effect of Entrained Air on Cavitation Pitting," Proceedings of the Joint Meeting of the International Association for Hydraulic Research, American Society of Civil Engineers, Minneapolis, MN, August.

Pierre Franc jean, Marie Michel, Jean 2004: Fundamentals of cavitation, Lluwer academic publications.

Pugh, C. A., 1984: "Modeling Aeration Devices for Glen Canyon Dam," Proceedings of the Conference on Water for Resource Development, American Society of Civil Engineers, Coeur d'Alene, Idaho, pp. 412-416, August 14.17.

Rao, N. S., Gangadharaiah, T., 1971: "Self-Aerated Flow Characteristics in Wall Region," Journal of the Hydaulics Division, American Society of Civil Engineers, vol. 97, No. 9, September.

Rao, P. V., Martin, C. S., Rao, B.C.S., Rao, N.S.L., 1981:"Estimation of Cavitation Eosion with Incubation Periods and Material Properties," Journal of Testing and Evaluation, American Society for Testing and Materials, pp. 189-197.

Regan, R. P.; Munch, A. V.; Schrader, E. K. 1979: Cavitation and erosion damage to sluices and stilling basins at two high-head dams, 13th ICOLD, Q 50, R 11.

Roger E. A. Arndt, 2009: cavitation in fluid machinery and hydraulic structures, St. Anthony Falls Hydraulic Laboratory, University of Minnesota, Minneapolis,Minnesota.

Rozanova N N & Ariel A. R., 1983: Cavitation and hydraulic studies of non-erodible energy dissipaters. Proc XXth IAHR Congress, Moscow Vol. 7. PP. 400-405.

Semenkov, V. M., Lentiaev, L. D., 1973: "Spillway with Nappe Aeration," Gidrotekhnicheskoe Stroitel'stvo, U.S.S.R., No. 5, pp. 16-20, May.

Stinebring, D. R., 1976:"Scaling of Cavitation Damage," master's thesis, Pennsylvania, State University, 160 pp., August.

Tomita, Y., Shima, A., 1986:"Mechanisms of Impulsive Pressure Generation and Damage Pit Formation by Bubble Collapse," Journal of Fluid Mechanics, vol. 169, pp. 535-564.

Vischer, D., Volkart, P., Siegenthaler, A., 1982:"Hydraulic Modelling of Air Slots in Open Chute Spillways," International Conference on the Hydraulic Modelling of Civil Engineering Structures, BHRA Fluid Engineering, Coventry, England, pp. 239-252, September.

Walter, D. S., 1957:"Rehabilitation and Modification of Spillway and Outlet Tunnels and River Channel Improvements at Hoover Dam," thesis for civil engineer degree, University of Colorado.

Wang X-R & Chou L-T 1979: The method of calculation of controlling (or treatment) criteria for the spillway surface irregularities.13th ICOLD Congress, New Delhi Vol. III, Q50, R56, PP. 977-1012.

Wang, X., Chou, L., 1979: "The Method of Calculation of Controlling (or Treatment) Criteria for the Spillway Surface Irregularities," Proceedings of the Thirteenth International Congress of Large Dams, Q50, R56, pp. 977- 1012, New Delhi, India.

Warnock, J. E., 1945: "Experiences of the Bureau of Reclamation," Proceedings of the American Society of Civil Engineers, vol. 71, No. 7, pp. 1041-1056.

Wei, C. Y., DeFazio, F. G., 1982: "Simulation of Free Jet Trajectories for the Design of Aeration Devices on Hydraulic Structures," 4th International Symposium of Finite Elements on Hydraulic Structures, Hannover, Germany, pp. l-11, June.

Yevdjevich, V., Levin, L., 1953:"Entrainment of Air in Flowing Water and Technical Problems Connected With It," International Association for Hydraulic Research, Proceedings of the Vth Congress, Minneapolis, MN, pp. 439.454.

CURRICULUM VITAE

Candidate's full name :		Mehdi Jahani
Place and date of birth:		Khoy , 21/03/1985
Permanent Address	**:**	Shahrake Ghods, Asatid Avenue, Amiran Building
University	**:**	Civil Engineering Bachelor degree from azad university of Urmia-Iran
Email	**:**	Me.jahani@gmail.com